



Publicly Accessible Penn Dissertations


1-1-2013

The Molecular Basis of Substrate Recognition by the Family of Pellino E3 Ubiquitin Ligases

Yu-San Huoh

University of Pennsylvania, yhuoh@mail.med.upenn.edu

Follow this and additional works at: <http://repository.upenn.edu/edissertations>

 Part of the [Biochemistry Commons](#), [Biophysics Commons](#), and the [Molecular Biology Commons](#)

Recommended Citation

Huoh, Yu-San, "The Molecular Basis of Substrate Recognition by the Family of Pellino E3 Ubiquitin Ligases" (2013). *Publicly Accessible Penn Dissertations*. 875.

<http://repository.upenn.edu/edissertations/875>

This paper is posted at Scholarly Commons. <http://repository.upenn.edu/edissertations/875>

For more information, please contact libraryrepository@pobox.upenn.edu.

The Molecular Basis of Substrate Recognition by the Family of Pellino E3 Ubiquitin Ligases

Abstract

The four mammalian Pellinos (Pellinos 1, 2, 3a, and 3b) are E3 ubiquitin ligases that have emerging roles in the regulation of Toll-like receptors, interleukin-1 receptor, T-cell receptor, Nod2, and TNF receptor signaling pathways. While each Pellino has a distinct role in facilitating various cellular processes, the underlying mechanisms by which these highly homologous proteins act selectively in these signaling pathways are not clear. In this dissertation, we elucidate the molecular basis of Pellino substrate specificity in order to gain a better understanding of the roles that individual Pellinos play in orchestrating inflammation and cell death. Pellino substrate recognition is mediated by a non-canonical FHA domain, a well-characterized phosphothreonine binding module. We identify a high-affinity Pellino-FHA domain binding motif in the Pellino substrate, interleukin 1 receptor associated kinase 1 (IRAK1). Binding analysis of the different Pellinos to a panel of pT-peptides reveals that each Pellino has a distinct binding specificity. This specificity also manifests in the interaction of Pellinos with a number of known Pellino substrates. These results argue that the non-redundant roles that Pellinos play in immune signaling are in part due to their divergent substrate specificities. In addition to elucidating Pellino substrate binding preferences, we also sought to determine how Pellinos interact with substrates. Through mutational analyses, we have found that the Pellino2 FHA domain $\beta 9/\beta 10$ loop mediates interactions with IRAK1, but is dispensable for pT-peptide binding. These results show that Pellino substrate binding determinants may require more than a short pT-peptide motif.

Degree Type

Dissertation

Degree Name

Doctor of Philosophy (PhD)

Graduate Group

Biochemistry & Molecular Biophysics

First Advisor

Kathryn M. Ferguson

Subject Categories

Biochemistry | Biophysics | Molecular Biology

THE MOLECULAR BASIS OF SUBSTRATE RECOGNITION BY THE FAMILY OF PELLINO E3

UBIQUITIN LIGASES

Yu-San Huoh

A DISSERTATION

in

Biochemistry and Molecular Biophysics

Presented to the Faculties of the University of Pennsylvania

in

Partial Fulfillment of the Requirements for the

Degree of Doctor of Philosophy

2013

Supervisor of Dissertation

Kathryn M. Ferguson, Associate Professor of Physiology

Graduate Group Chairperson

Kathryn M. Ferguson, Associate Professor of Physiology

Dissertation Committee

Gregory D. Van Duyne, Professor of Biochemistry and Biophysics

Ben E. Black, Associate Professor of Biochemistry and Biophysics

James Shorter, Associate Professor of Biochemistry and Biophysics

Michael J. May, Associate Professor of Veterinary Medicine

Roberto Dominguez, Professor of Physiology

Jeffrey L. Benovic, Professor of Biochemistry and Molecular Biology

THE MOLECULAR BASIS OF SUBSTRATE RECOGNITION BY THE E3 UBIQUITIN LIGASE

PELLINO

COPYRIGHT

2013

Yu-San Huoh

This work is licensed under the
Creative Commons Attribution-
NonCommercial-ShareAlike 3.0
License

To view a copy of this license, visit

<http://creativecommons.org/licenses/by-nc-sa/2.0>

ACKNOWLEDGMENT

First and foremost, I have to express my sincerest gratitude to Kate Ferguson for her continuous support during my PhD. I especially appreciate how much freedom Kate gave me to design and carry out experiments for various projects. Moreover, I am grateful for Kate's constant encouragement to stay positive about my work. There is no doubt that she is responsible for turning me into the independent and rigorous scientist that I am today.

I also have to thank Mark Lemmon for receiving me into his lab with open arms. Mark and his lab have been invaluable resources throughout my dissertation.

Kate and Mark have synergistically made a very exciting and stimulating research environment for me. I have to acknowledge certain members of the Ferguson and Lemmon labs who I would not have been able to complete this dissertation without: Dave Lin for teaching me everything there was to know about Pellinos; Karl Schmitz for mentoring me during my first few years in the lab and effortlessly making the lab environment (particularly our shared bay) so much fun; Jason Moore for helping me troubleshoot experiments, teaching me protein crystallography, and also being an awesome bay mate; Sung Hee Choi for taking the time to teach me various biochemical techniques; and Jeannine Mendrola for her help, encouragement, and lively opinions.

Of course, I also have to acknowledge former teachers and mentors that encouraged me to pursue higher education. I am particularly obliged to my undergraduate mentors Bingyu Zhao and Brad Day, who I fondly look up to even to this day. I also have to thank my friends and family for their patience and support. Last, but certainly not least, I would like to thank my boyfriend Jesse Platt who provides constant support and daily inspiration to always work harder.

ABSTRACT

THE MOLECULAR BASIS OF SUBSTRATE RECOGNITION BY THE FAMILY OF PELLINO E3 UBIQUITIN LIGASES

Yu-San Huoh

Kathryn M. Ferguson

The four mammalian Pellinos (Pellinos 1, 2, 3a, and 3b) are E3 ubiquitin ligases that have emerging roles in the regulation of Toll-like receptors, interleukin-1 receptor, T-cell receptor, Nod2, and TNF receptor signaling pathways. While each Pellino has a distinct role in facilitating various cellular processes, the underlying mechanisms by which these highly homologous proteins act selectively in these signaling pathways are not clear. In this dissertation, we elucidate the molecular basis of Pellino substrate specificity in order to gain a better understanding of the roles that individual Pellinos play in orchestrating inflammation and cell death. Pellino substrate recognition is mediated by a non-canonical FHA domain, a well-characterized phosphothreonine binding module. We identify a high-affinity Pellino-FHA domain binding motif in the Pellino substrate, interleukin 1 receptor associated kinase 1 (IRAK1). Binding analysis of the different Pellinos to a panel of pT-peptides reveals that each Pellino has a distinct binding specificity. This specificity also manifests in the interaction of Pellinos with a number of known Pellino substrates. These results argue that the non-redundant roles that Pellinos play in immune signaling are in part due to their divergent substrate specificities. In addition to elucidating Pellino substrate binding preferences, we also sought to determine how Pellinos interact with substrates. Through mutational analyses, we have found that the Pellino2 FHA domain $\beta 9/\beta 10$ loop mediates interactions with IRAK1, but is dispensable for pT-peptide binding. These results show that Pellino substrate binding determinants may require more than a short pT-peptide motif.

TABLE OF CONTENTS

ACKNOWLEDGMENT	III
ABSTRACT	IV
LIST OF TABLES.....	IX
LIST OF ILLUSTRATIONS	X
1. BACKGROUND	1
1.1. Pellino E3 ubiquitin ligases are critical mediators of innate receptor signaling	1
1.1.1. The role of Pellinos in TLR/IL-1R signaling.....	2
1.1.2. The role of Pellino3 in Nod2 signaling.....	3
1.2 The emerging roles of Pellino in other signaling pathways	4
1.2.1. The role of Pellino1 in TCR signaling	4
1.2.2. The role of Pellino3 in TNF signaling.....	4
1.3. Pellinos' relevance to inflammatory diseases	5
1.4. Pellino substrate specificity	6
1.4.1. Pellino substrate binding domain contains a non-canonical FHA domain.....	6
1.4.2. The Pellino FHA domain is important for immune signaling and cell death.....	7
2. THE PELLINO FHA-LIKE DOMAIN PT-PEPTIDE BINDING POCKET MEDIATES SPECIFIC INTERACTION WITH IRAK1	13
2.1. Mutations in Pellino pT peptide binding pocket disrupts Pellino association with IRAK1	13
2.2. Far western analysis of Pellino2:IRAK1 interaction	14
2.3. Pellino2 FHA domain can interact with Rad9p-derived peptide.....	15
2.4. Pellino2 can protect IRAK1 from threonine dephosphorylation	16
2.5. Mutation in the Pellino pT-peptide binding pocket disrupts IRAK1 polyubiquitination	16

3. THE DETERMINANTS OF PELLINO SUBSTRATE SPECIFICITY	24
3.1. Identification of an IRAK1-derived Pellino2 binding domain.....	24
3.2. Pellino pT-peptide +3 motif preferences	25
3.2.1. Pellino2 can specifically recognize IRAK1T141-derived pT-peptide	25
3.2.2. Pellino isoforms have different pT-peptide specificities	26
3.3. Pellinos have distinct specificities for RIP1 and TRAF6.....	28
3.4. Distribution of FHA binding motifs in Pellino substrates	28
3.5. Attempts to determine high resolution Pellino:phosphopeptide structure	29
3.6. Towards a Pellino3a-FHA structure	29
3.7. Homology modeling of Pellinos	30
3.8. Pellino substrate recognition may require more than pT-peptide recognition.....	30
3.8.1. Pellino2 interacts with IRAK1 mutants T54A and T141A	30
3.8.2. Pellino2 R224A disrupts interaction with IRAK1, but not pT-peptide.....	31
4. DISCUSSION OF CHAPTERS 2 AND 3.....	53
4.1. pT-peptide binding of Pellinos	53
4.2. Identifying more specific Pellino binding sites.....	53
4.3. Phosphorylation-dependent regulation of Pellino specificity and substrate recognition	55
4.3.1. Substrate phosphorylation may disrupt Pellino binding	55
4.3.2. Phosphorylation may affect Pellino specificity	56
4.4. Pellino substrate binding includes more than the recognition of a short pT-peptide sequence	56
4.5. Parallels between FHA and SH2 domains may assist in elucidating Pellino substrate specificity	58
4.6. Probing the regulation and biological functions of Pellinos	59
4.7. Therapeutic prospects of targeting Pellinos.....	60

5. THE MOLECULAR MECHANISMS OF PELLINO- AND TRAF6-MEDIATED	
UBIQUITINATION OF IRAK1	62
5.1. Attempts to determine the structure of the non-canonical Pellino RING domain	62
5.1.1. Pellino2 does not interact with Ubch7 and Ubc13	63
5.1.2. <i>E. coli</i> -derived full-length Pellino1 is more stable than Pellino2.....	64
5.1.3. Attempts to crystallize Sf9-derived Pellino2	65
5.2. Molecular basis of TRAF6 interaction with IRAK1.....	65
5.2.1. TRAF6 interacts with the C-terminal domain of IRAK1	65
5.2.2. TRAF6 and IRAK1 bind with 2:1 stoichiometry.....	67
5.3. Conclusion	68
6. METHODS.....	76
6.1. Expression vectors.....	76
6.2 Protein production and purification.....	76
6.2.1. <i>E. coli</i> -derived protein production and purification	76
6.3. HEK293T culture conditions and transfections	78
6.4. GST-Pellino pull-down assays.....	78
6.4.1. Pull-downs of Pellino substrates	78
6.4.2. Pull-down of Ubc13.....	79
6.5. Far western analyses.....	80
6.6. Peptide pull-down assays	80
6.7. Isothermal titration calorimetry	81
6.8. IRAK1 dephosphorylation protection assay	81
6.9. Detection of IRAK1 polyubiquitination	82
6.10. Fluorescence polarization peptide binding assays.....	82
6.11. Protein X-ray crystallography.....	83
6.11.1. Pellino:peptide co-crystallization screening.....	83

6.11.2. Peptide soaking of Pellino2 crystals.....	83
6.11.3. Pellino3a-FHA protein crystallization and structure determination.....	84
6.11.4. Pellino1 and 2 full length crystal screening	85
6.12. Surface plasmon resonance binding experiments.....	85
6.13. Analytical ultracentrifugation experiments	86
BIBLIOGRAPHY	87

LIST OF TABLES

Table 2.1. Summary of phosphothreonine peptide pull-downs of Pellinos	21
Table 3.1. Binding affinity of IRAK1-derived peptides to Pellino2-FHA domain.	37
Table 3.2. Binding affinity of IRAK1pT141+3 position variants to Pellino-FHA domains.	39
Table 3.3. Frequency of FHA binding motifs in Pellino substrates.	41
Table 3.4. FHA domain binding motifs in Pellino substrates.....	42
Table 3.5. Summary of co-crystallization screening of Pellino constructs with peptides	43
Table 3.6. Summary of optimized Pellino3a crystallization conditions.....	48
Table 3.7. Data collection statistics for Pellino2:pT141 peptide and Pellino3a-FHA	49
Table 5.1. Crystallization screening summary of full-length Pellinos	72
Table 5.2. K_D s of Pellino1 and Pellino1-FHA binding to pT-peptides	73

LIST OF ILLUSTRATIONS

Figure 1.1. Pellino-mediated signaling events downstream of IL-1R/TLR, Nod2, TCR and TNFR1 activation.....	9
Figure 1.2. The Pellino2 substrate binding domain is a non-canonical FHA domain.	11
Figure 1.3. Sequence alignment of select mammalian Pellinos	12
Figure 2.1. The Pellino FHA domain phosphothreonine-peptide binding pocket is essential for interaction with IRAK1.....	18
Figure 2.2. Far western analysis of Pellino2:IRAK1 interaction.....	19
Figure 2.3. Pellinos specifically interact with Rad9pT192 peptide.	20
Figure 2.4. Pellino2 can prevent complete threonine dephosphorylation of IRAK1.....	22
Figure 2.5 Mutation in the Pellino pT-peptide pocket disrupts IRAK1 polyubiquitination.....	23
Figure 3.1. Pellino2 interacts with IRAK1-197 in a phosphorylation dependent manner.....	33
Figure 3.2. Pellino2 specifically interacts with a peptide motif around pT141 of IRAK1-197.....	35
Figure 3.3. Pellinos have different phosphothreonine peptide binding specificities.....	38
Figure 3.4. Pellinos have different specificities for TRAF6 and RIP1.	40
Figure 3.5. Pellino1:pT141+3S peptide quasi crystals.....	45
Figure 3.6. The FHA domain pT-peptide binding site of Pellino2 crystal is a crowded environment.	46
Figure 3.7. Crystallization of Pellino3a-FHA	47
Figure 3.8. The Pellino β 4/ β 5 loop may confer Pellino substrate specificity.....	50
Figure 3.9. Pellino2 still interacts with IRAK1 T54A and T141A mutants	51
Figure 3.10. Pellino2 R224A disrupts interaction with IRAK1, but not Rad9pT192 peptide.	52
Figure 5.1 Pellino2 interactions with UbcH7 and Ubc13 are undetectable.....	70
Figure 5.2. <i>E. coli</i> -derived Pellino1 and Sf9-derived Pellino2 are more stable than <i>E. coli</i> -derived Pellino2.	71
Figure 5.3. TRAF6 interacts with IRAK1Ct	74
Figure 5.4. TRAF6 and IRAK1 bind with an apparent 2:1 stoichiometry	75

1. Background

1.1. Pellino E3 ubiquitin ligases are critical mediators of innate receptor signaling

One branch of innate immunity involves host surveillance of pathogens by the arsenal of pattern recognition receptors (PRRs). The evolutionarily conserved family of PRRs includes membrane-bound Toll-like receptors (TLRs) and the cytoplasmic nucleotide oligomerization domain (Nod)-like receptors (Nod1 and 2) and retinoic-acid-inducible-protein I (RIG-I)-like receptors (RLRs) [1]. Upon detecting conserved elements of invading microorganisms known as pathogen associated molecular patterns (PAMPS), these PRRs initiate various signaling cascades that culminate in the activation of transcription factors, such as nuclear factor-*kappa*B (NF- κ B) and interferon regulator factors (IRFs) [1-3], which up-regulate the synthesis and secretion of proinflammatory cytokines, chemokines, and interferons [1]. Regulation of PRR signaling networks relies heavily on carefully orchestrated phosphorylation and ubiquitination of the numerous signaling components.

Ubiquitination involves the covalent attachment of a 76 amino acid protein, ubiquitin, to a target protein [1,4]. This process involves the sequential actions of three ubiquitin ligases: first, the E1 ubiquitin-activating enzyme forms an ATP-dependent thioester bond between the C-terminus of ubiquitin and a cysteine within the E1 active-site; activated ubiquitin is then transferred to the active site cysteine of an E2 ubiquitin-conjugating (Ubc) enzyme; finally, an E3 ubiquitin-protein ligase facilitates the transfer of ubiquitin from the E2 enzyme to a lysine on the target protein [2-4]. Once a target protein is monoubiquitinated, the ubiquitin attached to the target can also undergo ubiquitination via one of its seven lysine residues [1,4] or N-terminus [5]. This leads to the formation of polyubiquitin chains on a target protein, where the type of ubiquitin linkage determines the biological function of the protein. For example, K48-linked polyubiquitination marks a protein for proteasomal degradation; on the other hand, K63-linked polyubiquitination marks proteins for non-degradative processes including the formation of signaling complexes and activation of protein kinases [6]. Like phosphorylation, ubiquitination is a

post-translational modification that is required for facilitating a variety of cellular processes. My dissertation focuses on the role of an E3 ubiquitin ligase family Pellino that mediates ubiquitination events in the context of innate immune signaling pathway regulation.

The Pellinos are one of several families of E3 ubiquitin ligases that have emerging roles in facilitating TLR and Nod2-dependent NF- κ B and IRF3/7 activation [7-10]. The family of Pellinos includes 4 mammalian isoforms: Pellino1, 2, and splice variants 3a and 3b. Although Pellinos were originally thought to simply be adaptor proteins that are recruited upon TLR and interleukin-1 receptor (IL-1R) stimulation, sequence analysis and *in vitro* ubiquitination assays identified that all mammalian Pellino isoforms are catalytically active RING E3 ubiquitin ligases that are able to form K48 and K63-ubiquitin linkages [11-13]. Here, we describe what is currently known about how Pellinos regulate these innate immune receptor signaling pathways (summarized in Figure 1.1A).

1.1.1. The role of Pellinos in TLR/IL-1R signaling

The Toll/IL-1R (TIR) superfamily comprises of the TLRs (numbered 1-10 and 1-12 in humans and mice, respectively) and IL-1R [14]. Each TIR member contains a cytoplasmic TIR domain that maintains homotypic interactions with adaptor proteins that also contain TIR domains [14]. Upon receptor stimulation, IL-1R and all TLRs, except for TLR3, can interact with the adaptor protein myeloid differentiation factor 88 (MyD88) to recruit and activate the family of interleukin-1 receptor (IL-1R) associated kinases (IRAKs) [2]. Recruited IRAKs subsequently trigger downstream signaling networks that lead to the activation of NF- κ B, and IRF7, along with the mitogen-activated protein kinases (MAPKs) [2]. TLR3 and also TLR4 alternatively recruit the adaptor molecule TRIF (TIR-domain-containing adaptor-inducing interferon- β), which targets TANK-binding kinase 1 (TBK1) and RIP1 (receptor-interacting serine/threonine-protein kinase) in order to activate NF- κ B and IRF3/7, and MAPK signaling pathways [2,15].

Pellinos play a crucial role in directing polyubiquitination events immediately following TLR/IL-1R stimulation [16-18]. For example, Pellino2 is implicated in the IL-1-dependent K63-

linked polyubiquitination of IRAK1 [18], which is a requirement for the activation of inhibitor of κ B kinase (IKK) complex that allows for NF- κ B to translocate into the nucleus [19,20]. By contrast, Pellino1 and 3 knockout mice studies show that both Pellinos are dispensable for NF- κ B activation in IL-1R signaling [17,21]. Instead, Pellino1 mediates RIP1 polyubiquitination, which is required for NF- κ B activation in TRIF-dependent TLR 3/4 signaling pathways [17]. In addition, Pellino1 E3 ligase activity is critical for the activation of type I interferon expression in the same TRIF-dependent signaling pathways, although Pellino1-mediated RIP1 polyubiquitination is not required for this process [22]. On the other hand, Pellino3 does not activate TLR3/4-mediated NF- κ B signaling, but instead modulates TLR3-mediated IRF7 activation [21]. Upon TLR3 stimulation, Pellino3 interacts with and polyubiquitinates the E3 ubiquitin ligase tumor necrosis factor receptor associated factor 6 (TRAF6); this modification prevents TRAF6 association with IRF7, which ultimately suppresses the TLR3-induction of type I interferon expression [21].

1.1.2. The role of Pellino3 in Nod2 signaling

Nod-like receptors (Nod1 and 2) are cytoplasmic PRRs that recognize peptides derived from bacterial peptidoglycans [23]. Instead of TIR domains, Nod-like receptors contain caspase-recruitment domains (CARDs) that directly make homotypic interactions with their cognate CARD-containing kinase, RIP2 (also known as RICK) [23]. Upon peptidoglycan-stimulation of Nod-like receptors, activated RIP2 interacts with transforming-growth-factor- β -activated kinase 1 (TAK1) complex, which ultimately leads to the stimulation of signaling pathways similar to TLR signaling [23]. Comparable to the IKK complex recognition of Lys63-linked polyubiquitinated IRAK1, TAK1 complex association requires Lys63-linked polyubiquitination of RIP2 [24]. Very recently, Pellino3 was found to be the E3 ligase that mediates Lys63-polyubiquitination of RIP2 and is a necessary signaling component involved with the activation of Nod2-dependent NF- κ B signaling pathway [10].

1.2 The emerging roles of Pellino in other signaling pathways

Recent gene targeting studies in mice have revealed new roles for Pellinos in the modulation of two processes outside the context of innate immune signaling: T-cell receptor (TCR) and tumor necrosis factor- α (TNF) signaling pathways (summarized in Figure 1.1B and C).

1.2.1. The role of Pellino1 in TCR signaling

Unlike Pellino2 and 3, Pellino1 is highly expressed in B- and T-cells. Upon further investigation of Pellino1's unique presence in B- and T-cells, it was discovered that Pellino1 surprisingly plays a role in maintaining proper T-cell activation [25]. T-cell activation is tightly controlled by the T-cell antigen receptor (TCR) and co-stimulatory receptors such as CD28 [26]. The stimulation of TCR/CD28 ultimately leads to the robust activation of NF- κ B [27]. While Pellino1 up-regulates NF- κ B signaling in TRIF-dependent TLR3/4 signal transduction [17], Pellino1 down-regulates NF- κ B signaling during TCR stimulation [25]. Pellino1 carries out this functional role by targeting cRel, a NF- κ B family member that is a critical mediator of T-cell activation [25]. Peli1 appears to facilitate the Lys48-linked polyubiquitination of cRel, which marks activated cRel for proteasomal degradation [25]. The inhibitory function of Pellino1 on T-cell activation is therefore crucial for maintaining self-tolerance and the suppression of autoimmunity.

1.2.2. The role of Pellino3 in TNF signaling

TNF is a pro-inflammatory cytokine responsible for mediating inflammation and apoptosis [15]. The interaction of TNF with its cognate receptor TNFR1 stimulates the trimerization of the receptor and subsequently the recruitment of a membrane-associated complex known as Complex I [15]. Complex I is made up of the adaptor protein TNFR1-associated death domain (TRADD), RIP1 and several ubiquitin E3 ligases, including TNFR-associated factor 2 (TRAF2), and cellular inhibitor of apoptosis proteins (cIAPs) 1 and 2 [15]. The formation of Complex I leads to the Lys63-linked polyubiquitination of RIP1, which ultimately activates NF- κ B and prevents cell

death [15]. Within 10-15 minutes after TNF stimulation, deubiquitylation enzymes A20 and cylindromatosis (CYLD) can remove Lys63-linked ubiquitin from RIP1 [15]. This process is known as ubiquitin editing, which is loosely defined as the replacement of polyubiquitination chains for different polyubiquitination chains that signal the target protein for alternative functional outcomes [3]. The ubiquitin editing of RIP1 leaves RIP1 unable to activate NF- κ B and associate with TNFR1 [15]. This then leads to the formation of the pro-apoptotic Complex II (also known as death-inducing signaling complex, DISC), which includes the adaptor FAS-associated death domain protein (FADD), caspase 8 and RIP1 [15]. Complex II formation triggers the activation of caspase 8, which subsequently initiates a downstream caspase cascade that ultimately leads to cell-death [15]. Activated caspase8 can also cleave RIP1 –further dampening the NF- κ B signaling pathway and augmenting pro-apoptotic signals [15].

While Pellino1 mediates RIP1 ubiquitination downstream of TLR3/4-activation [17], Pellino3 regulates RIP1, but in the context of TNFR1-activation [28]. In a TNF-dependent manner, Pellino3 interacts with RIP1 to impede the formation of Complex II and limit caspase 8-mediated cleavage of RIP1 [28]. By contrast, Pellino3 does not interact with RIP1 in Complex I, suggesting that Pellino3 does not regulate TNF-mediated NF- κ B activation [28]. Thus, Pellino3 is only responsible for down-regulating the pro-apoptotic affects of RIP1 activation in TNF-signaling [28].

1.3. Pellinos' relevance to inflammatory diseases

Links between individual Pellinos and the pathogenesis of specific inflammatory diseases have also been established. Pellino1 is a critical mediator of microglia activation and contributes to the onset of the mouse model for multiple sclerosis, autoimmune encephalomyelitis (EAE) [29]. Pellino3 deficiency enhances the pathogenesis of experimental murine models of colitis; this correlates with the lower Pellino3 expression levels that are consistently seen in colon samples from Crohn's disease patients [10]. Gaining insight into how Pellinos specifically regulate a variety

of immune signaling pathways will therefore also provide a better understanding of the molecular basis of these inflammatory diseases.

1.4. Pellino substrate specificity

1.4.1. Pellino substrate binding domain contains a non-canonical FHA domain

Previous structural studies of the human Pellino2 substrate-recognition domain revealed an unexpected, non-canonical example of a forkhead-associated (FHA) domain (Figure 1.2) [30]. The FHA domain is a well-characterized protein interaction module that binds to phosphorylated threonine (pT) in the context of a specific recognition sequence [31-35]. Sequence analysis was not able to predict the presence of an FHA domain in Pellino because its canonical FHA eleven-stranded β -sandwich contains two long insertions that form six additional β -strands [30] (Figure 1.2). These six β -strands form an adjacent subdomain or “wing” appendage that is not seen in any other FHA domain structures (see Figure 1.2). Despite the presence of the wing appendage, mutational analysis of the Pellino2 FHA domain suggests that Pellino2 association with IRAK1 is mediated by Pellino FHA domain recognition of specific pT-peptide sequences on IRAK1 ([30] and further described in detail in Chapter 2). The high sequence identity amongst the Pellinos suggests that all Pellinos contain FHA domains (Figure 1.3). The identification that Pellinos contain FHA domains provides the molecular basis for the IL-1 and TLR ligand-inducible nature of the Pellino:IRAK1 interaction [36,37] and its dependence on the phosphorylation of IRAK1 [11,38].

The discovery that all Pellinos possess a phospho-binding domain highlights the crosstalk that occurs between phosphorylation and ubiquitination events that are crucial for coordinating various cellular processes. Other FHA-RING E3 ubiquitin ligases include RING finger 8 (RNF8) and Checkpoint with FHA and RING (Chfr), which both serve as cell-cycle checkpoint proteins [39]. Phosphorylation-dependent ubiquitination of target proteins is a common theme in the kinase-mediated activation of NF- κ B [40]. In addition to Pellinos, Skp1-

Cullin-F-box (SCF) complex E3 ubiquitin ligases also contain phospho-binding modules (such as WD40 repeats) that coordinate ubiquitination of substrates upon TLR-stimulation [40,41].

1.4.2. The Pellino FHA domain is important for immune signaling and cell death

Studies suggest that Pellino substrate interactions involved in other signaling pathways are regulated in a similar manner as the Pellino-IRAK1 association. Pellino3 variants with mutations in the FHA-domain pT-peptide binding pocket disrupt both Pellino3-dependent Nod2 and TNF signaling events [10,28]. Intriguingly, while both the Pellino3 FHA domain and RING domains are necessary for proper Nod2 signaling, the Pellino3-mediated regulation of TNF signaling is only dependent on the Pellino3 FHA domain [28]; this implicates that the catalytic activity of Pellino3 is dispensable for mediating pro-apoptotic events.

Viruses have evolved a variety of strategies to target and suppress the host immune system. Interestingly, the *Melanoplus sanguinipes* entomopoxvirus genome contains an open reading frame that encodes a viral homolog of Pellino. Viral Pellino is predicted to form a canonical FHA domain without the wing appendage or RING domain [42]. This viral Pellino is capable of interacting with IRAK1 and can compete with mammalian Pellino3 for IRAK1 association [42]. Furthermore, viral Pellino is able to inhibit Toll and TLR signal transduction in *Drosophila* S2 cells and HEK293-TLR4 cells, respectively [42]; this suggests that viral Pellino has the ability to inhibit host immune responses. The fact that there exists a viral Pellino that can hijack the TLR signaling pathway suggests that Pellinos are indeed important mediators of immune signaling.

Clearly, Pellinos have non-redundant and contrasting roles in regulating immune receptor signaling and apoptosis. To mediate these various functions, Pellinos interact with a diverse set of substrates. However, little is known about how individual members of this highly conserved family of E3 ubiquitin ligases [43] selectively act upon components within the TLR, Nod2, TCR, and TNFR1 signaling pathways. In this investigation, we elucidate the molecular basis of Pellino

substrate specificity in order to gain a better understanding of the roles that individual Pellinos play in orchestrating inflammation and cell death.

Figure 1.1. Pellino-mediated signaling events downstream of IL-1R/TLR, Nod2, TCR and TNFR1 activation.

(A) The Toll/IL-1R (TIR) superfamily comprises of the TLRs (TLRs 1-10 in humans) and IL-1R. Each TIR member contains a cytoplasmic TIR domain that maintains homotypic interactions with adaptor proteins that also contain TIR domains. Upon receptor stimulation, IL-1R and all TLRs, except for TLR3, can interact with the adaptor protein myeloid differentiation factor 88 (MyD88) to recruit and activate the family of interleukin-1 receptor (IL-1R) associated kinases (IRAKs). Recruited IRAKs subsequently trigger downstream signaling networks that lead to the activation of NF- κ B, and IRF7. TLR3 and also TLR4 alternatively recruit the adaptor molecule TRIF (TIR-domain-containing adaptor-inducing interferon-BETA), which targets TANK-binding kinase 1 (TBK1) and RIP1 (receptor-interacting S/T-protein kinase) in order to activate NF- κ B and IRF3/7, and MAPK signaling pathways. Pellinos play a crucial role in directing polyubiquitination events immediately following TLR/IL-1R stimulation. For example, Pellino2 is implicated in the IL-1-dependent K63-linked polyubiquitination of IRAK1, which is a requirement for the activation of inhibitor of κ B kinase (IKK) complex. By contrast, Pellino1 and Pellino3 are dispensable for NF- κ B activation in IL-1R signaling. Instead, Pellino1 mediates RIP1 polyubiquitination, which is required for NF- κ B activation in TRIF-dependent TLR 3/4 signaling pathways. In addition, Pellino1 E3 ligase activity is critical for the activation of type I interferon expression in the same TRIF-dependent signaling pathways, although Pellino1-mediated RIP1 polyubiquitination is not required for this process. On the other hand, Pellino3 does not activate TLR3/4-mediated NF- κ B signaling, but instead modulates TLR3-mediated IRF7 activation. Upon TLR3 stimulation, Pellino3 interacts with and polyubiquitinates the E3 ubiquitin ligase tumor necrosis factor receptor associated factor 6 (TRAF6); this modification prevents TRAF6 association with IRF7, which ultimately suppresses the TLR3-induction of type I interferon expression. The cytoplasmic Nod-like receptors (Nod1 and 2) contain caspase-recruitment domains (CARDs) that directly make homotypic interactions with their cognate CARD-containing kinase, RIP2. Upon ligand-stimulation of Nod-like receptors, activated RIP2 interacts with transforming-growth-factor- β -activated kinase 1 (TAK1) complex, which ultimately leads to the stimulation of signaling pathways similar to TLR signaling. Pellino3 is implicated to be the E3 ligase that mediates Lys63-polyubiquitination of RIP2 and is a necessary signaling component involved with the activation of Nod2-dependent NF- κ B signaling pathway. (B) Pellino1 is critical for maintaining proper T-cell activation. T-cell activation is tightly controlled by the T-cell antigen receptor (TCR) and co-stimulatory receptors such as CD28. The stimulation of TCR/CD28 ultimately leads to the robust activation of NF- κ B. Pellino1 down-regulates NF- κ B signaling during TCR stimulation by targeting cRel, a NF- κ B family member. Peli1 facilitates the Lys48-linked polyubiquitination of cRel, which marks activated cRel for proteasomal degradation. (C) TNF is a pro-inflammatory cytokine responsible for mediating inflammation and apoptosis. The interaction of TNF with its cognate receptor TNFR1 stimulates the trimerization of the receptor and subsequently the recruitment of a membrane-associated complex known as Complex I. Complex I is made up of the adaptor protein TNFR1-associated death domain (TRADD), RIP1 and several ubiquitin E3 ligases, including TNFR-associated factor 2 (TRAF2), and cellular inhibitor of apoptosis proteins (cIAPs) 1 and 2. Complex I formation leads to the Lys63-linked polyubiquitination of RIP1, which ultimately activates NF- κ B and prevents cell death. Within 10-15 minutes after TNF stimulation, deubiquitylation enzymes A20 and cylindromatosis (CYLD) can remove Lys63-linked ubiquitin from RIP1. The ubiquitin editing of RIP1 leaves RIP1 unable to activate NF- κ B and associate with TNFR1. This then leads to the formation of the pro-apoptotic Complex II, which includes the adaptor FAS-associated death domain protein (FADD), caspase 8 and RIP1 [15]. Complex II formation triggers the activation of caspase 8, which subsequently initiates a downstream caspase cascade that ultimately leads to cell-death. In a TNF-dependent manner, Pellino3 interacts with RIP1 to impede the formation of Complex II and limit caspase 8-mediated cleavage of RIP1.

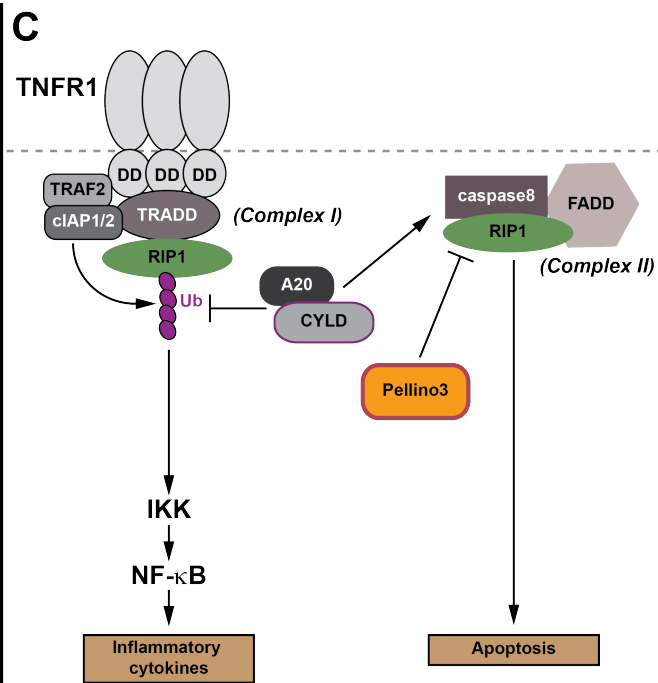
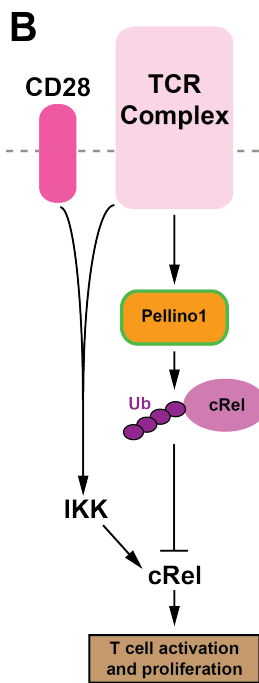
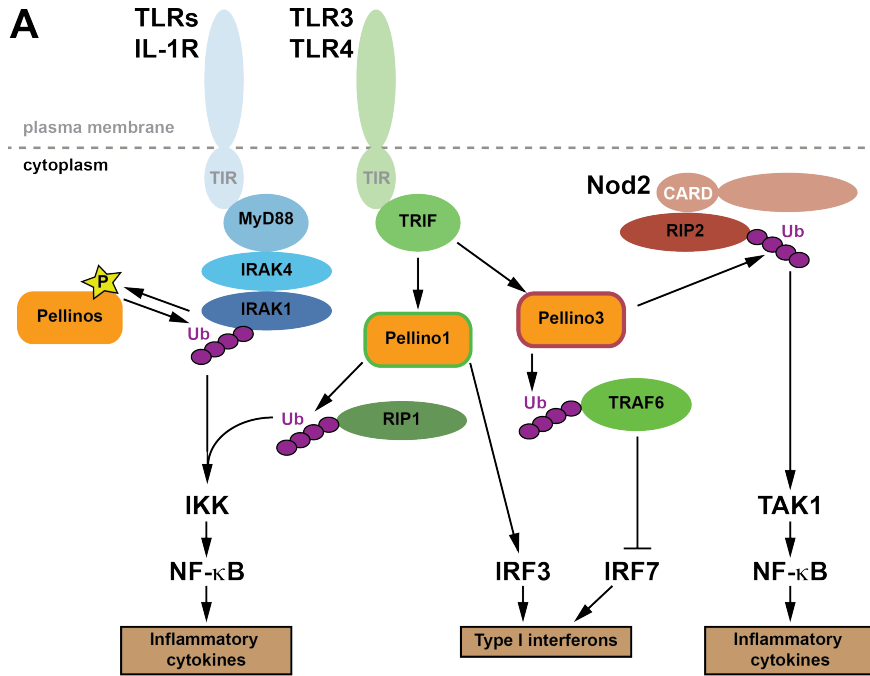
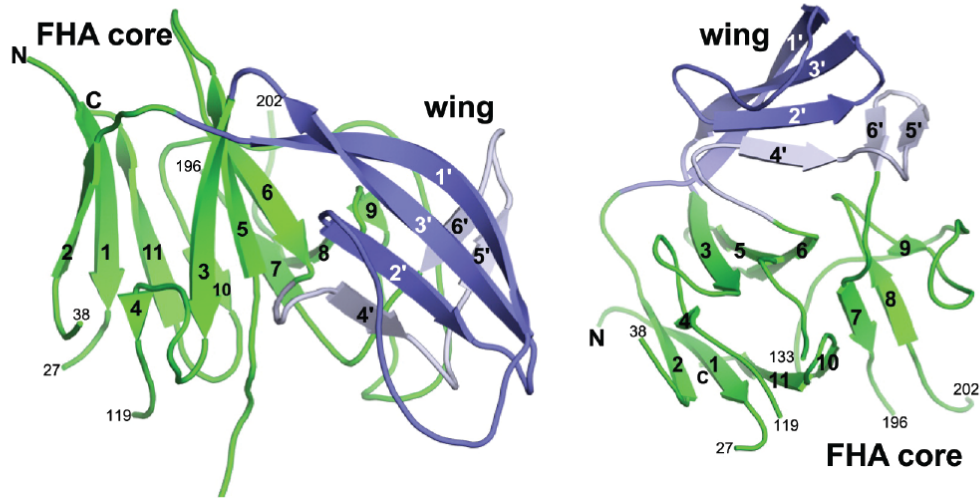


Figure 1.2. The Pellino2 substrate binding domain is a non-canonical FHA domain.

(A) Cartoon representations of the Pellino2 substrate binding domain structure. The canonical FHA core is colored green and the two insertions within the FHA core are highlighted in blue (amino acids 51-98 and 159-184 in dark and light blue, respectively). β -strands of the FHA core are numbered 1-11, while those of the wing are numbered 1'-6'. The N- and C-termini are labeled, as are the amino acids numbers at the beginning and end of each missing loop. (B) Schematic representation of the full-length Pellino2 domain architecture. This figure was reproduced from [30].

A



B

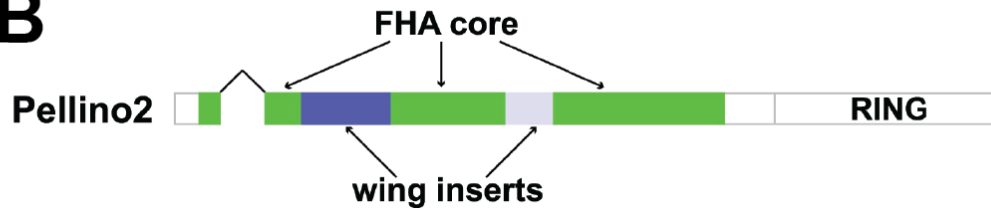
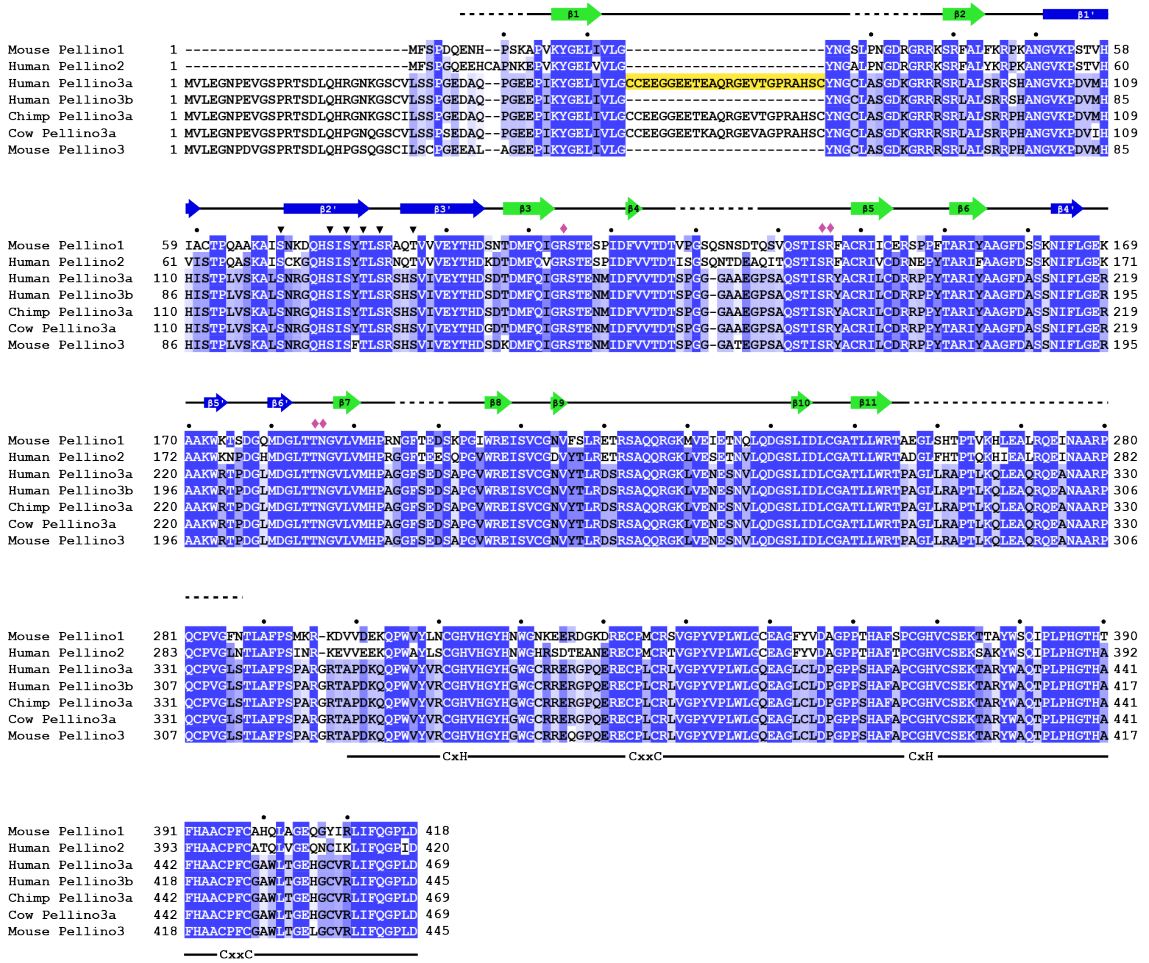


Figure 1.3. Sequence alignment of select mammalian Pellinos

A sequence alignment of mouse Pellino1 and 3, human Pellino2, 3a and 3b plus two representative examples of Pellino3a isoforms from other organisms (chimpanzee and cow). Sequences were aligned using Jalview 2.8 [44]. Shading represents percent sequence identity with the darkest blue indicating greatest sequence identity. Dots immediately above the sequence refer to every 10th amino acid of Pellino1. The 24 amino acid insert in human Pellino3a is highlighted in yellow. Structural information from Pellino2-FHA (PDB ID: 3EGA) is shown above the sequence. Arrows representing the position of the β -strands are colored in green for those in the FHA core and blue for those in the wing appendage. Dotted lines indicate the amino acids that are disordered in the Pellino2-FHA structure. The location of the RING motif is indicated under the sequences. The magenta diamonds mark the conserved residues in the Pellino FHA pT-peptide binding pockets. The black triangles mark sites of phosphorylation on Pellino1 associated with enhanced E3 ligase activity [45].



2. The Pellino FHA-like domain pT-peptide binding pocket mediates specific interaction with IRAK1

Parts of this chapter were adapted from [46].

2.1. Mutations in Pellino pT peptide binding pocket disrupts Pellino association with IRAK1

Various structural studies of FHA domains in complex with their cognate phosphopeptide ligands have elucidated how FHA domains specifically recognize their ligands. For example, the X-ray crystal structure of Rad53p-FHA1:Rad9p-peptide reveals that FHA-peptide binding is mediated by three loops at one end of the 11-stranded β -sandwich [32]. Five of the six highly conserved residues (G69, R70, S85, H88, and N107 in Rad53p) of the FHA domain family are located around the peptide-binding site. These residues make important interactions with the pT and peptide backbone, and maintain the structural integrity of the pT-peptide binding pocket. Alanine substitution of the analogous amino acids in this region of Pellino2 (such as R106 and T187/N188, highlighted in Figure 2.1A) abolish interaction with phosphorylated IRAK1 (pIRAK1) [30]. This demonstrates that the FHA domain pT-peptide binding pocket is well conserved in Pellino2. Pellinos share a high degree of sequence conservation (>70% sequence identity amongst the human Pellinos) and all are predicted to contain the non-canonical FHA domain, which includes the phosphothreonine binding pocket. R104A in Pellino1 and R131A in Pellino3b (mutations analogous to Pellino2 R106A) also ablate pIRAK1 binding (Figure 2.1B); these results confirm that the pT-peptide binding site is critical for interaction of all mammalian Pellinos with pIRAK1.

Pellino3a has previously been shown to be unable to associate with pIRAK1 in a pull-down assay [30]. Pellino3a differs from Pellino3b only in the presence of a glutamate-rich 24 amino acid insertion (Figure 2.1C). This insertion is predicted to lie adjacent to the FHA domain pT-peptide binding site (Figure 2.1A) and may occlude the binding pocket or compete for

substrate binding as a phosphomimetic motif. A Pellino3a variant lacking the central 7 amino acids of the insert (Pellino3a Δ 60-67) is unable to bind pIRAK1 (Figure 2.1D), whereas a Pellino3a variant with alanine substituted at all 6 glutamates in the insertion (Pellino3a E54-66A) gains the ability to interact with pIRAK1 almost to the extent observed for Pellino3b (Figure 2.1D). These observations argue against simple occlusion of the pT-peptide binding site. Rather, we suggest that the glutamates in the Pellino3a specific insertion mimic phosphorylated residues, bind to the pT-peptide binding pocket, and block pIRAK1 binding. In sum, these experiments affirm that the Pellino pT-peptide binding pocket is critical for mediating interaction with pIRAK1.

2.2. Far western analysis of Pellino2:IRAK1 interaction

A caveat of using lysates in our pull-downs is that we cannot tell whether Pellinos are directly interacting with IRAK1 or whether there is a bridging protein that mediates the Pellino-IRAK1 interaction. Furthermore, since our pull-down assays are only able to detect Xpress-tagged proteins that interact with Pellinos, our assays cannot distinguish whether Pellinos are able to discriminate between phosphothreonines on other proteins and specific phosphorylation sites on IRAK1. We used far western analysis to determine if Pellinos can directly target IRAK1 that has been transiently overexpressed in HEK293T cells. Complementary to western blotting, far western analysis can detect specific protein-protein interactions, but with a non-antibody probe – in our case, Pellino2. As seen in Figure 2.2, Pellino2 specifically detects IRAK1, despite the presence of multiple proteins with phosphothreonines (as detected by the α -pT western blot; Figure 2.2, 2nd left panel). By contrast, when using Pellino2 R106A variant as a probe, there is no detection of IRAK1 on the far western blot (Figure 2.2, far right panel). We conclude from these results that Pellino2 interacts directly with IRAK1 and not with any other phosphorylated protein in HEK293T cells.

2.3. Pellino2 FHA domain can interact with Rad9p-derived peptide

FHA domains can bind phosphothreonine-containing peptides, and typically show selectivity for phosphothreonine in a particular sequence context [47]. To determine whether the Pellino FHA-like domain shares this property, we investigated Pellino2's ability to bind phosphothreonine-containing peptides. We first analyzed binding to a phosphopeptide based on amino acids 188–196 of the Rad9 sequence (where T192 is phosphorylated). This peptide (Rad9pT192) has been shown to bind to Rad53-FHA1 [32,48] and EmbR-FHA [49]. As shown in Figure 2.3A, the Rad9pT192 peptide can also interact with Pellino2 in the context of a bead pull-down assay. The R106A mutation, which abolished IRAK1 binding by Pellino2, also prevents it from binding the Rad9pT192 peptide. Moreover, an unphosphorylated control peptide with the same sequence (Rad9T192) does not interact with Pellino2 –demonstrating this interaction is phosphorylation dependent (Figure 2.3A). Together, these data strongly suggest that the Pellino FHA core resembles other FHA domains in its ability to recognize phosphothreonine-containing sequences; furthermore, this mode of interaction is likely to contribute to recognition of phosphorylated IRAK1 by Pellinos.

There are no threonines in IRAK1 that are in a sequence context that resembles Rad9pT192. We tested binding of Pellinos to a series of phosphopeptides based on IRAK1 phosphorylation sites that have been reported in the literature [50,51] or that are predicted by NetPhos 2.0 [52] (Figure 2.3B-D and summarized in Table 2.1). None of these peptides interacts with Pellino2 in the qualitative bead pull-down assay (Figure 2.3B). While we found that Pellino1 and 3b can interact with the Rad9pT192 peptide, we could not detect interaction with any of the IRAK1-derived peptides (Figure 2.3C). In addition, the Pellino2 construct with only the FHA-like domain (Pellino2-FHA, residues 15-275) has the same binding preferences as full-length Pellino2 (Figure 2.3D). This suggests that the Pellino FHA-like domain is able to discriminate between the Rad9pT192 peptide and these IRAK1-derived peptides; therefore, Pellinos are able to recognize pT in a local sequence context.

One limitation to our peptide pull-down assay is that peptides need to be amine coupled to agarose beads. Since the amine coupling efficiency is dependent on the pI of the individual peptide, we could not ensure that equal amounts of individual peptides were coupled to the agarose beads. Thus, identifying interactions with certain pT-peptides may only occur within a narrow detection range. For investigating the determinants of Pellino pT-peptide specificity along with the identification of a cognate Pellino binding motif on IRAK1, we used a quantitative fluorescence polarization peptide binding assay (see Chapter 3).

2.4. Pellino2 can protect IRAK1 from threonine dephosphorylation

Previous Pellino2 pull-downs of calf intestinal phosphatase (CIP)-treated IRAK1 show that the removal of IRAK1 phosphorylation sites disrupts Pellino2 association and therefore, this association is phosphorylation dependent [30]. Our peptide binding assays now suggest that not only is the Pellino2:IRAK1 interaction phosphorylation dependent, this interaction relies upon Pellino2 recognition of specific phosphorylation sites on IRAK1. Corroborating with this result, when we treated IRAK1 with Antarctic phosphatase (AP) in the presence of excess Pellino2, we find that IRAK1 is not fully dephosphorylated (indicated by the lack of the lower band of the doublet seen in the AP-only lane; Figure 2.4, top panel). Even in the presence of Pellino2, AP-treatment increases the mobility of IRAK1, which suggests that there are phosphorylation sites that are not protected from dephosphorylation. Thus, we conclude that Pellino2 does not bind to all phosphorylation sites on IRAK1; rather, Pellino2 recognizes and binds to specific IRAK1 phosphorylation sites.

2.5. Mutation in the Pellino pT-peptide binding pocket disrupts IRAK1 polyubiquitination

Pellino association with substrate is a prerequisite for the ubiquitination of substrate. Thus, we presumed that mutations that disrupt substrate binding should also disrupt substrate ubiquitination. To test this, we transiently expressed Pellino2 and IRAK1 in HEK293T and

detected for polyubiquitination of IRAK1. Indeed, when Pellino2 and IRAK1 are transiently co-expressed, there is robust polyubiquitination of IRAK1 (Figure 2.5); by contrast, no polyubiquitination of IRAK1 is detected in the presence of the Pellino2 R106A variant. Interestingly, we find that when co-expressed with IRAK1, Pellino2 acquires post-translational modifications, as demonstrated in the mobility shift on the α -Xpress blot (Figure 2.5, lower panel). Since IRAK1 has been shown to phosphorylate Pellinos *in vitro* [13,45], we speculate that Pellino2 is phosphorylated by IRAK1. As expected, these modifications are also not detected on Pellino2 R106A.

Figure 2.1. The Pellino FHA domain phosphothreonine-peptide binding pocket is essential for interaction with IRAK1.

(A) Cartoon representation of the Pellino2-FHA structure (PDB ID: 3ega) looking onto the face of the pT-peptide binding pocket. The canonical FHA domain and the FHA wing are colored in green and blue, respectively. Highlighted in magenta are the highly conserved residues that are crucial for binding to phosphorylated peptides and proteins. Dashed lines represent the location and length of 2 disordered loops within the FHA domain. For Pellino3a, an additional 24 amino acids are predicted to be inserted within disordered loop 1. (B) Substitution of alanine at a key arginine in the FHA domain phosphothreonine (pT) binding pocket of Pellino1, 2, and 3b ablates IRAK1 interaction. (C) Sequence alignment of the β 1- β 2 region of the 4 Pellinos used in this study. The 24-residue, glutamate-rich insert unique to Pellino3a is highlighted. The β -strands 1 and 2 from the Pellino2 FHA domain structure (PDB ID: 3ega) are shown above the sequences. Starting from the residue 30 of Pellino3a, dots above the sequences indicate every 10th amino acids. Dashed lines represent disordered regions of Pellino2. (D) Pellino3a and a Pellino3a variant with a truncation in the glutamate-rich insert (Pellino3a Δ 60-67) do not interact with IRAK1. Substitution of alanine at every glutamate in the Pellino3a insertion confers IRAK1 binding property to Pellino3a. For (B) and (D), the indicated GST-fusions of Pellinos were incubated with HEK293T lysates that contained overexpressed Xpress-tagged IRAK1. Following washing, bound proteins were eluted by denaturation, analyzed by SDS-PAGE, and visualized by western analysis with α -Xpress to detect IRAK1, and Coomassie blue staining to detect the GST-fusion proteins. "In" indicates 4% of lysate. Positions of molecular mass markers are shown.

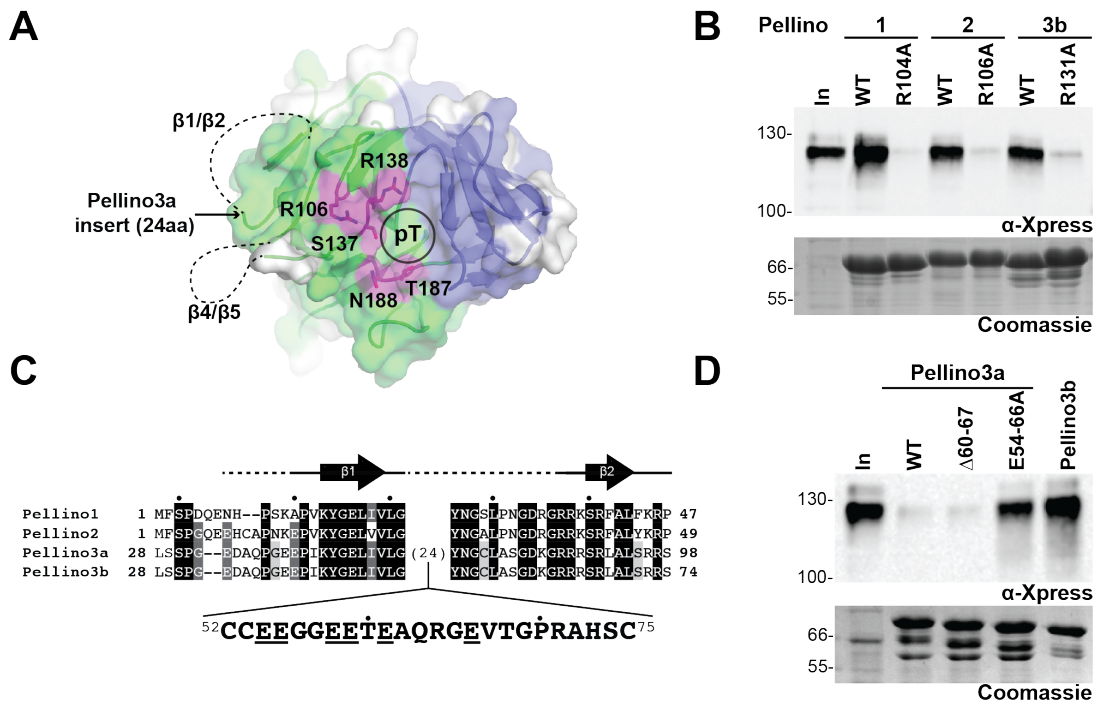


Figure 2.2. Far western analysis of Pellino2:IRAK1 interaction.

HEK293T lysates containing transiently expressed FLAG-IRAK1 was separated on SDS-PAGE and immobilized onto nitrocellulose membranes. Western blots were probed with α -FLAG, α -pT, α -His. Far western (FW) blots were probed with purified His₆-Pellino2 wild-type or R106A variant, then immunoblotted for α -His. While many bands appear on the α -pT blot, His₆-Pellino2, but not the R106A variant, only interacts robustly with IRAK1. Triangles represent increasing amounts of HEK293T lysates loaded on SDS-PAGE gels.

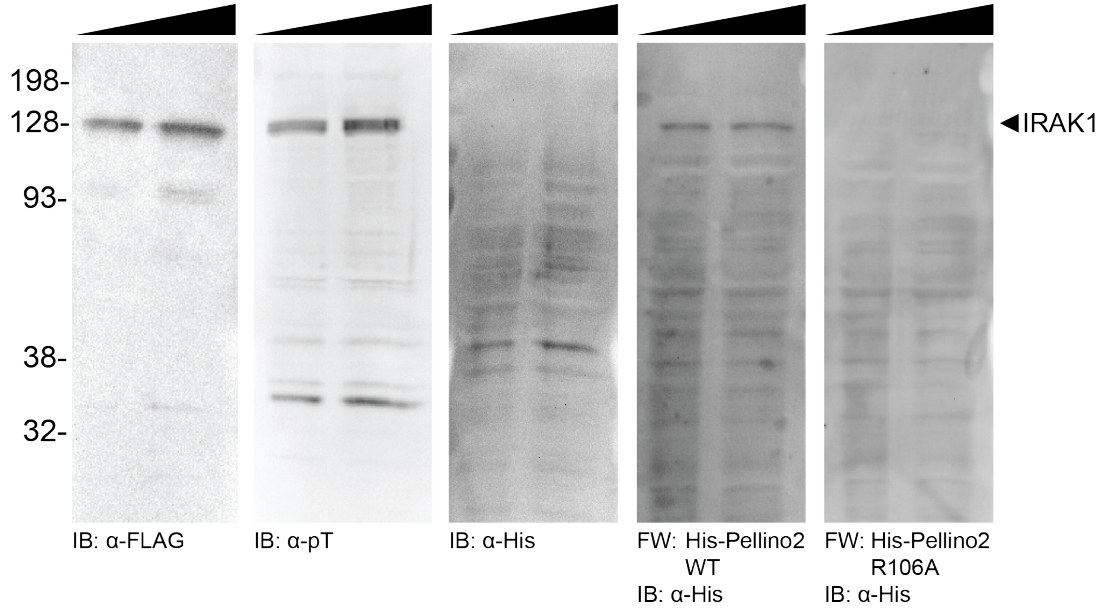


Figure 2.3. Pellinos specifically interact with Rad9pT192 peptide.

For A-D, peptides amine-coupled to agarose beads were incubated with purified Pellinos 1, 2, 2^{R106A}, 2-FHA, and 3b. Pellinos were then eluted by denaturation, analyzed by 12.5% SDS-PAGE and detected with Coomassie blue reagent. (A) Pellino2 interacts with the Rad9pT192 peptide, but not the unphosphorylated Rad9T192 peptide. The Pellino2 R106A variant, which does not interact with IRAK1 (Figure 2.1A), also does not interact with the Rad9-derived peptides. (B) Pellino2 does not interact with any of the IRAK1-derived peptides that were tested. (C) Like Pellino2, Pellinos 1 and 3b have similar binding preferences for Rad9pT192 and IRAK1-derived peptides. (D) Pellino2-FHA has the same peptide binding preferences as Pellino2, which indicates that the FHA-like domain mediates interaction with Rad9pT192 peptide. In indicates ~1% input. FTR1 peptide is a non-phosphorylated peptide used as a negative control. The sequences of the peptides used are summarized in Table 2.1.

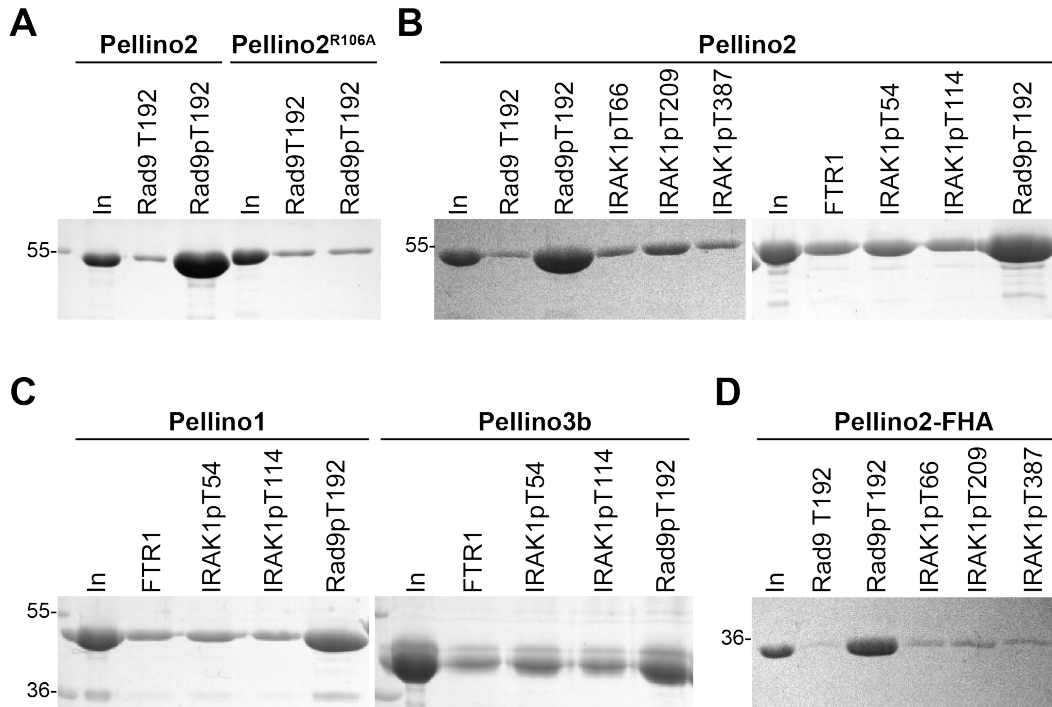


Table 2.1. Summary of phosphothreonine peptide pull-downs of Pellinos
 Peptide pull-downs were performed as described in Figure 2.3. “-“ indicates did not test.

Peptide	Peptide sequence	Interacts with Pellino1?	Interacts with Pellino2?	Interacts with Pellino3b?
IRAK1pT54	WVRDQpTELR	No	No	No
IRAK1pT66	SGQRpTASVLW	-	No	-
IRAK1pT114	WSPGTpTAPRP	No	No	No
IRAK1pT152	YPGSQpTHSES	-	No	-
IRAK1pT209	WISRGpTHNFSE	-	No	-
IRAK1pT387	TVRGpTLAY	-	No	-
Rad9 T192	WSLEV TEADT	-	No	-
Rad9pT192	WSLEVpTEADT	Yes	Yes	Yes
FTR1	GHLPF TKNLQ	No	No	No

Figure 2.4. Pellino2 can prevent complete threonine dephosphorylation of IRAK1.

HEK293T lysates containing transiently expressed Xpress-IRAK1 were incubated with or without Antarctic phosphatase (AP, 5U per reaction), and with or without Pellino2 (1 μ M). These lysates were separated on SDS-PAGE and visualized by western analysis using α -Xpress and α -pT. IRAK1 without AP or Pellino2 runs as a 125kDa band on both western blots. When treated with AP, two bands with faster mobility appear on the α -Xpress immunoblot: the slower band also appears on the α -pT blot and is therefore partially dephosphorylated (pIRAK1*); the faster migrating band is absent from the anti-pT immunoblot and therefore is presumed to be completely dephosphorylated IRAK1. When Pellino2 is added, the faster migrating band disappears – indicating specific threonines on IRAK1 are being protected from dephosphorylation.

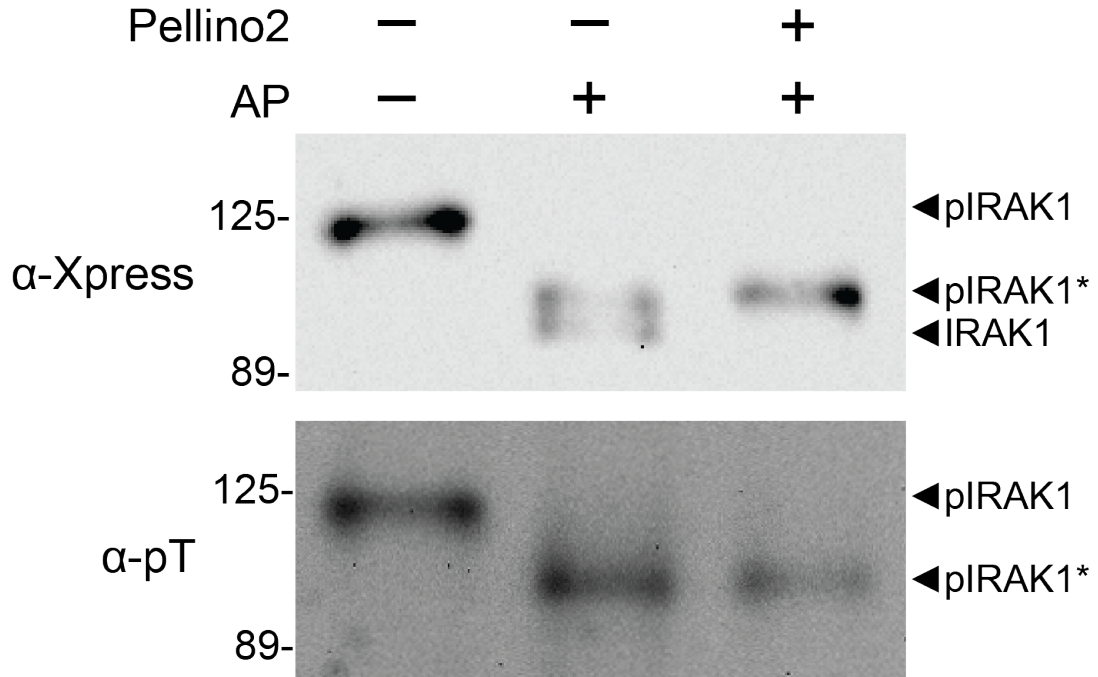
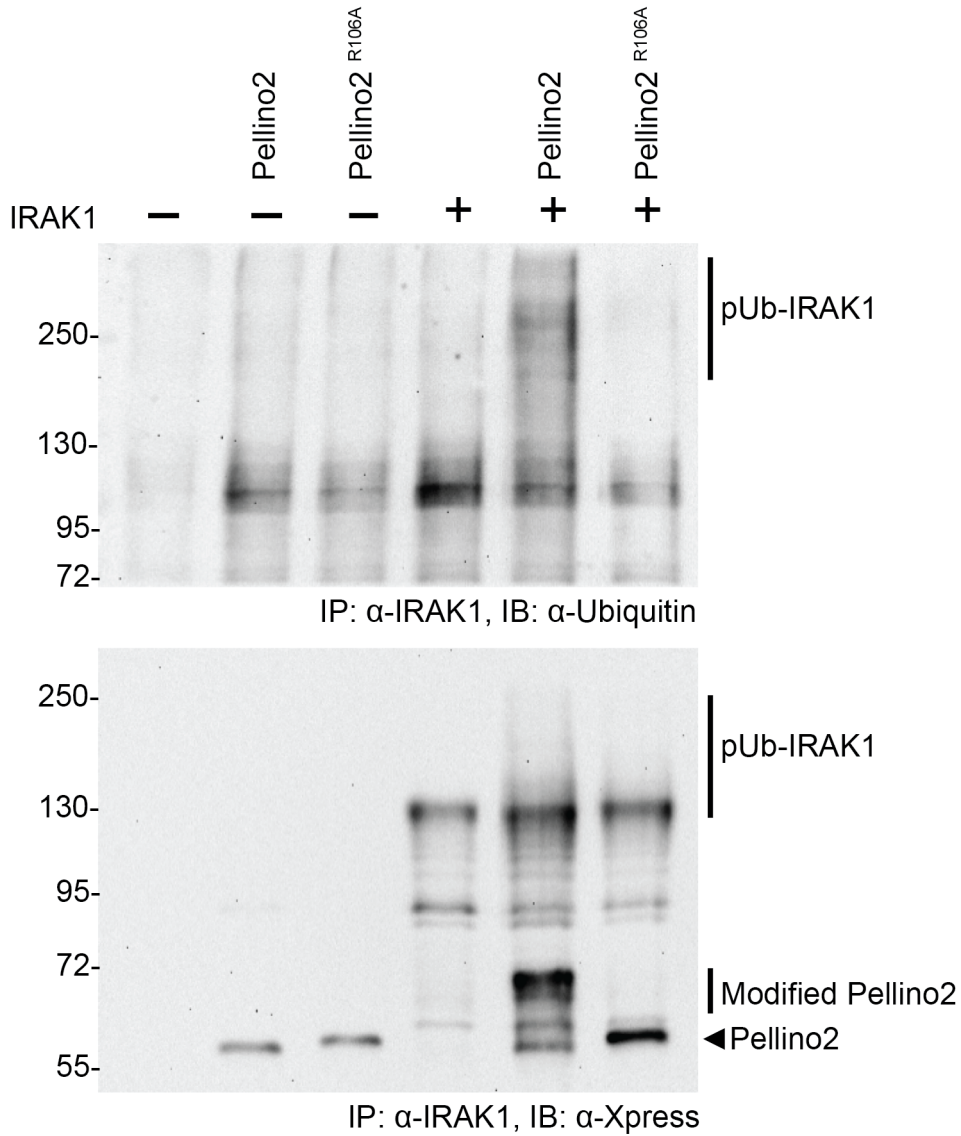


Figure 2.5 Mutation in the Pellino pT-peptide pocket disrupts IRAK1 polyubiquitination

Xpress-Pellino2 wild-type or R106A and Xpress-IRAK1 were either individually or co-transfected into HEK293T. Immunoblot analysis was performed on IRAK1 immunoprecipitated from these HEK293T lysates; α -ubiquitin was used to detect polyubiquitination of IRAK1 and α Xpress was used to detect IRAK1 and co-immunoprecipitated Pellino2. Substitution of alanine at a key conserved amino acid in the pT-binding region of the Pellino FHA core abolishes IRAK1 polyubiquitination in HEK293T cells. Furthermore, Pellino2 R106A has a mobility shift which indicates a loss of post-translational modifications.



3. The determinants of Pellino substrate specificity

Parts of this chapter were adapted from [46].

3.1. Identification of an IRAK1-derived Pellino2 binding domain

To gain additional insight into the binding determinants of Pellino2, we performed an IRAK1 truncation analysis to identify binding regions of IRAK1 that can interact with Pellino2. IRAK1 truncation variants (Figure 3.1A) were transiently overexpressed in HEK293T cells and tested for their ability to associate with GST-Pellino2 (Figure 3.1B). Deletion of the N-terminal death domain (IRAK1 Δ DD) significantly reduces the fraction of IRAK1 that binds to GST-Pellino2 –to the point where only a small proportion of the IRAK1 Δ DD input is enriched as compared to full-length IRAK1. Minimal interaction above background is observed for a truncation that also lacks the C-terminal domain (IRAK1 KDL) and for the kinase domain alone (IRAK1 KD). The trend in GST-Pellino2 pull-down of these 3 kinase domain-containing IRAK1 fragments is mirrored in the level of phosphorylation of each truncation, as assessed by anti-pT immunoblots (Figure 3.1B, middle panel).

A fragment containing only the first 197 amino acids of IRAK1 (IRAK1-197) robustly associates with Pellino2 in a phosphorylation dependent manner. At least three species of IRAK1-197 are observed on SDS-PAGE. Only the slowest migrating species contains significant phosphothreonine and is highly enriched in the GST-Pellino2 pull-down fraction (Figure 3.1B). Enzymatic dephosphorylation of IRAK1-197 results in undetectable levels of pT in this protein and abolishes interaction with GST-Pellino2 (Figure 3.1C). In addition, the Pellino2 pT-peptide binding site variant R106A does not interact with IRAK1-197 (Figure 3.1C). IRAK1-197 lacks the kinase domain and must be phosphorylated by kinases endogenous to HEK293T cells. We presume that the same endogenous kinases that are able to phosphorylate the kinase-dead IRAK1 variant (IRAK1 K239A) in IRAK1-null HEK293 cells (I1a cells) [53] can phosphorylate IRAK1-197. Finally, a truncation variant that lacks the proline/serine/threonine-rich (PST) domain and comprises only

the IRAK1 death domain (IRAK1 DD) is not phosphorylated in HEK293T cells and shows dramatically reduced binding to Pellino2 (Figure 3.1B). This suggests that the Pellino2 binding region may lie within the PST domain, or that this domain is required for appropriate phosphorylation of IRAK1-197.

Next, we sought to identify which threonine(s) in IRAK1-197 are important for interaction with Pellino2. There are 9 threonines in IRAK1-197: 5 are in the presumed unstructured PST domain and 4 in the death domain. Based on a structure-based sequence alignment with the IRAK2 death domain (PDB ID: 3mop) [54], only 3 of the 4 threonines in the IRAK1 death domain are predicted to be surface-exposed. We individually mutated to alanine each of these 8 presumed surface-exposed threonines and tested each IRAK1-197 variant for interaction with GST-Pellino2 (Figure 3.2A, B). Alanine substitutions at T54 and T141 significantly disrupt Pellino2 interaction (Figure 3.2B). In both cases, the IRAK1-197 variants show significantly reduced phosphorylation (Figure 3.2B middle panel). The phosphorylated fraction of IRAK1-197 T54A associates with Pellino2, whereas no phosphorylated IRAK1-197 T141A is pulled-down with Pellino2. This suggests that T54 in the death domain is important for phosphorylation of IRAK1-197 –perhaps through a change in structure or oligomerization. On the other hand, T141 in the PST domain is likely to represent a phosphorylation site directly recognized by Pellino2.

3.2. Pellino pT-peptide +3 motif preferences

3.2.1. Pellino2 can specifically recognize IRAK1T141-derived pT-peptide

Binding studies using synthetic phosphorylated peptides have been widely used to establish the specificity of many FHA domains [32,35,49,55,56]. To explore the specificity of Pellino2, we chose to test binding using the more stable Pellino2 truncation variant (Pellino2-FHA, residues 15-275) with fluorescently labeled phosphopeptides in a fluorescence polarization assay. A peptide comprising amino acids 137-145 of IRAK1 with a phosphothreonine at position 141 (pT141) binds to the Pellino2-FHA with a K_D value of 0.82 μ M (Figure 3.2C and Table 3.1). The

affinity for a scrambled version of pT141 is more than 100-fold weaker, and no binding is detected for the non-phosphorylated version of this peptide. These data demonstrate that high affinity binding to Pellino2 relies not only on a phosphorylated threonine, but also on the local sequence context around this moiety. In agreement with our IRAK1-197 mutational analysis, phosphothreonine-containing peptides derived from the sequences around IRAK1 T54 and T152 (pT54 and pT152) show markedly weaker affinities for the Pellino2 FHA domain than pT141 (Figure 3.2C and Table 3.1). To validate our fluorescence polarization peptide binding assay, we used isothermal titration calorimetry to measure the affinity of the Pellino2-FHA for the pT141 peptide (Figure 3.2D). We obtained a K_D value of 2.9 μM , which is reasonable when considering the differences in experimental setup and lack of multiple independent ITC experiments due to limited peptide quantities. These results further support the argument that the local sequence context around the pT is important for optimal Pellino2 binding. In addition, our studies identify the region around T141 in IRAK1 as a specific high-affinity Pellino2 recognition motif.

3.2.2. Pellino isoforms have different pT-peptide specificities

The major determinant of pT-peptide recognition for many FHA domains is the amino acid located 3 positions C-terminal to the phosphorylated threonine (+3 position) [32]. Peptide library screens performed on a diverse selection of FHA domains have identified four FHA pT-recognition motifs with different amino acids at the +3 position: pTxxD, pTxxI/L, pTxxY/M, and pTxxS/A [32]. The motif around T141 in IRAK1 falls in the last of these 4 groups with a serine at the +3 position. Henceforth, the peptide based on this IRAK1 sequence is referred to as pT141+3S. To determine whether pTxxS is the optimal Pellino2 pT-recognition motif, we analyzed binding of peptides with aspartate, isoleucine and tyrosine in place of serine at the +3 position (pT141+3D, pT141+3I and pT141+3Y, respectively) to Pellino2-FHA (Figure 3.3, Table 3.2). Pellino2-FHA binds most tightly to pT141+3Y with a K_D value 4.6 fold stronger than for pT141+3S. Aspartic acid at the +3 position is the most unfavorable binding motif with a 5-fold higher K_D value compared to pT141+3S,

whereas isoleucine at the +3 position shows a 2.6-fold higher K_D value compared to pT141+3S. These data indicate that Pellino2-FHA prefers the pTxxY binding motif 4.6-, 12-, and 23-fold compared to the pTxxS, pTxxI and pTxxD motifs, respectively (Table 3.2, Figure 3.3B).

We next asked whether the observed Pellino2 peptide binding preference is also seen for the other Pellinos. We measured binding to the same panel of fluorescently labeled peptides using Pellino1, 3a, and 3b truncations that contain only the FHA domain (amino acids 2-287, 40-305 and 2-304, respectively) (data summarized in Figure 3.3 and Table 3.2). All Pellinos bind to the original IRAK1 derived pT141+3S, which suggests that phosphorylation of T141 plays a role in association of IRAK1 with all of the Pellinos (Table 3.2). Pellino3a shows the weakest binding to pT141+3S (K_D value of 9.8 μ M), which is consistent with the lack of detectable binding between GST-Pellino3a and pIRAK1 (Figure 2.1D).

All Pellinos bind most tightly to the pT141+3Y peptide, and substantially disfavor binding to the pT141+3D motif (Table 3.2). However, differences arise in the extent to which each Pellino favors the pTxxY motif over the pTxxI and pTxxS motifs. As described above, Pellino2 clearly discriminated between all three, with the trend in K_D values of pTxxY < pTxxS < pTxxI. By contrast, Pellino1 shows minimal discrimination in binding between the peptides with tyrosine, serine and isoleucine at the +3 position (K_D values of 0.77, 1.7 and 1.8 μ M, respectively). Pellino3a and 3b, which differ only by the 24 amino acids insertion (Figure 2.1C), have very similar +3 motif preferences; although, the affinity in each case is ~2 fold weaker for Pellino3a compared to Pellino3b. Like Pellino1, the Pellino3 isoforms do not discriminate between serine and isoleucine at the +3 position. Yet unlike Pellino1, the Pellino3 isoforms do show more preference for tyrosine at the +3 position. The observed binding preferences revealed from this panel of pT-peptides suggest that each Pellino will have a distinct set of preferred substrates.

3.3. Pellinos have distinct specificities for RIP1 and TRAF6

Knockout studies in mice indicate that Pellino1 and Pellino3 have non-redundant functions in TLR signaling. These divergent functions have been attributed to differential polyubiquitination of RIP1 and TRAF6 by Pellino1 and 3, respectively [17,21]. Based on our observation that each Pellino has a different peptide binding profile, we postulated that Pellino1 selectively targets RIP1 over TRAF6, whereas Pellino3 is selective for TRAF6. We tested this hypothesis by examining the interaction of GST-Pellinos with these proteins transiently expressed in HEK293T cells. Much like IRAK1 (Figure 2.1 and 3.4A), we find that RIP1 interacts with GST-Pellino1, 2 and 3b, but not with GST-Pellino3a (Figure 3.4B). By contrast, TRAF6 does not interact with Pellino1 in this assay, whereas TRAF6 interaction is observed for Pellino2 and both isoforms of Pellino3 (Figure 3.4C). Since substrate binding is a prerequisite for substrate ubiquitination, this binding selectivity of Pellinos is likely responsible, at least in part, for their different cellular functions.

3.4. Distribution of FHA binding motifs in Pellino substrates

We next asked whether it is possible to rationalize the Pellino specificity differences observed in our simple GST-pull-down assay by using our peptide binding results and the distribution of pT+3 motifs in Pellino substrates (Tables 3.3 and 3.4) without any consideration of the *in vivo* phosphorylation state of these motifs. Pellino1 binds robustly to IRAK1 and RIP1 but not to TRAF6; this correlates with a requirement for pTxxY or pTxxS binding motifs, which are found in IRAK1 and RIP1, but not in TRAF6. These motifs are also found in cRel, another known Pellino1 substrate [25]. Pellino2 interacts more robustly with IRAK1 than with RIP1 and TRAF6; this may reflect the strong preference of Pellino2 for pTxxY motif (Figure 3.3B), which is more frequent in IRAK1 than in the other two substrates. It is hard to rationalize the binding of Pellino3a to TRAF6 and not to IRAK1 and RIP1 based on these very simple considerations. The only striking difference in the pT+3 motifs in TRAF6 is the representation of pTxxD, however the peptide

binding experiments do not suggest that Pellino3a shows any less discrimination against this motif than the other Pellinos.

3.5. Attempts to determine high resolution Pellino:phosphopeptide structure

To gain insight into the molecular basis of the different Pellino binding specificities, we sought to determine a high-resolution structure of a Pellino FHA-like domain in complex with a pT-peptide. Attempts to co-crystallize various constructs of Pellino1 and 2 with pT-peptides are summarized in Table 3.5 and Figure 3.5. In addition, pT-peptides were soaked into Pellino2-FHA crystals (see Chapter 6 for details), but crystals would immediately dissolve. Crosslinking Pellino2 crystals before pT141+3Y peptide soaks prevented crystals from dissolving, so data sets were collected on these crystals. Structures were solved by molecular replacement (MR) using PHASER [57] (see Chapter 6). There was no evidence for the peptide in the electron density maps generated with the MR phases. This is not surprising considering there are crystal contacts near the pT-peptide binding pocket that are likely impinged upon the presence of peptide (Figure 3.6).

3.6. Towards a Pellino3a-FHA structure

Since the Pellino3a glutamate-rich insertion most likely acts as a phosphomimetic peptide and occludes the FHA domain pT-peptide binding pocket, we speculated that the Pellino3a FHA-like domain structure could provide clues about pT-peptide recognition. We found that the Pellino3a-FHA construct (aa 40-305) could spontaneously crystallize (Figure 3.7A). After exhaustive screening for different crystallization conditions, we found that Pellino3a-FHA crystallized in conditions of 5-20% PEGs (400-20000 MWCO), ethylene glycol, or glycerol at very low ionic strengths and around neutral pH (Figure 3.7B for some examples). Many attempts were made to optimize these crystals (summarized in Table 3.6, and described in detail in Chapter 6) and improve X-ray diffraction (Figure 3.7C, D), but the best diffracting crystals were the ones originally

discovered to have formed spontaneously. We collected a 4.6Å data set on these Pellino3a-FHA crystals, but were not able to obtain a molecular replacement solution. Data collection statistics of Pellino3a-FHA crystals are summarized in Table 3.7.

3.7. Homology modeling of Pellinos

The peptide and substrate binding differences among the Pellinos are hard to reconcile due to their high degree of sequence identity and cannot be readily explained by the Pellino2 FHA domain crystal structure alone. Thus, we sought to perform structure-based homology modeling of the different Pellinos using SWISS-MODEL [58]. Although the residues that connect β 4 and β 5 strands (aa120-129) appear to be disordered in the crystal structure of the Pellino2 FHA domain, these residues form a short α -helix in the Pellino2 homology model (Figure 3.8A, D). Like Pellino2, the analogous residues in Pellino1 are also modeled to be a short α -helix (Figure 3.8C). However, in Pellino3a and 3b, the analogous residues are modeled to be predominantly unstructured, but with a significantly smaller α -helix compared to Pellino1 and 2 (Figure 3.8E). Interestingly, these 10 amino acids share low sequence identity (Figure 3.8B) near and are proximal to the FHA domain pT-peptide binding pocket (Figure 3.8A). The subtle structural differences predicted in these Pellino homology models may provide an explanation for the distinct phosphopeptide preferences and substrate specificities amongst the Pellinos.

3.8. Pellino substrate recognition may require more than pT-peptide recognition

The following experimental results suggest that Pellino substrate recognition may involve more than a short pT-peptide sequence.

3.8.1. Pellino2 interacts with IRAK1 mutants T54A and T141A

Despite the fact that the T54A and T141A mutations in IRAK1-197 abolish interaction with Pellino2, we found that these mutations in the context of full-length IRAK1 have no effect on

Pellino binding (Figure 3.9). This suggests that there are additional Pellino binding sites on IRAK1 that are not present on IRAK1-197. These additional binding sites could be other phosphorylation sites, as there are several threonines within 198-712 that have pTxxS/A and pTxxY motifs. In addition to multiple phosphorylation sites that Pellinos may recognize, it is possible that IRAK1 may contain non-phosphorylated determinants that enhance Pellino interaction; this could be an extension to the short peptide sequence surrounding the pT site, or additional binding sites (which may include secondary structure elements) more distal to the pT site. This has been demonstrated for the FHA-domain containing *Mycobacterium tuberculosis* FhaA, which prefers its cognate binding partner MivN over a library screen-optimized peptide due to an additional binding surface on a helix of MivN that make contacts with the FHA domain [59].

3.8.2. Pellino2 R224A disrupts interaction with IRAK1, but not pT-peptide

While the conserved amino acids in the FHA domain are responsible for mediating interaction with ligands and maintaining the structural integrity of the pT-peptide binding pocket, non-conserved amino acids in the interacting loops mediate sequence specificity for the pT+3 residue [55,56,60,61]. FHA domain structural studies also indicate that insertions between the β -strand connecting loops may attribute to the functional diversity of FHA domains [34]. The wing of the Pellino FHA-like domain is a very striking example of such insertions. Canonical FHA domains show more subtle variations such as an eight-residue helical insertion within the β 4/ β 5 loop of the human Rad53 homolog, CHK2 (check point kinase 2) FHA domain [33]. Based on the highly unusual insertions in the Pellino FHA domain, we speculated that the non-canonical features of the Pellino FHA-like domain (highlighted in Figure 3.10A-B) make additional contacts that mediate substrate recognition.

We performed a structure-based mutational analysis of conserved surface residues of the Pellino2 β 9/ β 10 loop and the unusual wing appendage that are on the same face of the pT-peptide binding pocket (Figure 3.10B). None of the mutations in the wing appendage (Q66L,

K69A, R85A, N165A) disrupted interaction with IRAK1 (Figure 3.10C). However, a substitution of alanine at R224 of the Pellino2 $\beta 9/\beta 10$ loop disrupts interaction with IRAK1 (Figure 3.10C). This mutation does not affect binding to pT-peptides (Figure 3.10D), confirming that loss of IRAK1 interaction is not due to the disruption of the structure of Pellino FHA R224A variant. This further supports the idea that Pellino substrate recognition may require protein-protein interactions additional to pT-peptide binding.

Figure 3.1. Pellino2 interacts with IRAK1-197 in a phosphorylation dependent manner.

(A) Schematic representations of IRAK1 and truncation variants indicating the amino acids of full length (FL) IRAK1 that are included in each variant generated. DD: Death domain; PST: proline/serine/threonine-rich domain; KD: kinase domain, Ct: C-terminal domain. (B) GST-Pellino2 pull down analysis of the indicated IRAK1 variants expressed in HEK-293T cells, essentially as described for Figure 1B. For each IRAK1 variant, three samples were analyzed: 4% of the HEK293 cell lysate (In), plus samples from GST alone and GST-Pellino2 pull-downs. Total Xpress-tagged protein was detected with α -Xpress antibody (upper panels). Western blots were probed with anti-phosphothreonine (α -pT) antibody (middle panel). Lower panel shows Coomassie stain to verify equal loading of GST and GST-Pellino2. IRAK1 (FL) and IRAK1-197 show robust interaction with Pellino2. IRAK1-197 migrates as several discrete bands, the range of which is indicated by a vertical line. The faster migrating species are not observed on the α -pT blot and presumed to represent unphosphorylated IRAK1-197. Expected positions of each IRAK1 variant is shown, as are positions of molecular weight markers. For clarity, the position of IRAK1 KD is indicated with a < on the left blots, since this species runs at the same position as the phosphorylated IRAK1-197. A * after the protein name indicates that this specie is detected on the α -pT blot. Non-specific interaction of α -pT with GST-Pellino2 partially obscures the IRAK1 Δ DD on this blot. (C) Pellino2-IRAK1-197 interaction is ablated when IRAK1-197 is treated with calf intestinal phosphatase (CIP) or when Pellino2 FHA domain pT-peptide binding pocket contains an alanine substitution at a key arginine (Pellino2 R106A). GST-pull downs were performed as for part B.

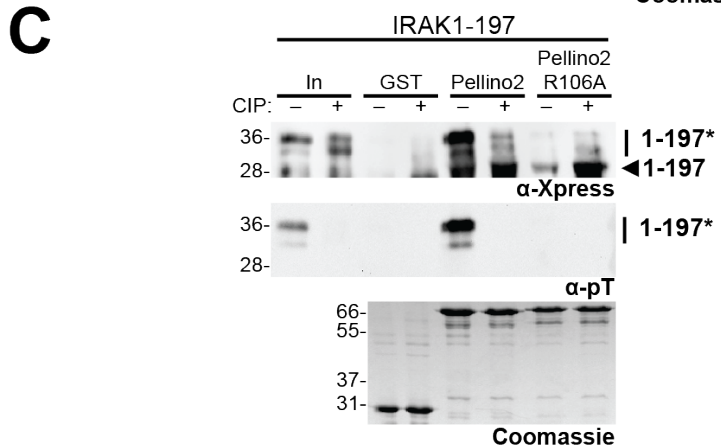
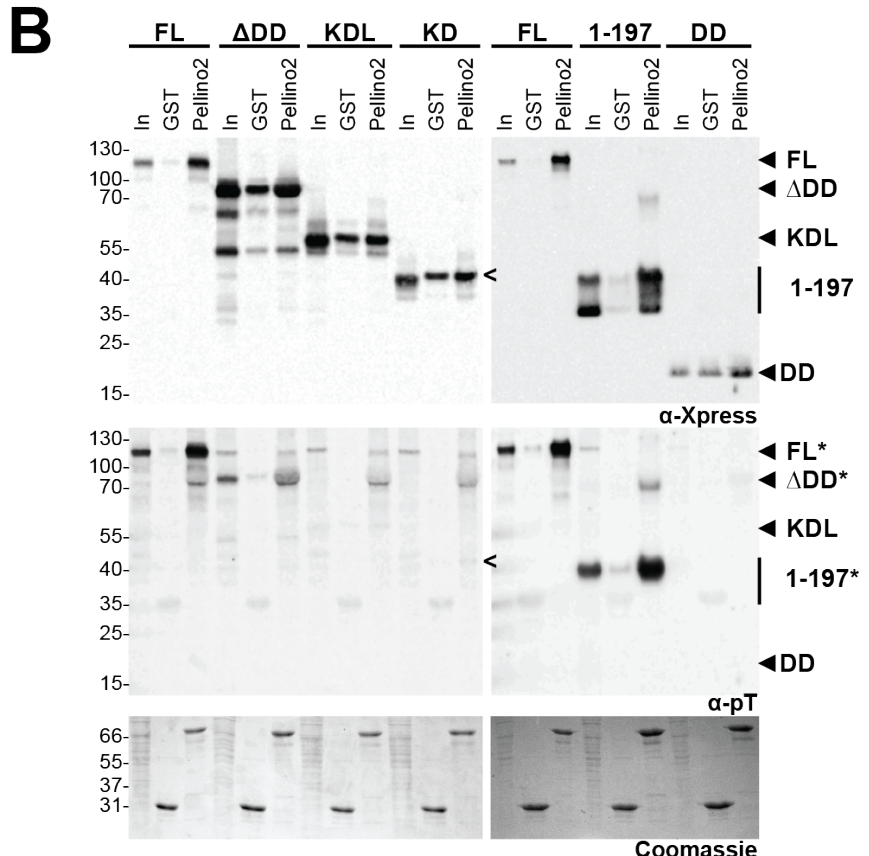
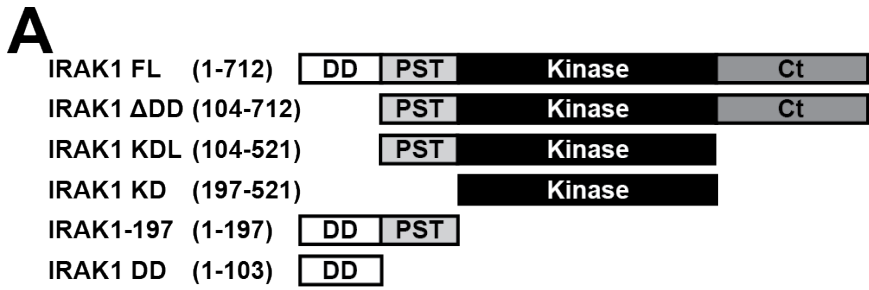


Figure 3.2. Pellino2 specifically interacts with a peptide motif around pT141 of IRAK1-197. (A-B) GST-Pellino2 was used to pull down Xpress-IRAK1-197 variants with alanine substituted at 8 different threonines. Only T54A and T141A show reduced interaction with Pellino2. (B) T54A and T141A also show reduced threonine phosphorylation. T152A is a representative example of variant that interacts with Pellino2 to the same extent as wild type IRAK1-197. Blots were generated as described in the legends to Figures 2.1 and 3.1. For A-B, a * after the protein name indicates that this specie is detected on the α -pT blot. (C) Binding of the indicated fluorescein-labeled peptides to increasing concentrations of Pellino2-FHA (Pellino2 15-275) as monitored by fluorescence polarization. A representative data is shown for each peptide. The curves indicate the fit to a simple binding isotherm for each data set shown. K_D values for at least three independent experiments are summarized in Table 3.1. (D) Binding of Pellino2-FHA to pT141+3S peptide using isothermal titration calorimetry (ITC). The top section shows the raw calorimetric data for the bottom section shows the integrated heat changes, corrected for heat of dilution, and fitted to a single-site binding model.

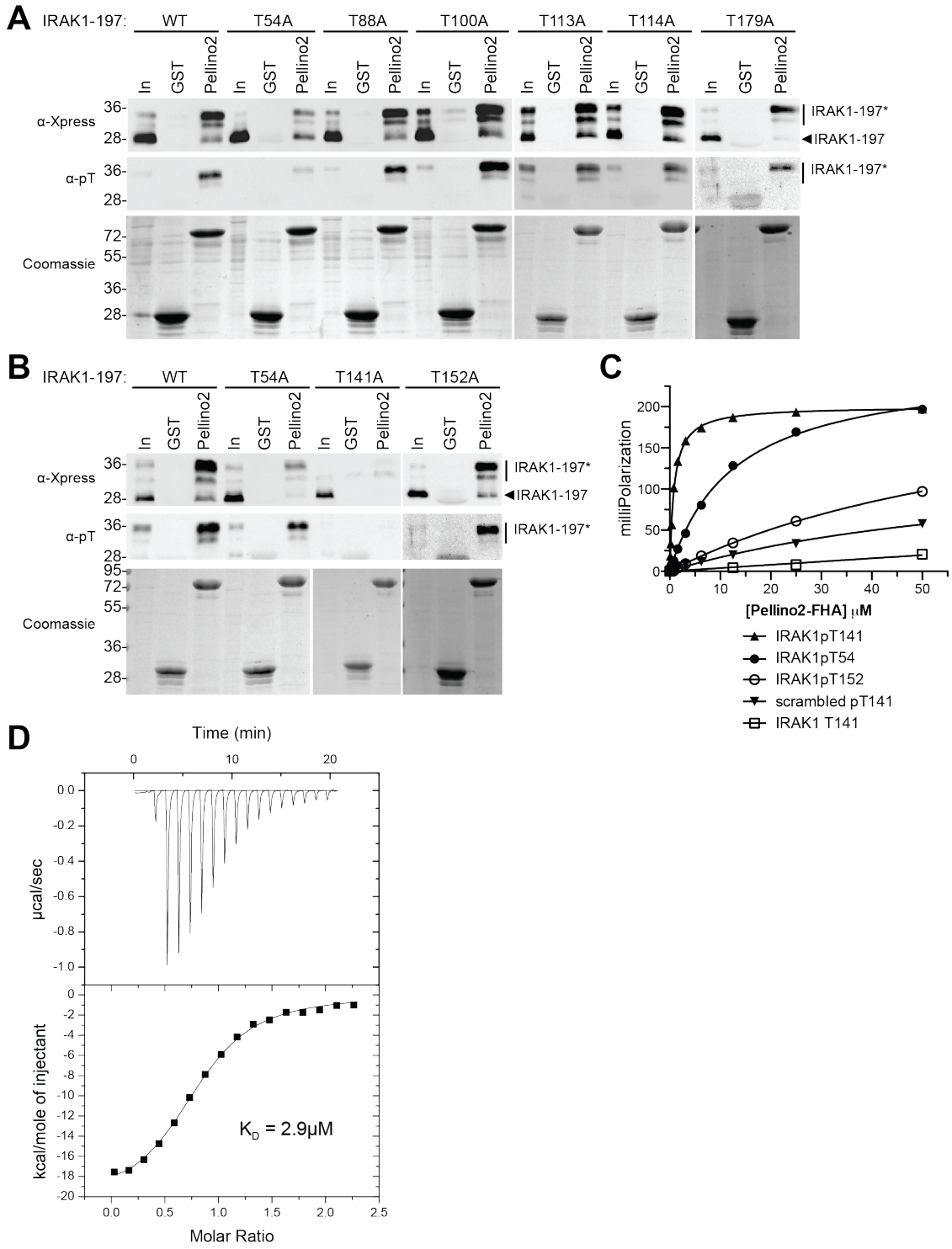


Table 3.1. Binding affinity of IRAK1-derived peptides to Pellino2-FHA domain.

The K_D values for binding of Pellino2-FHA to the indicated peptides were determined from at least three independent fluorescence polarization assays (Figure 3.2C). Baseline corrected data were fit to a simple binding equation. NB indicates no binding detected. All peptides include an N-terminal tyrosine to allow for spectroscopic quantification.

Peptide	Sequence	K_D (μM)
IRAK1T141	S-S-A-S- T-F-L-S-P	NB
IRAK1pT141	S-A-S-S-pT-F-L-S-P	0.82 ± 0.35
IRAK1pT141 scrambled	P-A-S-F-pT-S-S-L-S	> 50
IRAK1pT54	V-R-D-Q-pT-E-L-R-L	12.6 ± 1.8
IRAK1pT152	P-G-S-Q-pT-H-S-G-P	> 50

Figure 3.3. Pellinos have different phosphothreonine peptide binding specificities.

(A) The fold change in the K_D value for the binding of each Pellino to IRAKpT141 and derivative peptides relative to the binding of that Pellino to the pT141+3Y peptide (+3Y). Each Pellino binds the +3Y peptide with the highest affinity (Table 3.2), which is normalized to 1 as indicated by the dashed line. Fold change in K_D values for binding to the pT141+3D (+3D, white bars), pT141+3I (+3I, red bars) and pT141+3S (+3S, blue bars) are shown. (B) Fluorescence polarization binding assay for each Pellino with the pT141+3Y peptide, exactly as for Figure 3B. A representative data set is shown for the FHA domain of Pellino1 (red), Pellino2 (green), Pellino3a (black) and Pellino3b (blue). Curves indicate the fit to a simple binding isotherm for each data set shown. K_D values for at least three independent experiments are summarized in Table 3.2.

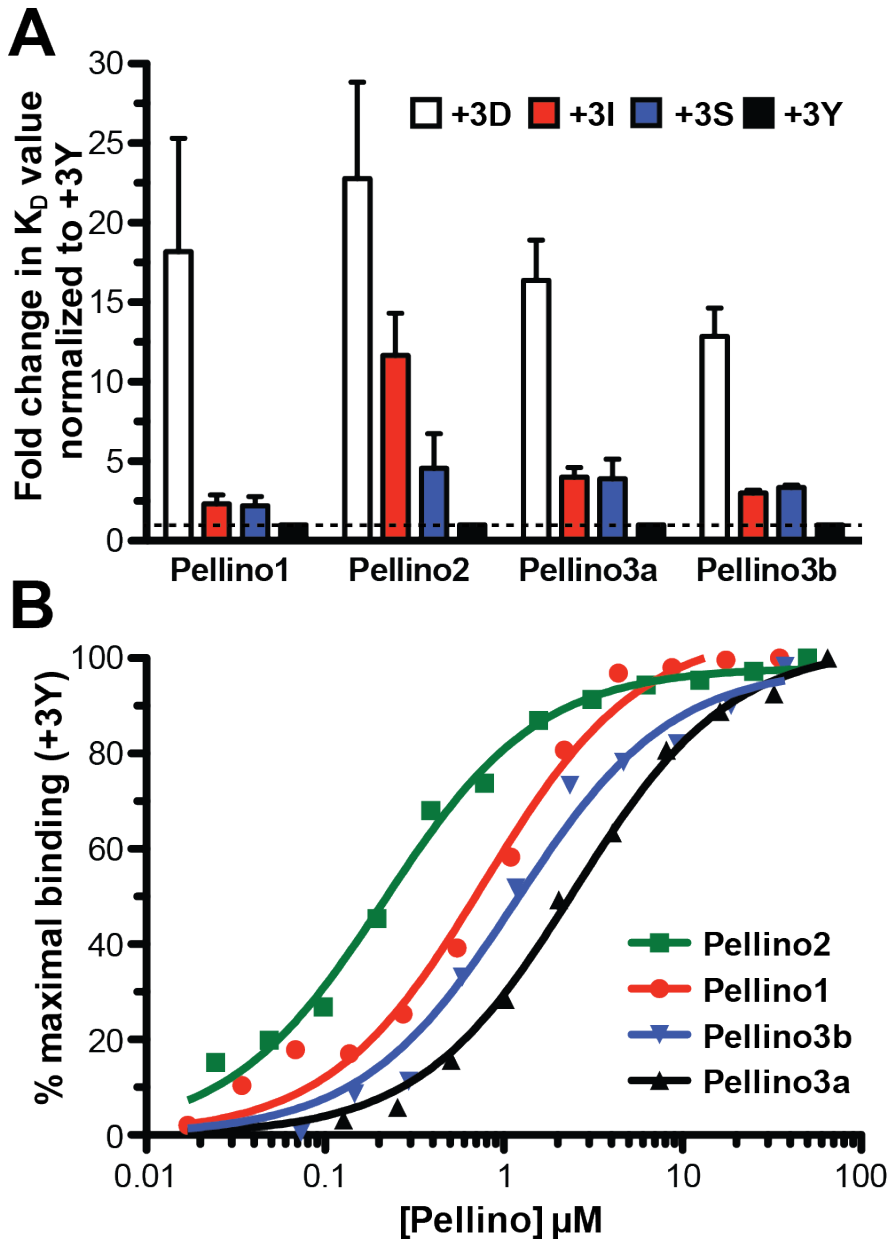


Table 3.2. Binding affinity of IRAK1pT141+3 position variants to Pellino-FHA domains.
The K_D values for binding of the FHA domain of each Pellino to the indicated peptides were determined as described in the legend to Table 3.1.

Peptide	Sequence	K_D (μ M)			
		Pellino1	Pellino2	Pellino3a	Pellino3b
IRAK1pT141+3D	S-A-S-S-pT-F-L-D-P	14 \pm 4.4	4.1 \pm 0.6	41 \pm 3.9	18 \pm 3.7
IRAK1pT141+3I	S-A-S-S-pT-F-L-I-P	1.8 \pm 0.1	2.1 \pm 0.1	10 \pm 1.0	4.2 \pm 1.7
IRAK1pT141+3S	S-A-S-S-pT-F-L-S-P	1.7 \pm 0.2	0.82 \pm 0.35	9.8 \pm 2.8	4.7 \pm 1.1
IRAK1pT141+3Y	S-A-S-S-pT-F-L-Y-P	0.77 \pm 0.18	0.18 \pm 0.04	2.5 \pm 0.3	1.4 \pm 0.4
	+3 position preference	Y \approx S \approx I \ll D	Y $<$ S $<$ I $<$ D	Y $<$ S \approx I \ll D	Y $<$ S \approx I \ll D

Figure 3.4. Pellinos have different specificities for TRAF6 and RIP1.

GST-Pellino pull-downs of (A) Xpress-IRAK1 and (B) Xpress-RIP1 show that only Pellino3a cannot interact with IRAK1 and RIP1. (C) GST-Pellino pull-downs of Xpress-TRAF6 show that only Pellino1 cannot associate with TRAF6. This demonstrates that Pellinos have different substrate specificities. All pull-downs were performed as described in Figure 2.1.

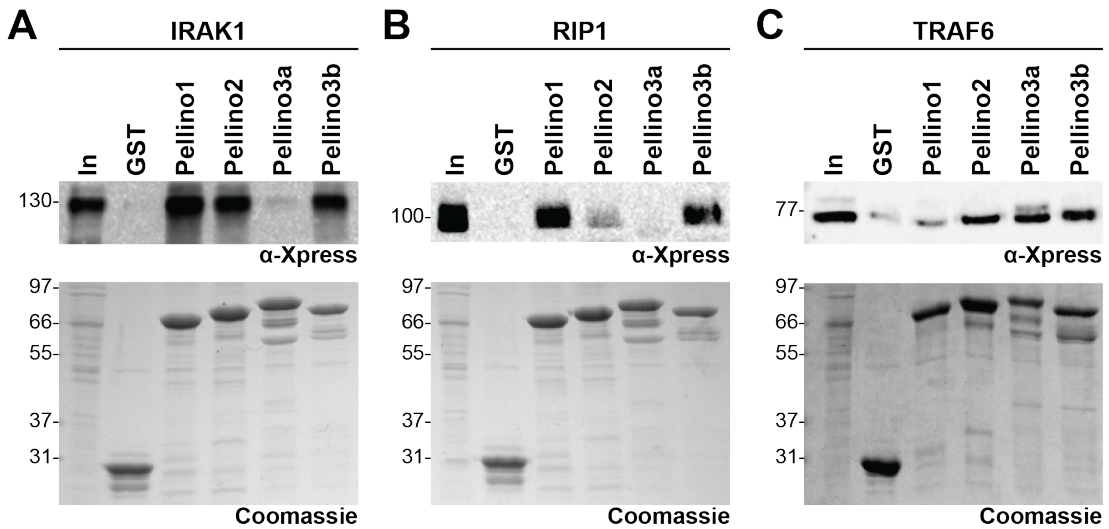


Table 3.3. Frequency of FHA binding motifs in Pellino substrates.

The number of times each motif appears in these Pellino substrates is indicated. Where there are two possible amino acids in the +3 position in the FHA motif, the occurrence of the amino acid analyzed in this study (I, S, Y) is listed first, followed by the occurrence of the second amino acid.

	pTxxD	pTxxI / L	pTxxS / A	pTxxY / M
IRAK1	-	- / 3	1 / 5	2 / -
RIP1	-	- / 4	5 / -	1 / 2
TRAF6	4	2 / 2	- / -	- / 2
RIP2	-	2 / 3	4 / -	2 / 1
cRel	3	- / 5	6 / -	1 / 1

Table 3.4. FHA domain binding motifs in Pellino substrates

The FHA domain binding motifs of IRAK1, RIP1, TRAF6, RIP2, and cRel are listed. Positions refer to the amino acid number of the threonine shown in large, bold font. The amino acids in the +3 position in the sequence is colored according to the binding motif (pTxxD, pTxxI/L, pTxxS/A and pTxxY/M). The +3 amino acids that were investigated in this study - D, I, S and Y - are colored in purple, green, red, and blue, respectively. The +3 amino acids that were not investigated in this study - L, A and M - are indicated in pale green, pink and light blue respectively.

Protein	Position	Sequence	+3 motif	Protein	Position	Sequence	+3 motif
IRAK1	141	SSAS T FLSP	S	RIP2	12	SALP T IPYH	Y
IRAK1	234	VMRN T VYAV	A	RIP2	31	GASG T VSSA	S
IRAK1	322	ILLG T ARAI	A	RIP2	53	LHIH T PLLD	L
IRAK1	387	TVRG T LAYL	Y	RIP2	95	LGIV T EYMP	M
IRAK1	398	EYIK T GRLA	L	RIP2	139	LHN M T P PLL	L
IRAK1	426	RAVK T HGAR	A	RIP2	149	HDLK T QNIL	I
IRAK1	431	HGAR T KYLK	L	RIP2	189	PEGG T IYIM	Y
IRAK1	455	STQS T LQAG	A	RIP2	233	FEDV T NPLQ	L
IRAK1	512	RPP M TQVYE	Y	RIP2	360	GSP E T S RS L	S
IRAK1	551	YVSS T GRAH	A	RIP2	412	DHKT T PCSS	S
RIP1	38	CFHR T OGLM	L	RIP2	482	STKP T RTSK	S
RIP1	110	AEM S TPLSV	S	RIP2	493	QLLD T TDIQ	I
RIP1	189	KNGG T LYYM	Y	cRel	46	DNNR T YPSI	S
RIP1	206	NAKP T EKSD	S	cRel	67	ITLV T KN D P	D
RIP1	437	EGKG T AYSS	S	cRel	164	HGNL T TALP	L
RIP1	476	HGFG T RP L D	L	cRel	183	RAPN T AELR	L
RIP1	508	PVPE T NYLG	L	cRel	246	IVFK T PPY C	Y
RIP1	514	YLG N T P TMP	M	cRel	258	TEPV T VK M Q	M
RIP1	525	SLPP T DE S I	S	cRel	296	KKQ K T T LL F	L
RIP1	552	EIGG T SS S L	S	cRel	324	LELL T SG D P	D
RIP1	579	IFDN T T S LT	L	cRel	330	GDP P T L AS Q	S
TRAF6	31	CSAV T KD D S	D	cRel	378	REMP T GV S S	S
TRAF6	42	GTAS T GNLS	L	cRel	419	VAH P T P RS G	S
TRAF6	220	EYCN T ILIR	I	cRel	425	RSGN T N P LS	L
TRAF6	237	LDCP T AP I P	I	cRel	433	SSF S T R T L P	L
TRAF6	317	IREL T AK M E	M	cRel	435	FSTR T L P SN	S
TRAF6	322	AKME T Q S MY	M	cRel	500	VNMM T T S SD	S
TRAF6	336	RTIR T LE D K	D	cRel	501	NMM T T S SDS	D
TRAF6	429	PFQ G T I RL T	L				
TRAF6	433	TIR L T I L D Q	D				
TRAF6	501	CEV S T R FD M	D				

Table 3.5. Summary of co-crystallization screening of Pellino constructs with peptides

Protein	Construct	Peptide	Screens	Details	Results
Pellino1	1-418	pT141+3S	Emerald Wizard I-III, Greg Van Duyne Boxes 1-4 (In house), Hampton Index, Hampton Peg/Ion, Qiagen Classics, Qiagen Protein Complex Suite	Hanging drop diffusion, 1:1.1 protein to peptide molar ratio	Quasi crystals (Figure 3.5) in Greg Van Duyne Box 2 #22 (50mM Imidazole pH 7, 5% PEG 3350, 100mM CaCl ₂). Crystals disappeared and then appeared a few weeks later. Not able to reproduce.
Pellino1	1-418	pT141+3S	Emerald Wizard III, Emerald Cryo I and II, Greg Van Duyne Boxes 1-4 (In house), Hampton Peg/Ion, Qiagen Classics, Qiagen Protein Complex Suite	Protein complex purified on superose 12 column, hanging drop diffusion, 1:1.2 protein to peptide molar ratio	No hits
Pellino1	2-287	IRAK1pT141L	Silver bullet in 10mM HEPES pH 7.0, 150mM NaCl, 5mM βME	Hanging drop diffusion, 1:1.1 protein to peptide molar ratio	No hits
Pellino1	2-287	pT141+3S	Emerald Wizard III, Emerald Cryo I and II, Greg Van Duyne Boxes 1-4 (In house), Hampton Peg/Ion, Qiagen Classics, Qiagen Protein Complex Suite	Protein complex purified on superose 12 column, hanging drop diffusion, 1:1.2 protein to peptide molar ratio	No hits
Pellino1	2-287	pT141+3Y	Greg Van Duyne Boxes 1-4 (In house)	Hanging drop diffusion, 1:1.1 protein to peptide molar ratio	No hits
Pellino2	15-275	IRAK1pT141L	Emerald Wizard I and II, Greg Van Duyne Boxes 1-4 (In house), Qiagen Classics, Qiagen Protein Complex Suite	Hanging drop diffusion, 1:1.1 protein to peptide molar ratio	No hits
Pellino2	15-275	pT141+3S	Emerald Wizard I-III, Emerald Cryo I and II, Greg Van Duyne Boxes 1-4 (In house), Hampton Index, Hampton Peg/Ion, Qiagen	Hanging drop diffusion, 1:1.1 protein to peptide molar ratio	No hits

Pellino2	15-275		pT141+3S	Classics, Qiagen Protein Complex Suite Emerald Wizard III, Emerald Cryo I and II, Greg Van Duyne Boxes 1-4 (In house), Hampton Peg/Ion, Qiagen Classics, Qiagen Protein Complex Suite	Hanging drop diffusion, hanging reverse drop diffusion, 1:1.2 protein to peptide molar ratio	No hits
Pellino2	15-275		pT141+3S	Emerald Wizard III, Emerald Cryo I and II, Greg Van Duyne Boxes 1-4 (In house), Hampton Peg/Ion, Qiagen Classics, Qiagen Protein Complex Suite	Supplemented with 22.5% sucrose, hanging drop diffusion, 1:1.2 protein to peptide molar ratio	No hits
Pellino2	15-275		pT141+3S	Greg Van Duyne Boxes 1-4 (In house)	Seed screening with Pellino2 15-275 crystals that come out in Sodium Formate, pH 5. Hanging drop diffusion, 1:1.1 protein to peptide molar ratio	No hits
Pellino2	15-275		pT141+3Y	Greg Van Duyne Boxes 1-4 (In house), Qiagen Classics, Qiagen Protein Complex Suite	Hanging drop diffusion, 1:1.1 protein to peptide molar ratio	No hits
Pellino2	15-275		Rad9pT192	Emerald Wizard I and II, Greg Van Duyne Boxes 1-4 (In house), Qiagen Classics	Hanging drop diffusion	No hits
Pellino2	15-275, V61M/L232M		IRAK1pT141L	Emerald Wizard I-III, Emerald Cryo I and II, Greg Van Duyne Boxes 1-4 (In house), Hampton Peg/Ion, Qiagen Classics, Qiagen Protein Complex Suite	With and without TCEP in protein buffer, hanging drop diffusion, 1:1.1 protein to peptide molar ratio	No hits
Pellino2	15-275, V61M/L232M		Rad9pT192	Greg Van Duyne Boxes 1-4 (In house), Qiagen Classics	Hanging drop diffusion	Hits with and without peptide. Molecular replacement solutions did not contain peptide.

Figure 3.5. Pellino1:pT141+3S peptide quasi crystals

Equal volumes of full-length Pellino1 and pT141+3S peptide (1:1 molar ratio, 10mg/ml total in 10mM HEPES pH 7, 80mM NaCl, 1mM DTT) and reservoir solution (50mM Imidazole pH 7, 5% PEG 3350, 100mM CaCl₂) were mixed and equilibrated over the reservoir solution at 20°C. Quasi crystals would grow up to ~10-15µm in size and would also appear without peptide. Clusters of crystals are ~30µm² in the pictured dimension.

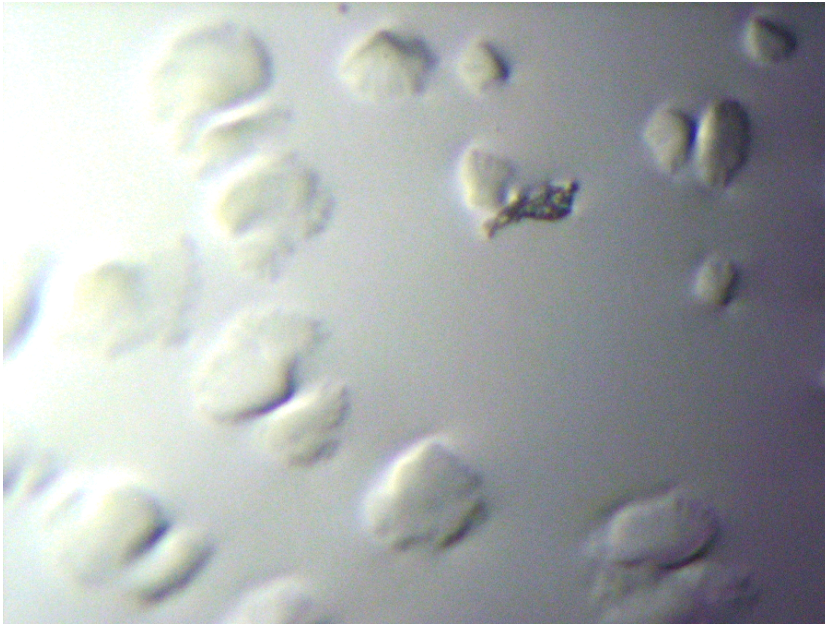


Figure 3.6. The FHA domain pT-peptide binding site of Pellino2 crystal is a crowded environment.

Close up view of the pT-peptide binding pockets of Rad53-FHA1 domain (gray, PDB ID: 1gxc) superimposed onto the Pellino2-FHA domain (green, PDB ID: 3ega). Arginine 106 of Pellino2-FHA domain is highlighted in magenta. Highlighted in orange is the Rad9p peptide bound to Rad53-FHA1. The Rad9p peptide clashes with the Pellino2-FHA domain symmetry mate (cyan), suggesting that the crowded environment may not be able to accommodate pT-peptide.

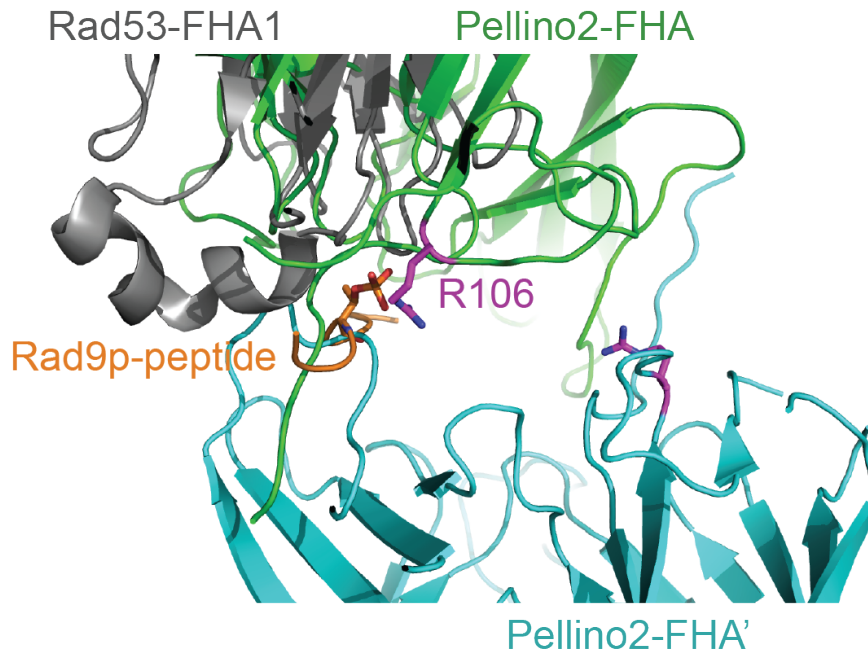


Figure 3.7. Crystallization of Pellino3a-FHA

(A) Pellino3a-FHA (residues 40-305) crystals that formed in 10mM HEPES pH 7, 150mM NaCl, 5mM β ME. The left panel shows crystals that spontaneously formed during a 6-week incubation period at 4°C in a 1.5ml microcentrifuge tube. The right panel shows optimized Pellino3a-FHA crystals formed by hanging drop vapor diffusion. See Table 3.7 for data collection statistics on a data set from a Pellino3a-FHA crystal that formed spontaneously. (B) Other conditions that yield Pellino3a-FHA crystals: 75mM HEPES pH 7, 600mM sodium tartrate (left panel); 0.1M MES pH 6.5, 6% (w/v) PEG 20,000 (middle panel); 100mM HEPES pH 7.5, 2M ammonium formate (right panel). (C) Dehydration of Pellino3a-FHA crystals improves X-ray diffraction quality. Pellino3a-FHA crystals were transferred to 1-2 μ l drops containing 10mM HEPES pH 7, 150mM NaCl, and 5mM β ME with or without 10-15% ethylene glycol. The drops were equilibrated with the same solution in the reservoir for ~16 hours at 20°C. 66% ethylene glycol, 10mM HEPES pH 7, 150mM NaCl, and 5mM β ME was slowly added to the drops until the concentration of ethylene glycol was ~33%. Crystals were flash frozen directly from the drop. Diffraction data was collected at the UPenn X-ray home source. (D) Seeding Pellino3a-FHA crystals also improved crystal formation. A 1:1000 dilution of crushed Pellino3a-FHA crystals was streak seeded into Pellino3a (2.8-8.5mg/ml) and reservoir solution (75mM HEPES 7, 600mM sodium tartrate) mixed in equal volumes and equilibrated over reservoir solution at 20°C.

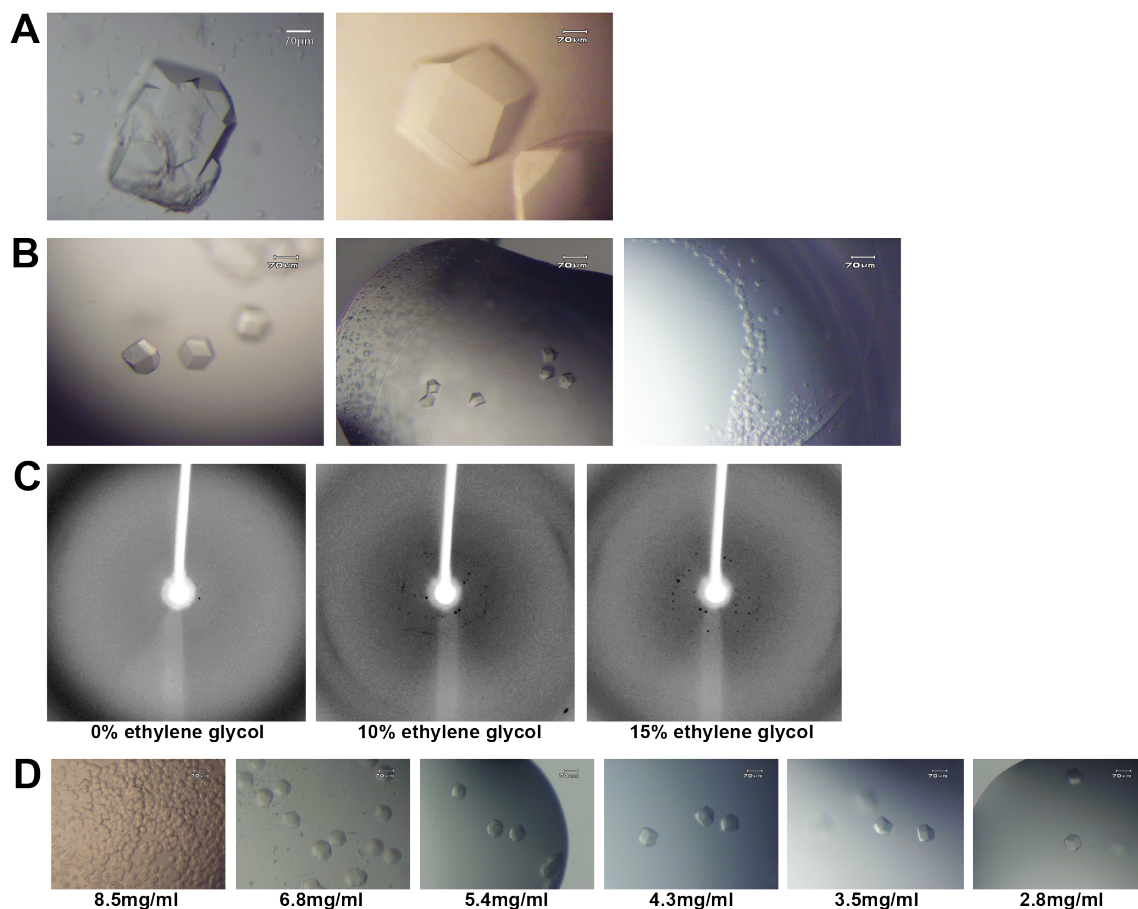


Table 3.6. Summary of optimized Pellino3a crystallization conditions

Pellino32-FHA crystals grew to 100-400 μm^3 . Pellino3a-FHA (6-10mg/ml) was crystallized in these conditions.

Condition	Buffer	pH	Precipitant	Salt/Additive
1	10mM HEPES	7	150mM NaCl	5mM β ME
2	75mM HEPES	7	600mM NaTartrate	
3	100mM MES	6.5	3% PEG 3350	
4	100mM MES	6.5	2.5% PEG 8,000	
5	100mM NaPhosphate	6.5	5% PEG 8,000	
6	100mM NaPhosphate	7	3-5% PEG 5,000	
7	100mM HEPES	7	6% PEG 10,000	37.5mM MgCl_2

Table 3.7. Data collection statistics for Pellino2:pT141 peptide and Pellino3a-FHA

Numbers in parentheses refer to the last resolution shell. $R_{\text{sym}} = \sum |I_h - \langle I_h \rangle| / \sum I_h$, where I_h = average intensity over symmetry equivalent measurements.

	Pellino2:pT141 peptide	Pellino3a-FHA
Space group	F222	I2 ₁ 3
Cell dimensions	a=84.4, b= 86.7, c = 163.6	a, b, c = 170.0Å
X-ray source	APS 23-ID-B	APS 23-ID-B
Wavelength (Å)	1.0332	1.0331
Resolution limit (Å)	2.05	5.2
Measured/Unique	130244 / 17956	109705 / 3231
Fold redundancy	3.3 (3.2)	6.2 (6.3)
Completeness (%)	97.4 (98.8)	99.2 (100)
R_{sym} (%)	5.4 (61.0)	7.7 (44.5)
<I/σ>	22.6 (2.7)	25.8 (4.9)

Figure 3.8. The Pellino $\beta 4/\beta 5$ loop may confer Pellino substrate specificity

(A) Cartoon representations of superimposed homology models of Pellino1, 2 and 3b. Pellino3a and Pellino3b are essentially modeled the same except for the 24 amino acid insertion. We therefore did not include the Pellino3a homology model to avoid redundancy. The $\beta 1/\beta 2$ loops in Pellinos 1, 2, and 3b are modeled to be very similar in structure and was removed for a better view of the FHA domain pT-peptide binding pocket. (B) Sequence alignment of the residues in $\beta 4/\beta 5$ loop of Pellino1, 2, 3a and 3b. The secondary structure elements of the Pellino2-FHA core (PDB ID: 3ega) are shown above the sequence alignment; the dotted line represents residues that are disordered in the structure. Residues are colored by percent sequence identity (darkest blue represents the greatest sequence identity). (C-E) Close up views of the Pellino FHA domain pT-peptide binding pocket and the modeled $\beta 4/\beta 4$ loop of Pellino1 (C), Pellino2 (D), and Pellino 3b (E). R104, R106, and R131 of Pellino 1, 2, and 3b, respectively, are highlighted in magenta.

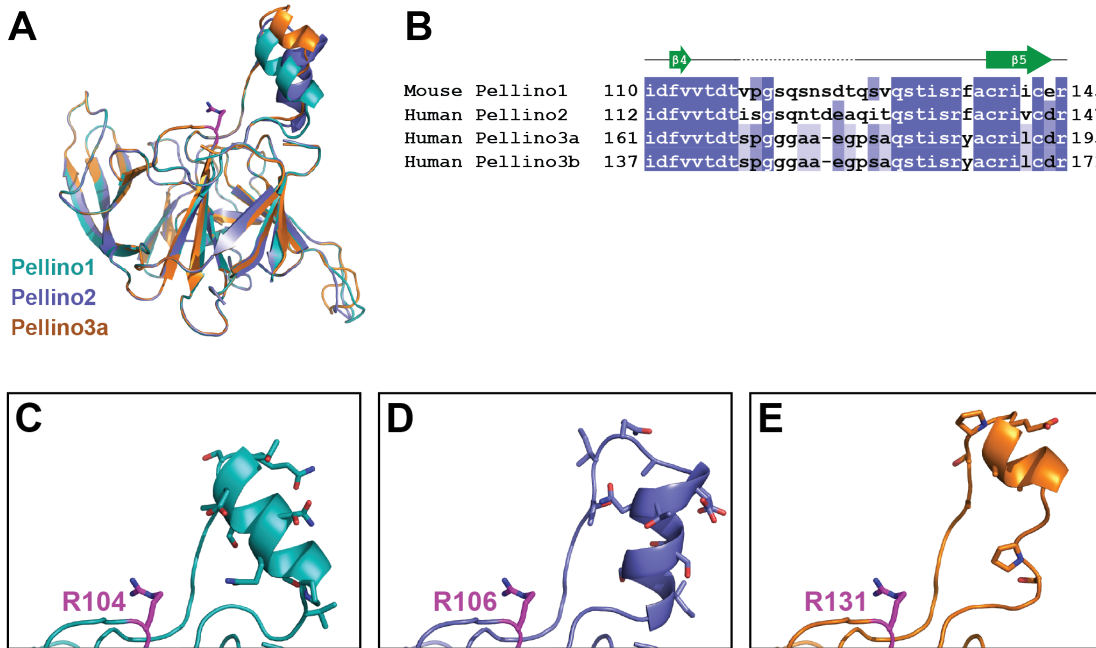


Figure 3.9. Pellino2 still interacts with IRAK1 T54A and T141A mutants

Pull-downs of IRAK1 and IRAK1 variants from HEK293T cells with immobilized GST-Pellino2. Experiments were performed exactly as described in Figure 3.1. T54A and T141A mutations do not disrupt IRAK1-Pellino2 association.

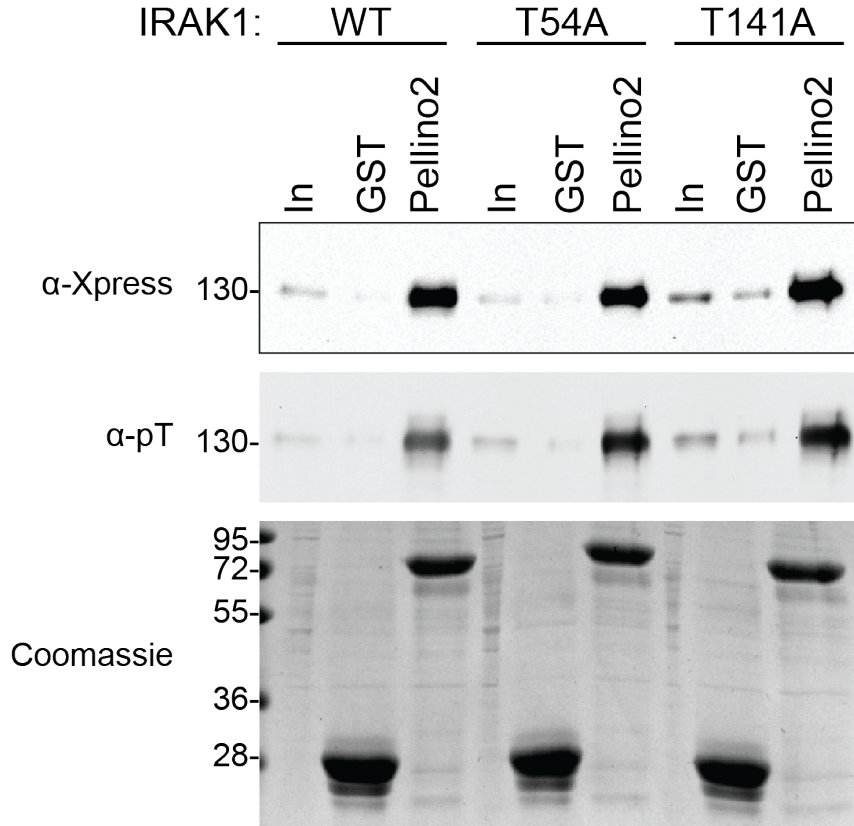
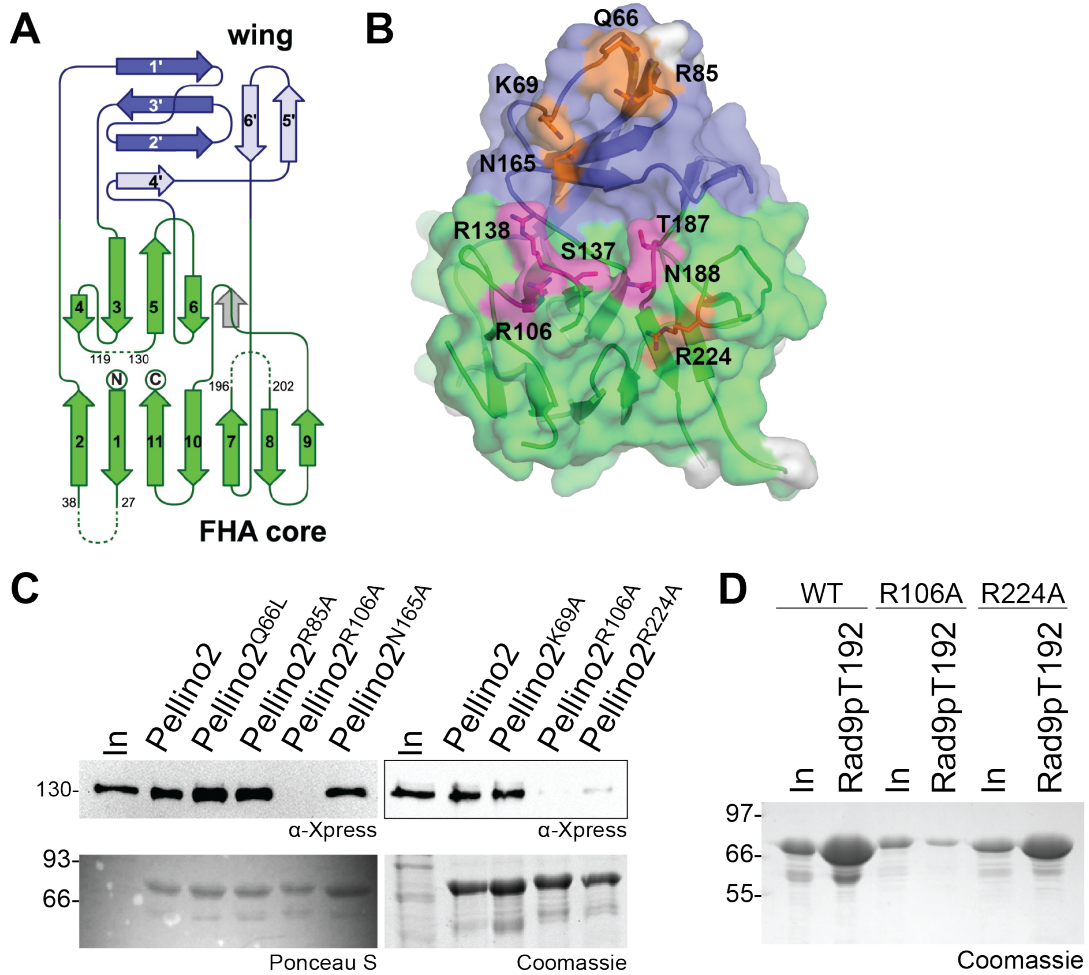


Figure 3.10. Pellino2 R224A disrupts interaction with IRAK1, but not Rad9pT192 peptide.
 (A) A topology diagram of the Pellino2 substrate binding domain structure highlights the non-canonical features of the Pellino FHA-like domain: the Pellino wing (in blue) and the $\beta 9/\beta 10$ loop within the FHA core. For comparison, the position of the $\beta 9$ -strand in canonical FHA domains is shown in gray. (B) Cartoon representation of the Pellino2 FHA core pT-peptide interaction surface. Conserved residues that are part of the FHA core pT-peptide binding pocket are highlighted in magenta. Residues that were mutated in (C) are highlighted in orange. (C) Pull-downs of IRAK1 from HEK293T cells with immobilized GST-Pellino2 and Pellino2 mutants. Both R224A and R106A mutations disrupt interaction with IRAK1. (D) Rad9pT192 peptide pull-downs of GST-Pellino2 and Pellino2 variants. Unlike Pellino2 R106A, Pellino2 R224A can still interact with the Rad9pT192 peptide. (A) was adapted from [30].



4. Discussion of Chapters 2 and 3

Parts of this chapter were adapted from [46].

4.1. pT-peptide binding of Pellinos

When comparing peptide binding affinities between the Pellinos, Pellino2 interacts most tightly with all 4 pT141 peptide variants (Table 3.2). This may reflect the fact that we have focused most of our efforts to elucidate the molecular basis of Pellino2-IRAK1 interaction. However, if this high-affinity binding is an intrinsic property of Pellino2 compared to the other members of this family of E3 ligases, this may explain the difficulty in identifying the true physiologically relevant Pellino2 substrates based on experiments using overexpression or incomplete knockdown of this protein. Alternatively, high affinity binding may be a property of all Pellino FHA domains, but we have not identified the optimal binding motif for Pellino1, 3a and 3b in this study.

Our mutational analysis of Pellino3a suggests that its unique insertion attributes to substrate specificity and therefore should affect pT-peptide binding as well. Indeed, our pT-peptide binding experiments show that compared to all the Pellinos, Pellino3a binds the weakest to the pT141 peptide variants. However, the fact that Pellino3a is able to interact with these peptides only 2-fold weaker than Pellino3b suggests that the Pellino3a unique insertion only binds very weakly with the Pellino3a FHA domain pT-peptide binding pocket. Future studies should determine the binding affinity of Pellino3b for a peptide derived from the Pellino3a insertion. Moreover, it would be interesting to see if Pellino3b is still able to interact with IRAK1 in the presence of the same peptide.

4.2. Identifying more specific Pellino binding sites

To our knowledge, this is the first identification of a specific Pellino2 binding site on one of its physiologically relevant substrates. Here, we provide some ideas on how to characterize more Pellino binding motifs.

Despite the fact that we assayed a very limited set of peptides, our study has found a pT-peptide, pT141+3Y peptide, that can interact with Pellino2 with a K_D of 180nM (Table 3.2). This is quite impressive considering the highest affinity known for an FHA domain-pT peptide interaction is for the Rv0020c FHA domain with its peptide library screen-derived peptide that has a K_D of ~100nM [35]. Thus, our study's approach of dissecting the Pellino-IRAK1 interaction may also successfully elucidate the specific sites on other substrates that Pellinos target.

Consideration of the physiologically relevant phosphorylation state of Pellino substrates will also assist in identifying more Pellino binding motifs. In our studies, phosphorylation of Pellino substrates is entirely dependent on substrate overexpression, which is presumed to stimulate substrate phosphorylation by autophosphorylation or an endogenous kinase. A more refined approach would be to look for Pellino interaction with substrates that become phosphorylated upon appropriate stimulation of immune receptors. Examining the substrate specificity of kinases that are responsible for phosphorylating Pellino substrates may additionally provide clues to physiologically relevant phosphorylation sites on Pellino substrates.

An extension of the dephosphorylation protection assay we performed on IRAK1 can also help to identify other phosphorylation sites on IRAK1 and other Pellino substrates. Mass spectrometry-based analyses of phosphatase-treated substrates in the presence Pellinos can elucidate the phosphorylation sites that are protected by Pellinos. In addition, comparing the dephosphorylation protection profiles of all 4 Pellinos can hypothetically uncover more specificity differences amongst the Pellinos.

Interestingly, the TxxY sequence is found in the activation loops of IRAK1 (T387), RIP1 (T189), and RIP2 (also at T189). Kinase activation frequently involves the phosphorylation of specific residues within the activation loop [62] so these threonines are most likely phosphorylated *in vivo*; in fact, Thr387 of the IRAK1 activation loop is an autophosphorylation or IRAK4 phosphorylation site crucial for the activation of IRAK1 kinase activity [50,63]. The common occurrence of TxxY in these kinase activation loops suggests that the Pellinos may

target these sites. Mutational analyses of the RIP1, RIP2 and IRAK1 kinase activation loops may be too disruptive to test whether Pellinos bind to these regions. In fact, alanine substitution of IRAK1 T387 disrupts kinase activity [50]. While we were not able to detect IRAK1pT387-derived peptide (pT387 peptide) interaction with Pellino2 in our qualitative peptide pull-down assay (Figure 2.3), we have not had the opportunity to measure Pellino2 binding to pT387 peptide using a quantitative assay due to limited peptide quantities. Future studies should measure Pellino binding to peptides derived from the kinase activation loops of Pellino substrates.

4.3. Phosphorylation-dependent regulation of Pellino specificity and substrate recognition

4.3.1. Substrate phosphorylation may disrupt Pellino binding

Based on our peptide binding analysis, all 4 Pellinos show the weakest binding to the IRAK1pT141-derived peptide variant containing the pTxxD motif –in each case at least 13 times weaker than for the pT141+3Y peptide (Table 2 and Figure 4A). This trend against aspartate (a phosphomimetic residue) at the +3 position could reflect negative selection of binding sites with a phosphorylated residue in this position. Phosphorylation of a pTxxS motif would be expected to reduce Pellino binding and could represent a regulatory mechanism of Pellino substrate recognition.

There is evidence to suggest that this form of regulation may occur at the IRAK1pT141 site that we found to be a specific Pellino2 target. Upon stimulation of THP-1 cells with R-848 (a TLR7/8 ligand), IRAK1 is known to become phosphorylated at a number of specific serines and threonines in the PST domain around T141 [64]. Interestingly, the same IRAK1 PST region is the target of two other IRAK1 binding partners involved in TLR signaling, the prolyl isomerase Pin1 and the substrate recognition domain of the SCF- β -TrCp E3 ubiquitin ligase (β -TrCp) [64,65]. In fact, Pin1 and β -TrCp require phosphorylation of serines adjacent to T141 (including S144 at the +3 position) for association with IRAK1. Our pT peptide binding analysis suggests that phosphorylation of these adjacent serines would disfavor Pellino binding. Thus, the IRAK1

phosphorylation state may dictate which post-translational modifiers can associate with IRAK1 and hence, influence the regulation of downstream TLR signaling events. It would be interesting to investigate whether these IRAK1-binding proteins are activated under the same TLR-stimulation conditions and if so, determine an order in which these proteins associate with IRAK1. Moreover, future studies should look at whether Pellinos compete with Pin1 and β -TrCp for IRAK1 association.

4.3.2. Phosphorylation may affect Pellino specificity

Pellino phosphorylation has previously been shown to enhance the catalytic activity of Pellinos *in vitro* [13,45], however it remains unclear whether phosphorylation also affects Pellino substrate specificity. Phosphorylation of the E3 ubiquitin ligase Nedd4-2 inhibits substrate binding and is a regulatory mechanism to maintain proper epithelial Na⁺ transport [66]. In a similar manner, phosphorylation of Pellinos may also modulate substrate specificity. In our study, we found that Pellino3a contains a phosphomimetic insert that prevents IRAK1 association. We speculate that other Pellinos can be phosphorylated in a manner that mirrors auto-inhibition of Pellino3a substrate binding. One potential site is the disordered serine/threonine-rich β 4/ β 5 loop, which homology modeling suggests may confer differences in Pellino specificity (Figures 1.3, 3.8). Performing mutational analyses of this β 4/ β 5 loop in Pellinos will provide insight into whether this loop is not only important for substrate recognition, but also for the regulation of Pellinos. In addition, more *in vitro* studies are necessary to determine the changes in Pellino substrate specificity (if any) when mammalian Pellino family members are phosphorylated.

4.4. Pellino substrate binding includes more than the recognition of a short pT-peptide sequence

The discovery that R224 of the β 9/ β 10 loop within the Pellino FHA core mediates interaction with substrate and not pT-peptide motifs suggests that there are other binding determinants that mediate Pellino substrate recognition. Future studies should look at whether these other binding

determinants enhance Pellino binding affinities as seen with the *M. tuberculosis* FHA domain-containing FhaA protein, which interacts with its cognate binding partner, MviN, 2-fold stronger than a peptide library screen-optimized pT-peptide [35,59]. A feasible starting point would be to look at the Pellino2 binding to IRAK1-197. Large enough quantities of phosphorylated IRAK1-197 can potentially be crudely purified from HEK293T lysates for more quantitative binding studies with Pellino2. We have tried to capture Xpress-tagged IRAK1-197 on an α -Xpress surface plasmon resonance (SPR) sensor chip, but the capturing conditions were not suitable for maintaining protein stability. In the future, these conditions need to be optimized in order for IRAK1-197 to be immobilized on a SPR sensor chip. Binding studies with longer IRAK1-derived pT peptides or pT peptides with more than one phosphorylation site may also be useful tools in further probing the molecular basis of Pellino substrate recognition.

While we initially reasoned that the Pellino3a unique insertion acts as a phosphomimetic peptide that blocks the FHA domain pT-peptide binding pocket, we now cannot rule out the possibility that the insertion blocks some other part of Pellino3a such as the β 9/ β 10 loop. The β 9/ β 10 loop may be necessary for Pellino3b association with IRAK1 and RIP1, but not for TRAF6. This may explain why Pellino3a can only interact with TRAF6 (Figure 3.4C), yet Pellino3a and 3b have essentially the same pT+3 motif preferences. More mutational analyses are required to determine precisely how the Pellino3a insertion blocks IRAK1 and RIP1 binding.

The FHA wing appendage is an extreme example of β -strand insertions that may mediate FHA domain specificity. Though we have not found any residues that are critical for IRAK1 association, our mutational analysis of the FHA wing appendage did not take into account the fact that Pellino phosphorylation sites are mapped to the wing appendage (Figure 1.3) [45]. Thus, it is still entirely possible that the Pellino wing facilitates substrate interaction only when phosphorylated. Again, it will be important to elucidate whether Pellino phosphorylation is able to modulate substrate specificity; doing so will provide insight into the function of the Pellino wing appendage.

4.5. Parallels between FHA and SH2 domains may assist in elucidating Pellino substrate specificity

Analogous to FHA domains, Src homology 2 (SH2) domains are phospho-binding modules that recognize phosphotyrosine (pY) in a sequence specific manner. Also similar to FHA domains, SH2 are capable of recognizing short phosphopeptide sequences. Directed pY-peptide library screens of SH2 domains have revealed SH2 peptide binding motifs in the same way that the pT+3 motifs were discovered for FHA domains [67]. Interestingly, various analyses on the peptide binding preferences of SH2 domains have shown that different SH2 domains can recognize the same peptide motifs with similar affinities *in vitro* [68]. As mentioned earlier, this is also the case for many FHA domains (including Pellinos) that are able to bind to the same Rad9p-derived peptide. We have also shown that while Pellinos have different substrate specificities, Pellinos can bind to the pT141 peptide variants within the same micromolar range. Thus, it remains elusive as to how FHA and SH2 domains are able to recognize cognate binding partners and discriminate against phosphorylated proteins that are not actual targets *in vivo*. The structure of the N-terminal SH2 domain of phospholipase C γ in complex with the tyrosine kinase domain of FGFR1 reveals that there is a secondary binding site that facilitates SH2 domain selectivity and enhances binding affinity to FGFR1 [69]. Again, the presence of an additional binding determinant for SH2 domain recognition is a reflection of the FhaA:MviN interaction [59]. Since there are far more extensive studies on elucidating SH2 domain specificities and function, we should take into consideration the previous SH2 domain studies and design analogous experiments that can elucidate Pellino FHA domain specificity and function. The far western analysis and phosphatase protection assays used in this study were originally inspired by experiments performed on SH2 domains [70,71]. Future studies should focus on emulating studies that were used to probe SH2 domain specificity in a high-throughput manner and SH2 domain functions *in vivo*.

4.6. Probing the regulation and biological functions of Pellinos

As alluded to in Chapter 1, gaining insight into Pellino substrate specificity will lead to a better appreciation of the roles that individual Pellinos play in orchestrating immune receptor signaling. Here, we suggest how our new studies can provide new tools to investigate the regulation and biological functions of Pellinos.

Our results together with gene targeting studies in mice suggest that Pellinos mediate non-redundant roles in immune signaling, in part, by interacting with distinct substrates. An understanding of how Pellinos precisely mediate these divergent immune signaling pathways will require the identification of *bona fide* Pellino substrates. Despite the fact that the Pellino1 and 3 knockout mice studies have identified novel signaling components that Pellinos regulate, it is not clear whether Pellino family members are directly or indirectly acting upon these signaling components. For instance, while Pellino1 has been shown to mediate TCR signaling by down-regulating cRel [25], there is no evidence that Pellino1 directly interacts with and ubiquitinates cRel *in vivo*. Moreover, Pellino3 knockout mice studies have shown to disrupt the levels of TRAF6 ubiquitination *in vivo* [21], but experiments have failed to detect Pellino3 directly polyubiquitinating TRAF6 *in vitro*. To help distinguish between Pellino binding partners or simply downstream signaling components, we propose to perform far western analyses similar to the setup that was used to study the Pellino2-IRAK1 interaction (Chapter 2).

So far, only the FHA domain Pellino3 has been demonstrated to be essential for mediating proper immune signaling function and apoptosis [10,28]. While we have shown that disrupting the Pellino2 FHA domain pT-peptide binding pocket abrogates IRAK1 polyubiquitination in a transfection model, it remains to be determined whether disrupting the Pellino2 FHA domain pT-peptide binding pocket will affect IRAK1 polyubiquitination and subsequently NF- κ B activation *in vivo*. Moreover, it is unclear whether the Pellino1 FHA domain is required for modulating TRIF-mediated TLR signaling and T-cell activation. Future studies should

address the functional consequence of inhibiting the Pellino-substrate interaction by using Pellino variants with mutations that disrupt the FHA domain pT binding pocket. Our studies have introduced additional Pellino variants (Pellino2R224A and Pellino3a E54-66A) that should be pursued further to provide insight into the Pellino FHA domain-mediated regulation of immune signaling.

Pellinos have now been shown to participate in a variety of immune signaling pathways. As many other E3 ubiquitin ligases are involved in the same signaling pathways, being able to specifically inhibit Pellino catalytic activity will be necessary to decouple irrelevant ubiquitination events that modulate immune processes from those that are Pellino-mediated. Since we have shown that Pellinos have different phosphothreonine motif specificities, using pT-peptides that block individual Pellino substrate-binding domains would be a novel way to inhibit Pellinos and explicitly probe different branches of signaling that are specific to Pellinos.

4.7. Therapeutic prospects of targeting Pellinos

As mentioned earlier, Pellinos are implicated in having both augmentative and protective effects on inflammatory diseases. Pellino1 is a critical mediator of microglia activation and contributes to the onset of the mouse model for multiple sclerosis, autoimmune encephalomyelitis (EAE) [29]. On the other hand, Pellino3 deficiency enhances the pathogenesis of experimental murine models of colitis [10]. The different Pellino substrate specificities can feasibly be exploited for pharmacological advantage in treating inflammatory diseases that have been recently linked to the aberrant regulation of Pellinos.

As seen for a NEMO-binding domain peptide that blocks NF κ B-activation and reduces tumor growth in a canine model of spontaneous diffuse large B-cell lymphoma [72], the use of high-affinity peptides to inhibit Pellino substrate binding and block Pellino-mediated immune signaling may be of therapeutic relevance. Here, we postulate how to make use of therapeutic peptides that target Pellinos. If indeed Pellino1 mediates the onset of multiple sclerosis in

patients, one could focus on developing a peptide or peptide mimetic that specifically interacts with and inhibits Pellino1. In this case, minimal interaction with Pellino3a and 3b would be necessary because Pellino3 isoforms may provide protection against Crohn's disease. Now that both Pellino3 isoforms have been implicated in regulating TNF α -induced apoptosis [28], targeting Pellino3 can potentially be promising anti-cancer therapeutics. Only the Pellino3 FHA domain and not the catalytic RING domain is responsible for regulating TNF α -induced apoptosis [28]; thus, peptide-based inhibition can be a very specific way to block TNF signaling while preserving Pellino3 function in other immune signaling pathways. In order to develop a Pellino3-specific drug, one would first need to determine whether a peptide library screen-optimized pT-peptide binds to Pellino3 isoforms with high affinity. Since Pellinos most likely have redundant roles in regulating IRAK1-dependent pathways, peptides that target the entire family of Pellinos may be very useful as well. A starting point for an anti-inflammatory drug that binds to all Pellinos could be a peptide that contains a pTxxY motif.

Our results on Pellino pT-peptide binding and substrate specificity strongly encourages the prospects of therapeutics that can be developed to specifically target an individual Pellino with minimal off-target effects. However, we are still very far away from pursuing a Pellino inhibitor. It still remains elusive whether disrupting the Pellino FHA domain has an effect on the onset or prevention of inflammatory disease states linked to the aberrant regulation of Pellinos; investigations in the near future should address this. Moreover, in order to determine if Pellinos would make good drug targets, future studies should probe the molecular basis of Pellino substrate specificity even further in hopes to better understand Pellinos' roles in specific cellular processes and the pathogenesis of inflammatory diseases.

5. The molecular mechanisms of Pellino- and TRAF6-mediated ubiquitination of IRAK1

Upon IL-1R/TLR stimulation, Pellinos and TRAF6 are the E3 ubiquitin ligases that are implicated in the K63-linked polyubiquitination of IRAK1 [13,20]. While Pellinos and TRAF6 target the same substrate, it remains unclear whether these two very different E3 ubiquitin ligases have distinct functional roles in the IL-1R/TLR signaling pathways. As seen with signaling components targeted by multiple ubiquitin ligases, IRAK1 may actually be subjected to the ubiquitin editing process that is common in NF- κ B signaling [3] (see Figure 1.1 for a well-characterized example of ubiquitin editing on RIP1). When IRAK1 becomes activated by TLR/IL-1R stimulation, TRAF6, Pellinos and also SCF- β -TrCp E3 ubiquitin ligases may actually come together to form complexes involved with coordinating the different polyubiquitination linkages that have been previously reported for IRAK1 [73,74]. Gaining insight on the molecular basis of Pellino- and TRAF6-mediated ubiquitination of IRAK1 will elucidate the mechanisms by which these E3 ubiquitin ligases regulate IRAK1 and other substrates in immune signaling pathways. In this chapter, we describe attempts to determine the structure of the non-canonical Pellino RING domain and to investigate the molecular basis of TRAF6 association with IRAK1.

5.1. Attempts to determine the structure of the non-canonical Pellino RING domain

RING domains confer specificity for E2 ubiquitin ligases, which result in specific ubiquitin linkages on substrates [75]. The classical RING domain is defined as a conserved sequence of cysteines and histidines: C-X₂-C-X₍₉₋₃₉₎-C-X₍₁₋₃₎-H-X₍₂₋₃₎-C/H-X₂-C-X₍₄₋₄₈₎-C-X₂-C (also known as the C3HC4 motif) [75]. Intriguingly, Pellinos contain non-canonical RING domains, which have the cysteine and histidine pattern: Cys-X₁-His-X₁₉-Cys-X₂-Cys-X₃₀-Cys-X₁-His-X₂₅-Cys-X₂-Cys (CHC2CHC2 motif) [11]. A better understanding of the Pellino RING domain specificity for E2 ubiquitin ligases

will elucidate the type of linkages Pellinos can generate, thereby providing insight into Pellinos' regulatory role in immune receptor signaling. Our goal was to solve the structures of (1) full-length Pellino2 in complex with E2 ubiquitin ligases and (2) more stable forms of full-length Pellinos 1 and 2.

5.1.1. Pellino2 does not interact with UbcH7 and Ubc13

Full-length Pellino2 expressed and purified from *E. coli* undergoes rapid degradation of the C-terminal RING domain resulting in a stable FHA-only fragment. This suggests that the Pellino RING domain in this *E.coli*-derived protein may be misfolded and/or intrinsically structurally disordered. We reasoned that in an E2 ubiquitin ligase-Pellino complex, the Pellino C-terminal RING domain would be stabilized by the interaction with the E2 ubiquitin ligase and protected from proteolysis. We chose to use the E2 ubiquitin ligases, UbcH7 and Ubc13, because the structures of these E2 ubiquitin ligases in complex with E3 ubiquitin ligases have been previously characterized [76,77]. In addition, Ubc13 in conjunction with *E. coli*-derived Pellinos 1 and 3b form K63-linked polyubiquitin chains *in vitro* even without the addition of IRAK1 [13]. Purified UbcH7 and Ubc13 were individually mixed with full-length Pellino2 and assayed for complex formation by size exclusion chromatography as was done with TRAF6 and Ubc13 [77]. Ubc13 and UbcH7 do not co-elute on a gel filtration column (Figure 5.1A, B), which suggests that Pellino2 does not interact with these E2 ubiquitin ligases – suggesting that the K_D values for interaction of Pellino2 with these E2 ubiquitin ligases is greater than one micromolar. We also assayed for Pellino2:Ubc13 interaction by performing a GST-Pellino2 pull-down, but also did not detect association with Ubc13 (Figure 5.1C). This is in contrast to the TRAF6-Ubc13 interaction where the K_D value is measured to be $1.48\mu\text{M}$ [77]. Future studies should use other protein binding assays such as analytical ultracentrifugation sedimentation equilibrium to determine if there are protein-protein interactions at higher protein concentrations.

While we did not detect E2 ubiquitin ligase interaction with Pellino2, we only tested 2 out of the ~40 mammalian E2 ubiquitin ligases. Further studies should be tried to determine whether Pellino2 interacts with any of the E2 ubiquitin ligases that have been shown to form ubiquitin chains with Pellino1 [45]. However, caution must be taken when interpreting the results if Pellino2 binding to these E2 ubiquitin ligases cannot be detected because IRAK1-catalyzed *in vitro* Pellino ubiquitination assays have failed to demonstrate actual IRAK1 ubiquitination [13,45]. We suspect that the E2 ubiquitin ligases used in these assays are not physiologically relevant.

Further studies should also attempt to detect Ubc13 interaction with Pellino1 and 3b. It is possible that in addition to having different substrate specificities, Pellinos also have different E2 ubiquitin specificities.

5.1.2. *E. coli*-derived full-length Pellino1 is more stable than Pellino2

Since the Pellino2 RING domain is sensitive to proteolysis, we attempted to crystallize full-length Pellino1, which is more stable when expressed and purified from *E. coli* (Figure 5.2A, B).

Crystallization screening attempts with Pellino1 are summarized in Table 5.1.

When we tested full-length Pellino1 for pT-peptide binding, we found that Pellino1 consistently bound to pT-peptides ~10 times tighter than Pellino1-FHA (Table 5.2). This is not expected because solely the FHA domain is presumed to be mediating interaction with phosphopeptides. These results suggest that Pellino1 RING domain may be directly involved with mediating phosphopeptide interaction, or may stabilize the Pellino1-FHA domain to optimize interaction with peptide. This is not observed for Pellino2, where the affinities for full-length Pellino2 and Pellino2-FHA binding to pT141+3S peptide are similar (Table 5.2). The peptide binding affinity differences we see between Pellino1-FHA, full-length Pellino1 and Pellino2 reiterate that Pellinos have distinct substrate specificities. Why only the Pellino1 RING domain contributes to pT-peptide binding is hard to reconcile due to the fact the RING domains between the Pellinos also share high sequence identity. Future structural characterization of Pellino1 alone

or bound to pT-peptide will be needed to provide insight into the molecular basis of Pellino1 substrate binding.

5.1.3. Attempts to crystallize Sf9-derived Pellino2

We also expressed Pellino2 in insect (Sf9) cells using the baculovirus expression system to test whether Pellino2 RING domain may be more stable when produced in an eukaryote. Pellino2 expressed in Sf9 cells was not as sensitive to proteolysis and could be purified to homogeneity. Crystallization screening attempts with Pellino2 are summarized in Table 5.1.

As previously mentioned, *E. coli*-derived full-length Pellino2 is sensitive to C-terminal protein degradation. It is entirely possible that the reason we could not detect Pellino2 association with Ubc13 and UbcH7 is due to the C-terminal RING domain being misfolded. Thus, Sf9-derived Pellino2 should be assayed for E2 interaction. It will also be interesting to see whether the more stable insect cell expressed Pellino2 binds more tightly to pT-peptides than Pellino2-FHA, as we observed for *E. coli* expressed Pellino 1.

5.2. Molecular basis of TRAF6 interaction with IRAK1

5.2.1. TRAF6 interacts with the C-terminal domain of IRAK1

Previous structural studies have shown that the TRAF6 substrate binding domain recognizes a P-X-D-X-X-(aromatic/acidic residue) sequence motif known as the TRAF6 binding motif [78]. The IRAK1 C-terminal domain (Ct) contains three of these TRAF6 binding motifs (referred to as IRAK1 Ct motif 1-3, 1 being the most N-terminal). Mutations within these binding motifs in IRAK1 disrupt TRAF6-mediated activation of the NF- κ B. However, short IRAK1-derived peptides containing these individual TRAF6 binding motifs interact with TRAF6 with rather weak affinities (K_D values of 50-500 μ M, Figure 5.3A). These observations led us to postulate that TRAF6 association with IRAK1 may involve binding determinants additional to the TRAF6 binding motif, or may involve binding of multiple TRAF6 molecules to a single IRAK1 substrate.

To address this, we investigated the interaction of the TRAF6 substrate-binding domain (residues 346-504, TRAF6-C) with an IRAK1 Ct construct (residues 522-712) that contains all three putative TRAF6 binding motifs. We first employed surface plasmon resonance to determine the binding of TRAF6-C to IRAK1 Ct that had been amine coupled to a CM5 Biosensor chip. We found that TRAF6-C binds to IRAK1 Ct with a K_D value of $6\mu\text{M}$ – a 10-fold tighter affinity than previously reported for the strongest binding IRAK1-derived peptide (IRAK1 Ct motif 3; Figure 5.3A,C). Ye *et al* also measured binding to peptides derived from the intracellular region of CD40 (a TNF receptor family member). They report no difference in affinity for peptide of 9 and 30 amino acids in length (centered on the TRAF6 motif; K_D values of $59.9\mu\text{M}$ and $84\mu\text{M}$, respectively) [78], suggesting that the low affinity for the 8-10 amino acid peptides is not simply due to the length. A number of factors may account for the higher affinity observed for interaction of TRAF6 with IRAK1 Ct: the TRAF6 binding motifs may be presented in an optimal configuration in this larger protein domain; there may be additional contacts with TRAF6 involving parts of IRAK1 Ct outside the short TRAF6 binding motifs; and the increase in affinity may be due to the presence of multiple TRAF6 binding motifs in IRAK1 Ct. To distinguish between these two possibilities, future experiments should involve a mutational analysis of IRAK1 Ct and competitive IRAK1-derived peptide binding experiments.

We have found the tightest binding yet for a TRAF6-substrate interaction ($K_D = 6\mu\text{M}$). Elucidation of the TRAF6-IRAK1 interaction could potentially be advantageous for therapeutic modulation. TRANCE-R (another TNF receptor family member)-derived peptides that weakly bind to TRAF6 ($K_Ds \geq 78\mu\text{M}$ [78]) have already shown to specifically inhibit TRAF6 and block osteoclastogenesis [79]. However, further studies that investigate the molecular basis of TRAF6 substrate binding should not overlook working with protein constructs as opposed to solely looking at peptide binding.

5.2.2. TRAF6 and IRAK1 bind with 2:1 stoichiometry

The physiologically relevant stoichiometry of TRAF6 remains elusive. Structural studies have shown that the catalytic portion of TRAF6 (including the RING domain) forms a dimer when bound to Ubc13 [77]. Disruption of the TRAF6 dimerization interface abrogates TRAF6 catalytic activity *in vitro* [77]. However, the substrate binding domains of TRAF6 and other TRAF family members form trimmers in solution [78,80-82]. In addition, the oligomerization state of TRAF6 when bound to substrates is unclear due to the fact that some known substrates have 1-3 putative TRAF6 binding motifs and some substrates, including IRAK1, are known to dimerize.

We sought to determine the stoichiometry of the TRAF6:IRAK1 complex. Again, we used the TRAF6-C construct, which has been reported to be monomeric in solution at micromolar concentrations [78]. Using sedimentation velocity analytical ultracentrifugation analyses, we find that IRAK1 Ct and TRAF6 sediment as simple monomeric species with sedimentation coefficients of 1.4 S and 1.9 S, respectively (Figure 5.4A). The molecular weights of both proteins are 20kDa, so the differences seen in sedimentation coefficients suggest differences in the hydrodynamic properties of the proteins. This is not surprising considering IRAK1 Ct is proline-rich and is predicted to be a disordered region of IRAK1. We therefore assume that IRAK1 Ct is not a globular protein. A mixture comprising of a 1:1 molar ratio of TRAF6-C and IRAK1 Ct shows two species with sedimentation coefficients of 1.6 S and 2.6 S. The smaller of these species has a sedimentation value close to that of IRAK1 Ct alone and likely represents unbound IRAK1 Ct. The larger species is consistent with formation of a species containing IRAK1 monomer bound to TRAF6-C.

We then turned to sedimentation equilibrium analytical ultracentrifugation experiments to elucidate the TRAF6:IRAK1 stoichiometry. Sedimentation equilibrium data plotted as $\ln A_{280\text{nm}}$ against the square of the radial position reveals a straight line with a slope proportional to the sample's weight average molecular weight. TRAF6-C sediments as a 20kDa globular protein, indicating that it is a monomer at a protein concentration of 45 μM (Figure 5.4B). Much like the

sedimentation velocity experiments, IRAK1 Ct sediments like a smaller protein compared to TRAF6-C, but in actuality, it is sedimenting as a non-globular protein. When we mix TRAF6-C and IRAK1 Ct in equimolar concentrations, the sample sediments as a 40kDa globular protein. However, a sample containing a 2:1 molar ratio of TRAF6-C to IRAK1 Ct sediments larger than 40kDa globular protein. When we increase the amount of TRAF6-C to a 3:1 molar ratio of TRAF6-C and IRAK1 Ct, the size of the sedimenting species decreases to the size of the species in a 1:1 mixture. We presume that the 1:1 and 3:1 TRAF6-C:IRAK1Ct mixtures sediment approximately the same size because both mixtures have excess IRAK1Ct or TRAF6-C, which lowers the average molecular weight of the sample. These data suggest that TRAF6-C forms a 2:1 complex with IRAK1 Ct. It is likely that the TRAF6 interacts with the second and third motifs in IRAK Ct and not with the first motif, which in the peptide binding studies bound TRAF6 with a much weaker affinity ($K_D = 518\mu\text{M}$). We have purified an IRAK1 Ct construct that does not contain IRAK1Ct motif 1 (IRAK1CtS, residues 549-712), but this construct is not amenable to SPR binding experiments because it did not immobilize under the amine coupling conditions. Future studies should determine whether IRAK1CtS binds TRAF6-C with the same affinity as IRAK1Ct using other experimental means, such as isothermal titration calorimetry (ITC).

In vivo FRET experiments of full-length TRAF6 suggest that upon LPS stimulation, TRAF6 forms high-order oligomers that can be visualized under the microscope [77]. The aggregation of TRAF6 could act as a functionally relevant scaffold for downstream signaling components. It would be interesting to determine the oligomeric state of full-length TRAF6 and IRAK1 and determine its relevance to IL-1/TLR signaling.

5.3. Conclusion

We have now elucidated the Pellino and TRAF6 binding determinants on IRAK1. Because their substrate binding specificities and RING domains are both quite different, we suspect that these E3 ubiquitin ligases do not play redundant roles in the IL-1/TLR signaling pathways. To gain a

better understanding of the distinct functional roles these E3 ubiquitin ligases play, future studies should compare the timing and location of TRAF6- and Pellino-mediated IRAK1 polyubiquitination. One approach to do this would be to monitor the ubiquitination state of IRAK1 in the presence of cell-permeable TRAF6 or Pellino decoy peptides upon TLR/IL-1R stimulation. Furthermore, it would be insightful to figure out which E2 ubiquitin ligases interact with TRAF6 and Pellinos. It is possible that differences in IRAK1 polyubiquitination can lead to different interactions with downstream components that would in turn, lead to different cellular consequences. Pellino3 have recently been shown to interact with and regulate TRAF6 in the context of the TLR3/4-mediated IRF7 activation pathway [21]. It is possible that Pellinos act upon TRAF6 in a similar manner within the NF- κ B activation pathway.

Figure 5.1 Pellino2 interactions with UbcH7 and Ubc13 are undetectable

(A) Superimposed size exclusion chromatography profiles of Pellino2, Ubc13 or a 1:1 molar ratio mixture of the two proteins (5 μ M each). (B) Superimposed size exclusion chromatography profiles of Pellino2, UbcH7 or a 1:1 molar ratio mixture of the two proteins (5 μ M each). (C) GST or GST-Pellino2 immobilized to glutathione agarose beads were incubated with 10 μ M of Ubc13. Bound protein was eluted by SDS-PAGE loading buffer, analyzed by SDS-PAGE, and detected with Coomassie staining. "In" represents 5% input. In A-C, there is no detectable Pellino2 association with the E2 ubiquitin ligases.

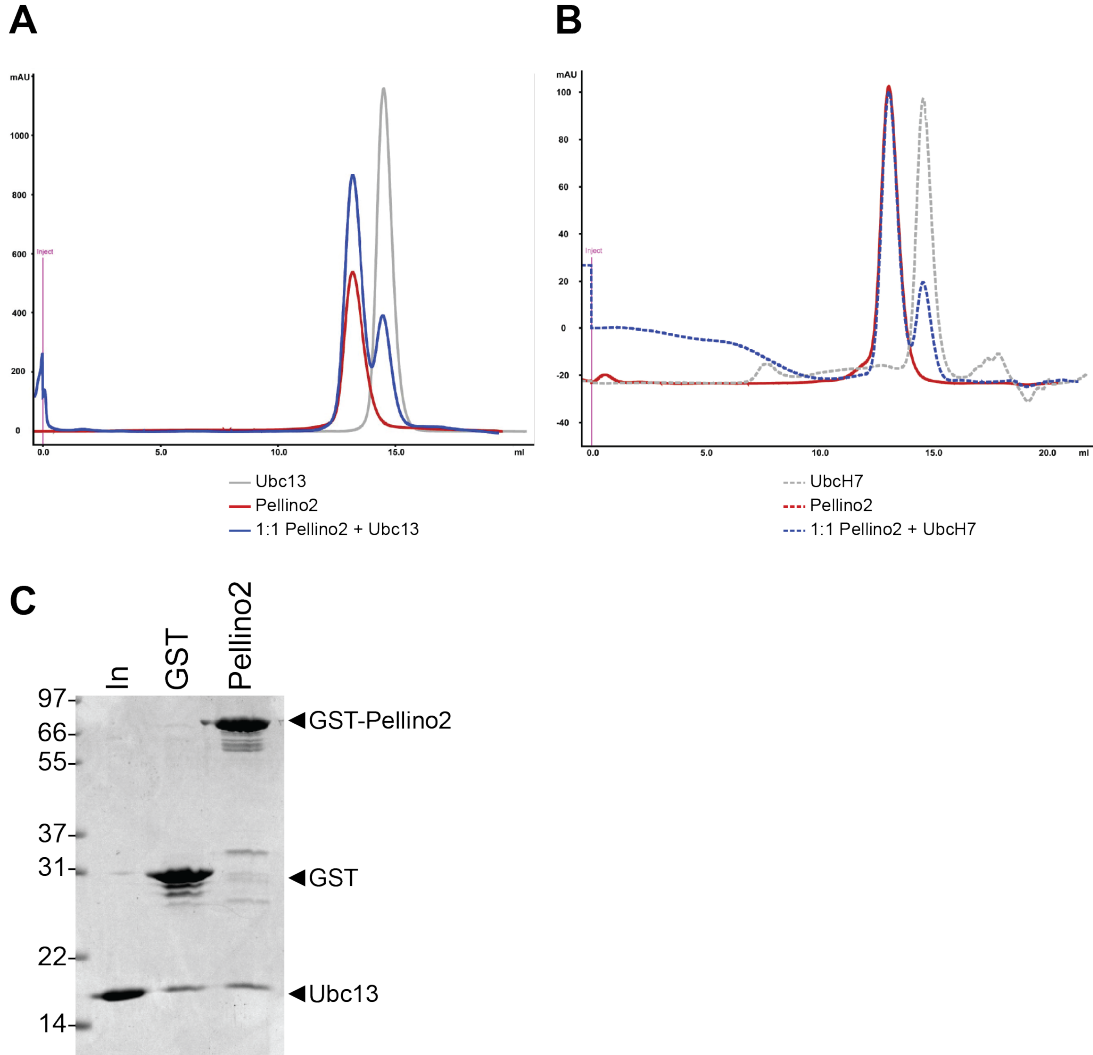


Figure 5.2. *E. coli*-derived Pellino1 and Sf9-derived Pellino2 are more stable than *E. coli*-derived Pellino2.

(A-C) Ni²⁺-NTA gravity flow chromatography fractions at the indicated imidazole concentrations of His₆-tagged proteins analyzed by SDS-PAGE, and detected with Coomassie staining. (A) *E. coli*-derived His₆-Pellino2 is already partially proteolyzed after the first protein purification step. (B) *E. coli*-derived His₆-Pellino1 is not as degraded as Pellino2 after the first protein purification step. (C) There appears to be minimal protein degradation with Sf9-derived His₆-Pellino2.

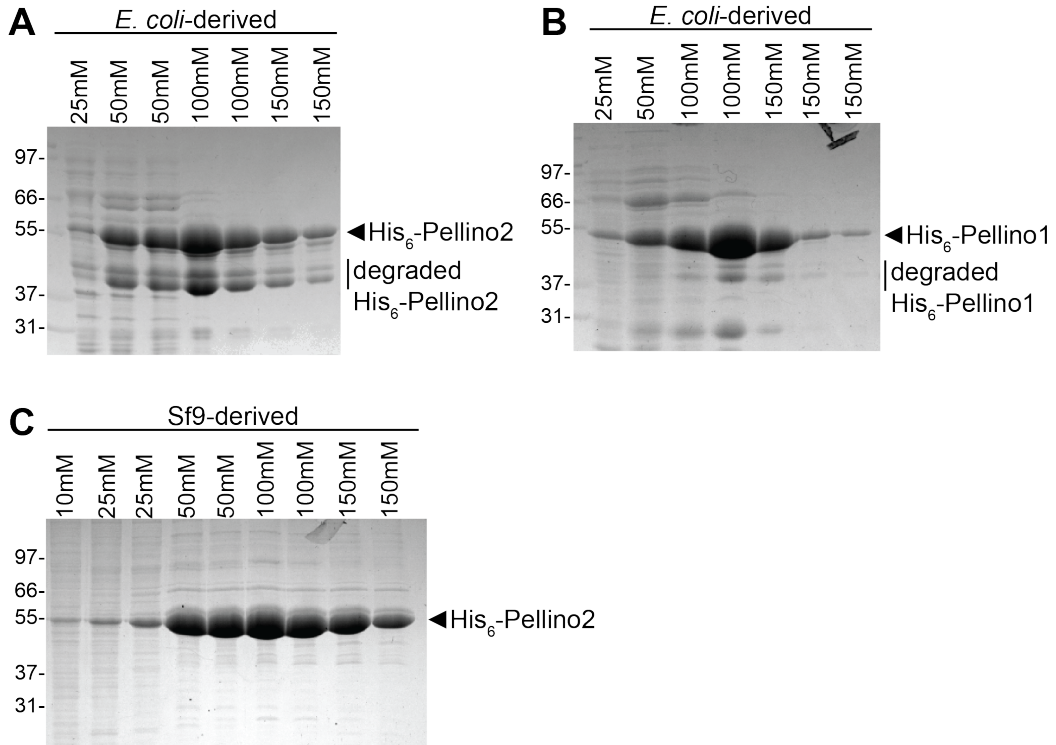


Table 5.1. Crystallization screening summary of full-length Pellinos

Protein	Screens	Details	Details	Results
<i>E. coli</i> -derived Pellino1	Emerald Wizard I-III, Greg Van Duyne Boxes 1-4 (In house), Hampton Index, Hampton Peg/Ion, Qiagen Classics, Qiagen Protein Complex Suite	At 20°C, hanging drop diffusion	Quasi crystals in Greg Van Duyne Box 2 #22 (50mM Imidazole pH 7, 5% PEG 3350, 100mM CaCl ₂)	Crystals seemed to be temperature sensitive? They would disappear and then appear a few weeks later. Not able to reproduce this hit.
Sf9-derived Pellino2	Emerald Wizard I-III, Emerald Cryo I and II, Greg Van Duyne Boxes 1-4 (In house), Hampton Index, Hampton Peg/Ion, Qiagen Classics	At 20°C, hanging drop diffusion	Small, thin clusters in Hampton Index #12 (0.1M TRIS pH 8.5, 3M NaCl) Quasi crystals in Greg Van Duyne Box 2 #22 (50mM Imidazole pH 7.0, 5% PEG 3350, 100mM CaCl ₂)	Could not reproduce these hits.
Sf9-derived Pellino2	Emerald Wizard I-III, Emerald Cryo I and II, Greg Van Duyne Boxes 1-4 (In house), Hampton Index, Hampton Peg/Ion, Qiagen Classics	At 4°C, hanging drop diffusion	Needles in Wizard I #38 (1M Na/K Tartrate, 0.1M CHES pH 9.5, 0.2M Li ₂ SO ₄ , final pH 9.7) Needles in Cryo II #40 (40% MPD, 0.1M CHES pH 9.5) One cluster in Greg Van Duyne Box 4 #14 (50mM Imidazole pH 7, 35% MPD, 0.2M Ammonium Acetate)	Could not reproduce these hits.

Table 5.2. K_D s of Pellino1 and Pellino1-FHA binding to pT-peptides

The K_D values for binding of Pellino1, Pellino1-FHA, Pellino2 and Pellino2-FHA to the indicated peptides were determined. Baseline corrected data were fit to a simple binding equation. All peptides include an N-terminal tyrosine to allow for spectroscopic quantification. -- : not measured.

Peptide	Sequence	Pellino1	Pellino1-FHA	Pellino2	Pellino2-FHA
IRAK1pT141+3D	S-A-S-S-pT-F-L-D-P	0.73	14 ± 4.4	--	4.1 ± 0.6
IRAK1pT141+3I	S-A-S-S-pT-F-L-I-P	0.15	1.8 ± 0.1	--	2.1 ± 0.1
IRAK1pT141+3S	S-A-S-S-pT-F-L-S-P	0.20 ± 0.14	1.7 ± 0.2	0.94	0.82 ± 0.35
IRAK1pT141+3Y	S-A-S-S-pT-F-L-Y-P	0.14 ± 0.08	0.77 ± 0.18	--	0.18 ± 0.04

Figure 5.3. TRAF6 interacts with IRAK1Ct

(A) K_D values for TRAF6-C binding to peptides derived from TRAF6 binding motifs on IRAK1 as determined by isothermal titration calorimetry (ITC). TRAF6 binding motifs on IRAK1 are numbered 1-3, starting from the most N-terminal motif. The asterisked binding data were obtained from [78]. (B) Domain architecture of TRAF6 and IRAK1 along with the constructs used in (C) and Figure 5.4. DD: death domain; PST: Proline, serine, threonine-rich region; Ct: C-terminal domain; Z_{1,4}: TRAF6 zinc fingers; CC: coiled-coiled domain; TRAF: C-terminal TRAF6 substrate binding domain. The molecular weights of both IRAK1Ct and TRAF6-C are 20kDa. (C) SPR analysis of TRAF6-C binding to IRAK1 Ct. A series of samples of TRAF6-C at the indicated concentrations was passed over a CM5 chip to which IRAK1 Ct had been immobilized. The curve indicates the fit of a representative data set to a simple one-site binding equation. The K_D value is 6.0 μ M.

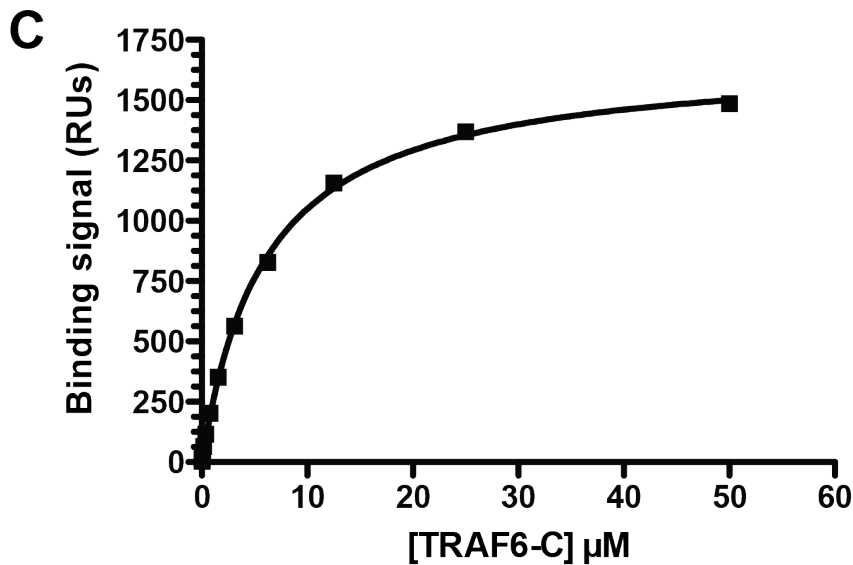
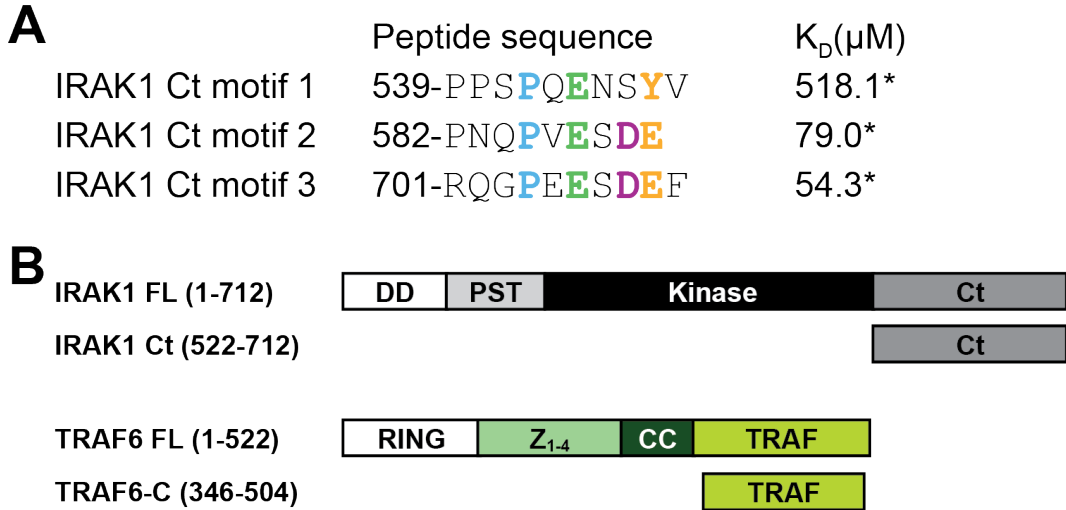
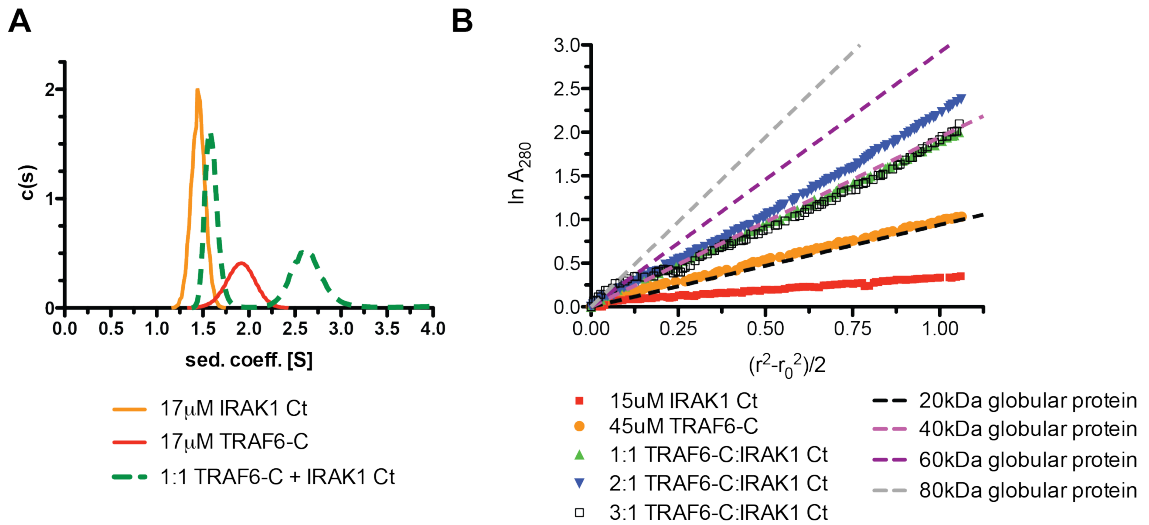


Figure 5.4. TRAF6 and IRAK1 bind with an apparent 2:1 stoichiometry

TRAF6-C, IRAK1Ct, or mixtures of both proteins were analyzed by sedimentation velocity (A) and sedimentation equilibrium (B) analytical ultracentrifugation. All experiments were conducted in 12.5mM MES, 150mM NaCl, 2mM β ME, 1mM TCEP. (A) Sedimentation velocity analytical ultracentrifugation analysis of 17 μ M of TRAF6-C, IRAK1Ct and a 1:1 mixture of TRAF6-C and IRAK1Ct (17 μ M each) by sedimentation coefficient distribution, $c(s)$. (B) TRAF6-C (45 μ M) and IRAK1Ct (15 μ M) with or without increasing concentrations of TRAF6-C (15, 30, 45 μ M) were centrifuged at 20,000rpm. Sedimentation data are plotted as $\ln A_{280}$ against $(r^2 - r_0^2)/2$, where r is the radial position in the sample and r_0 is the radial position of the meniscus. This representation gives a straight line with a slope proportional to the sample's average molecular mass. The dotted lines represent simulated sedimentation equilibrium data for globular proteins at the specified molecular weights.



6. Methods

6.1. Expression vectors

All proteins are human homologs except for mouse Pellino1, which differs by only one amino acid from the human homolog (S146 is asparagine in human). The cDNA for RIP1 (Open Biosystems) was inserted into pcDNA4/HisMaxC (Invitrogen). IRAK1 in p3xFLAG-CMV-14 (Sigma) and pcDNA4/HisMaxC, Pellino2 and TRAF6 in pcDNA4/HisMaxC were generous gifts from Lisolette Jensen (Temple University, Pennsylvania). Expression plasmids for GST-Pellinos and His₆-Pellinos are described in [30]. The appropriate coding regions for truncated IRAK1 and Pellinos were inserted into pcDNA4/HisMaxC and into a pET21-derived HTUA vector (generously provided by Gregory Van Duyne, UPenn), respectively. The cDNA for Ubc13 and UbcH7 (Open Biosystems) were inserted into HTUA. The appropriate coding region for TRAF6-C-His₆ was subcloned into the pET21 vector. The Quikchange site-directed mutagenesis strategy (Stratagene) was used for creating alterations in pcDNA4/HisMaxC-IRAK1-197, His₆- and GST-Pellinos. Full-length Pellino2 was subcloned into the pFastBacHT vector (Invitrogen); the Bac-to-Bac expression system (Invitrogen) was then used for generation of recombinant baculovirus and for protein expression in *Spodoptera frugiperda* (Sf9) insect cells.

6.2 Protein production and purification

6.2.1. *E. coli*-derived protein production and purification

GST- and His₆-Pellino constructs, His₆-Ubc13, His₆-UbcH7, TRAF6-His₆, and His₆-IRAK1 constructs, were expressed in *E. coli* BL21 (DE3) pLys cells at 37°C and induced with 0.5mM IPTG at 25°C for 3-6 hours. Afterwards, cells were pelleted and resuspended in lysis buffer (50mM HEPES, 300mM NaCl, 10% glycerol, pH 7) supplemented with 1mM phenylmethylsulfonyl fluoride (PMSF) and stored at -20°C until ready for use. Cells were thawed and kept at 4°C throughout the purification process unless otherwise noted, and were sonicated 3-5 times at 60%

amplitude for 20-30 seconds (1 second on, 1 second off). Cell lysates were then spun at 35,000g for 25-45 minutes to clear insoluble cellular debris.

Glutathione agarose beads were incubated with cleared lysates containing GST-Pellinos for 30-90 minutes, washed 3 times in 3 bead volumes (BV) 50mM sodium phosphate, 300mM NaCl, pH 7.4, and resuspended in 20mM sodium phosphate, 150mM NaCl, pH 7.4 (PBS). To ensure addition of equal amounts of immobilized GST-proteins for pull-down assays, the amount of immobilized GST-proteins were visualized using SDS-PAGE and normalized with the addition of blank glutathione agarose beads.

Ni²⁺-NTA agarose beads were incubated with cleared lysates containing His₆-tagged proteins for 30-90 minutes. The beads were then resuspended in 5-7 BV of wash buffer (25mM imidazole, 50mM Tris, 300mM NaCl, pH 8) and loaded onto a gravity flow column. Following an additional wash, His₆-tagged proteins were eluted with duplicate 2 BV imidazole concentrations of 50, 100, 150mM (with 50mM Tris, 300mM NaCl, pH 8). Imidazole elutions of 80-90% purity were pooled. To remove the His₆-tag, His₆-Pellino constructs, His₆-IRAK1Ct constructs, His₆-Ubc13, His₆-UbcH7 were incubated with TEV protease [83] (~100µg for every 5mg of His₆-tagged protein) and dialyzed overnight against various dialysis buffers.

His₆-Pellinos were dialyzed against 10mM HEPES, 300mM NaCl, and 5mM β-mercaptoethanol (βME), pH 7.0. His₆-Ubc13 and His₆-UbcH7 were dialyzed against 10mM HEPES, 150mM NaCl, and 5mM βME, pH 7.0. TRAF6-C-His₆ was dialyzed against 10mM MES, 80-150mM NaCl, and 5mM βME, pH 6.5. Dialysis was performed overnight at 4°C for Pellino1 and 2, His₆-Ubc13, His₆-UbcH7, and TRAF6-C-His₆ at 22°C for Pellino3a and 3b. Digested, untagged Pellinos, Ubc13, and UbcH7, and TRAF6-C-His₆ were buffer exchanged into ~80mM NaCl, 5mM βME, in the appropriate pH and purified by cationic exchange chromatography (Source S, GE Healthcare) at pH 6 (Pellinos1, 2 and 3b, Ubc13, UbcH7) or pH 5.5 (Pellino3a). His₆-IRAK1Ct constructs were dialyzed overnight at 4°C against 10mM HEPES, 80mM NaCl, 5mM βME, pH 7.5. TEV-digested, untagged IRAK1 Ct constructs were purified by anion

exchange chromatography (Source Q, GE Healthcare) at pH 7.5. Following ion exchange chromatography, protein fractions were pooled and further purified by size exclusion chromatography (Superose 12, GE Healthcare) in 10mM HEPES, 150mM NaCl, 5mM β ME, pH 7.0 (Pellino constructs, Ubc13, Ubch7, and IRAK1Ct constructs) or 10mM MES, 150mM NaCl, 5mM β ME, pH 6.5 (TRAF6-C-His).

6.2.2. Sf9-derived Pellino2 production and purification

Sf9 cells at $1.5\text{--}2 \times 10^6$ /ml were infected with freshly amplified, recombinant baculovirus and harvested by centrifugation 3 days post infection. Sf9 cells expressing His₆-Pellino2 were then resuspended in lysis buffer (50mM HEPES, 300mM NaCl, 10% glycerol, pH 7) supplemented with general protease inhibitor cocktail (Sigma) plus 1mM PMSF and stored at -20°C until ready for use. Subsequent purification steps of His₆-Pellino2 were exactly the same as *E. coli*-derived protein.

6.3. HEK293T culture conditions and transfections

Human embryonic kidney (HEK) 293T cells were cultured in DMEM supplemented with 10% FBS, 1% Pen-Strep, and 1% L-glutamine at 37°C, 5% CO₂ and split 10-15-fold every 3-4 days. One day prior to transfection, 2.5×10^5 HEK293T cells were seeded per well in a 6-well plate. The next day, cells were at ~75% confluence and transfected with 2 μ g of total DNA plus FuGENE6 (Promega, 4.7 μ l FuGENE6 + 60 μ l DMEM per well in 6 well plate).

6.4. GST-Pellino pull-down assays

6.4.1. Pull-downs of Pellino substrates

Two days post-transfection, HEK293T cells overexpressing IRAK1, IRAK1 truncation mutants, TRAF6, or RIP1 (all Xpress-tagged) were washed with PBS and lysed by vigorous scraping against the tissue culture dish in HEK293T lysis buffer (50mM HEPES pH 7.5, 150mM NaCl,

5mM β ME, 0.1% IGEPAL [octylphenoxyethoxyethanol, Sigma], supplemented with 20mM β -glycerophosphate, 1mM EDTA, 50mM NaF, 1mM Na_3VO_4 , protease inhibitor cocktail [Sigma]. For HEK293T cells overexpressing RIP1, HEK293T lysis buffer was additionally supplemented with PhosSTOP (Roche). Lysates were subsequently kept at 4°C unless otherwise noted. After incubation for 20 minutes on ice, lysates were spun at 16,000g to clear cellular debris. Lysates were incubated with GST-Pellino proteins immobilized on glutathione agarose beads (50 μ l) for 4 hours to overnight. Beads were washed 3 times with HEK293T lysis buffer and resuspended in SDS-PAGE loading buffer for western blot analysis.

For dephosphorylation of IRAK1-197, HEK293T cells overexpressing Xpress-IRAK1-197 were lysed in 50mM HEPES pH 7.5, 100mM NaCl, 10mM MgCl_2 , 5mM β ME, 0.1% IGEPAL supplemented with protease inhibitor cocktail (Sigma) and incubated for 1 hour at 37°C with or without calf intestinal phosphatase (CIP, New England Biolabs; 10U/100 μ l of lysate). CIP treatment was stopped with 5mM EDTA and the addition of 1mM sodium vanadate or PhosSTOP (Roche).

Western blots were probed with α -Xpress (Invitrogen) or α -phosphothreonine (pT, Invitrogen or Cell Signaling) and detection used horseradish peroxidase conjugated to α -mouse and α -rabbit (GE Healthcare), or IRDye680RD- α -rabbit and IRDye800CW- α -mouse (Li-COR Biosciences).

6.4.2. Pull-down of Ubc13

GST-Pellino immobilized to agarose beads was incubated with 200 μ l of 10 μ M Ubc13 in binding buffer (10mM HEPES, 150mM NaCl, 5mM β ME) for 1 hour at 4°C. Beads were washed 3 times with binding buffer and proteins were eluted with SDS-PAGE buffer. Bound protein was eluted by 60 μ l SDS-PAGE loading buffer, analyzed by SDS-PAGE, and detected with Coomassie staining.

6.5. Far western analyses

HEK293T lysates overexpressing FLAG-IRAK1 were separated by SDS-PAGE, transferred to nitrocellulose membranes, and analyzed by western and far western blotting. α -FLAG (Sigma), α -His₄ (Qiagen), and α -pT (Invitrogen) were used for western blots. For far western blots, nitrocellulose membranes were incubated with 6ml of Pellino2 or Pellino2R106A (10 μ g/ml) in 10mM HEPES, 150mM NaCl, 5mM β ME, 0.3% bovine serum albumin (BSA) for 2 hours at 25°C. Far western blots were washed 3 times with 50mM Tris, 150mM NaCl, 0.05% Triton X-100 (TBST) and subsequently probed with α -His₄ as if performing a western blot.

6.6. Peptide pull-down assays

Peptides were synthesized using standard Fmoc chemistry with free N-termini and purified by reverse-phase HPLC (made in the laboratory of P. Leslie Dutton, UPenn). The purity and molecular mass were confirmed by MALDI time-of-flight mass spectrometry. The following peptides were made: IRAK1-derived peptides WVRDQpTELRL; SGQRpTASVLW; WSPGTpTAPRP; WISRGpTHNFSE; TVRGpTLAY; Rad9-derived peptides: WSLEVpTEADT (Rad9pT192); WSLEVTEADT (Rad9T192). Some experiments used the Rad9p peptide YSLEVpTEADT, which was purchased from Bio Basic Inc. Lyophilized HPLC-purified peptides were resuspended in DMSO and amine coupled to Affi-Gel 15 agarose beads (Bio-Rad) according to the manufacturer's protocol. Peptide-coupled beads were equilibrated with binding buffer (25 mM HEPES, 300 mM NaCl, and 1 mM DTT, pH 7.0). For each pull-down reaction, 100 μ l of Pellino1, 2, 3b, Pellino2-FHA (residues 15-275) or Pellino2 R106A (50 μ M, in binding buffer) was incubated with 20 μ l peptide-coupled beads for 1 hour at 4°C. The beads were washed three times with binding buffer supplemented with 0.1% Triton X-100. Bound protein was eluted by 40 μ l SDS-PAGE loading buffer, analyzed by SDS-PAGE, and detected with Coomassie staining.

6.7. Isothermal titration calorimetry

Pellino2-FHA and pT141+3S peptide used in the ITC experiment were dialyzed overnight into 25 mM HEPES pH 7.0, 150mM NaCl, 5mM β ME at 4°C. Protein and peptide solutions were quantified by UV spectrophotometry. Extinction coefficients for proteins were determined by Protein Calculator v3.3 (<http://www.scripps.edu/~cdputnam/protcalc.html>). The ITC experiment was performed using an ITC200 microcalorimeter (MicroCal Inc). pT141+3S peptide (275 μ M) was titrated into a sample cell containing Pellino2-FHA (25 μ M) in 16 serial injections at 20°C. Experimental data was analyzed using ORIGIN software as per the manufacturer's instructions.

6.8. IRAK1 dephosphorylation protection assay

HEK293T cells transfected with Xpress-IRAK1 were lysed with HEK293T lysis buffer. Cleared lysates were first incubated with protein G agarose (Invitrogen) for 1 hour at 4°C to remove proteins that non-specifically interact with protein G agarose beads. IRAK1 was immunoprecipitated from the lysates by using IRAK1 antibody (Santa Cruz Biotechnologies) and protein G agarose beads overnight. IRAK1 immobilized onto beads were washed with wash buffer (50mM HEPES, 150mM NaCl, 5mM β ME, pH 7.5) and then treated with or without Antarctic phosphatase (AP, 5U per reaction) in the presence of Pellino2 (1 μ M) in Antarctic phosphatase (AP) reaction buffer (wash buffer supplemented with 1mM MgCl₂ and 0.1mM ZnCl₂) for 45 minutes at 37°C with gentle agitation. After 1 wash with wash buffer, IRAK1 was then eluted from protein G agarose by denaturation, separated by SDS-PAGE, and visualized by immunoblotting. Xpress-antibody was used to visualize IRAK1, pT-antibody was used to visualize phosphorylated threonines, and detection used horseradish peroxidase conjugated to α -mouse and α -rabbit (GE Healthcare).

6.9. Detection of IRAK1 polyubiquitination

Xpress-Pellino2, and FLAG-IRAK1 (2 μ g of DNA total) was transfected into HEK293T cells. Cells were lysed 1 day after transfection. Cleared lysates were first incubated with protein G agarose (2.5 μ l, Invitrogen) for 20 minutes at 4°C to remove proteins that non-specifically interact with protein G agarose beads. IRAK1 was immunoprecipitated from the lysates by using IRAK1 antibody (Santa Cruz Biotechnologies) and protein G agarose beads (20 μ l) overnight. Beads were washed 3 times with HEK293T lysis buffer and resuspended in SDS-PAGE loading buffer for western blot analysis. Western blots were probed with α -Xpress (Invitrogen) and α -ubiquitin (Dako); detection used horseradish peroxidase conjugated to α -mouse and α -rabbit (GE Healthcare).

6.10. Fluorescence polarization peptide binding assays

C-terminally amidated peptides were purchased from Bio Basic Inc., AnaSpec, or Keck Biotechnology Resource Laboratory (Yale University). These peptides were N-terminally labeled with fluorescein-5-isothiocyanate (FITC) or 5,6-Carboxyfluorescein (5,6-FAM) by the manufacturer, or in-house. For in-house labeling, amine-reactive FITC (Invitrogen) dissolved in DMSO (10mg/ml) was added to peptide in 0.1M sodium bicarbonate at pH 9.0 (~10mg/ml). The reaction was constantly stirred for 60-120 minutes at room temperature. To remove excess FITC label, the reaction was spun through a BioSpin6 (Bio-Rad) column pre-equilibrated in PBS.

Due to the light-sensitivity of fluorescein, peptides' exposures to light were kept to a minimum. Peptide binding reactions (100 μ l) contained 50nM fluorescein-labeled peptide plus increasing concentrations of Pellinos (0-190 μ M) in PBS. Fluorescence polarization for each sample was measured using a Beacon 2000 system (Panvera) –use of which was generously provided by Prof. Gregory Van Duyne (UPenn). Data were fitted to a simple binding isotherm using Prism (GraphPad Software). All fluorescence polarization (mP) values were normalized to the mP value from no added Pellino. For binding experiments with low affinity peptides, protein

concentrations did not reach maximum specific polarization (B_{max}), so data fitting required a constrained B_{max} ; the constrained B_{max} values used were from B_{max} values obtained from experiments with the same Pellino proteins binding to IRAK1-derived pT141+3S peptide.

6.11. Protein X-ray crystallography

6.11.1. Pellino:peptide co-crystallization screening

Peptides (>99.5% purity) that were used in crystallization studies were dissolved and dialyzed against 10mM HEPES pH 7 and 80mM NaCl for 2-3 days at 4°C to ensure removal of trifluoroacetic acid (TFA). The IRAK1pT141 long peptide (IRAK1pT141L) has the following sequence: YKLPSSASpTFLSPAFP (Bio Basic Inc.). The pH of the peptides was always checked to ensure the TFA had been fully removed. Gel filtration fractions of Pellino1, Pellino2, and truncation variants were pooled, concentrated, and buffer exchanged into 10mM HEPES pH 7, 75mM NaCl and reducing agent [5mM β ME, 1mM dithiothreitol (DTT), or 2mM *tris*(2-carboxyethyl)phosphine (TCEP)]. Concentrated proteins were mixed with 200-1000 μ M peptides in varying ratios to make up 10mg/ml of total protein. The Mosquito Crystal (TTP Labtech) was used to set up 96-well hanging-drop crystal screens: 100 μ l of screening conditions were dispensed into 96 well plate, 100-300nl of ~10mg/ml protein were mixed with 200-400nl of reservoir solution and equilibrated over 100 μ l of reservoir solution at 20°C.

6.11.2. Peptide soaking of Pellino2 crystals

Expression and purification methods for Pellino2-FHA^{V61M/L232M} are exactly the same as Pellino2-FHA. Gel filtration fractions of Pellino2-FHA^{V61M/L232M} were pooled, concentrated, and buffer exchanged into 10mM HEPES pH 7, 75mM NaCl and 5mM β ME. Pellino2-FHA^{V61M/L232M} was crystallized using the hanging-drop vapor diffusion method. Equal volumes of Pellino2-FHA^{V61M/L232M} (10mg/ml) and reservoir solution (100mM sodium acetate pH 4.6 or 4.8 and 3.25M

sodium formate) were mixed and equilibrated over the reservoir solution at 20°C. 2µl of 8.5% glutaraldehyde was placed next to the drop containing crystals and the drops were left to equilibrate with reservoir for 10-15 minutes until the protein started precipitating from drops containing crystals. Precipitation caused the transfer of cross-linked crystal to be very tedious, so alternatively, crystals would be transferred to stabilization solution (reservoir plus 5% ethylene glycol) prior to crosslinking. Cross-linked crystals were transferred into cryoprotectant [reservoir solution plus ~150mM pT141+3Y peptide, supplemented with either 6% glycerol, 6% ethylene glycol, 6% 2-methyl-2,4-pentanediol (MPD) or 7.5% PEG 400, 7.5% PEG 1000] for 1-5 minutes. The cross-linked crystals were flash frozen from cryoprotectant. Data were collected at the Advanced Photon Source GM/CA 23-ID-B beam line. Data were processed with HKL-2000 [84] and solved by molecular replacement in the program PHASER [57]. The canonical FHA core of the Pellino2-FHA structure (PDB ID: 3ega) was used as a search model.

6.11.3. Pellino3a-FHA protein crystallization and structure determination

For the spontaneous crystallization of Pellino3a-FHA, gel filtration fractions of Pellino3a-FHA were pooled, concentrated to ~9mg/ml (300µl), and incubated in a 1.5ml microcentrifuge tube at 4°C for ~6 weeks. Pellino3a-FHA crystals also formed by the hanging drop vapor diffusion by setting up 1-5µl drops of Pellino3a-FHA (6-10mg/ml) and equilibrating over gel filtration buffer (10mM HEPES pH 7, 150mM NaCl, 5mM βME) at 20°C. Pellino3a-FHA at high protein concentrations (>6mg/ml) was very sensitive to spontaneous nucleation so precautionary steps were taken to reduce the amount of nucleations: concentrating small volumes of protein at a time (~30µl final concentrated volume); keeping highly concentrated, 0.22µM filtered Pellino3a-FHA at 20°C; using low-retention 1.5ml microcentrifuge tubes; changing pipet tips after setting up each crystallization drop; keeping pipet tip direct contact with tube and cover slip surfaces at a minimum; setting up drops as quickly as possible. To improve X-ray diffraction of these Pellino3a-FHA crystals, we also tried dehydrating crystals. Crystals were transferred to 1-2µl drops

containing 10mM HEPES pH 7, 150mM NaCl, and 5mM β ME with or without 10-15% ethylene glycol. The drops were equilibrated with the same solution in the reservoir for ~16 hours at 20°C.

For other crystallization conditions using the hanging drop vapor diffusion method, equal amounts of Pellino3a-FHA (6-10mg/ml) were mixed with and equilibrated over reservoir solutions at 20°C. We also attempted to control crystal growth by crystal seeding into lower concentrations of Pellino3a-FHA. A Pellino3a-FHA crystal (~70 μ m³ in size) was transferred to 75mM HEPES pH 7, 600mM sodium tartrate, 5% ethylene glycol and crushed with a seed bead (Hampton) as per the manufacturer's instruction. A 1:1000 dilution of crushed Pellino3a-FHA crystals was streak-seeded into Pellino3a (2.8-8.5mg/ml) and reservoir solution (75mM HEPES pH 7, 600mM sodium tartrate) mixed in equal volumes and equilibrated over reservoir solution at 20°C.

All crystals were cryoprotected by adding gel filtration buffer supplemented with 66% ethylene glycol until the concentration of ethylene glycol reached ~33% and directly flash frozen from the drop. Data was collected at the Advanced Photon Source GM/CA 23-ID-B beam line. Data was processed with HKL-2000 [84] and was solved by molecular replacement (MR) in the program PHASER [57]. The canonical FHA core of the Pellino2-FHA structure (PDB ID: 3ega) was used as a search model.

6.11.4. Pellino1 and 2 full length crystal screening

Gel filtration fractions of Pellino1 and 2 were pooled, concentrated, and buffer exchanged into 10mM HEPES pH 7, 75mM NaCl and reducing agent (5mM β ME, 1mM DTT, or 2mM TCEP). Hanging drops for crystallization screens were set up exactly like the Pellino:peptide co crystallization screens. Crystallography screening trays were incubated at 4°C or 20°C.

6.12. Surface plasmon resonance binding experiments

SPR experiments were performed on a Biacore3000 instrument (GE healthcare) at 25°C in 25mM HEPES, 150mM NaCl, 3 mM EDTA, 0.005% Tween-20, pH 7.5. The hydrogel matrix of a

Biacore CM5 biosensor chip was activated with N-ethyl-N'-(dimethylaminopropyl)-carbo-diimide hydrochloride and N-hydroxysuccinimide. IRAK1Ct (100µg/ml in 10 mM sodium acetate, pH 4.5) was flowed over this activated surface at a rate of 5 µl/min for 7 minutes. The remaining reactive sites were blocked with 1 M ethanolamine-HCl (pH 8.5). The signal contributed by immobilized IRAK1 constructs ranged from 1100-1850 response units (RUs). TRAF6 binding response values are reported after reference (mock-coupled surface binding) subtraction. Data were analyzed using Prism (GraphPad).

6.13. Analytical ultracentrifugation experiments

Sedimentation velocity and sedimentation equilibrium analytical ultracentrifugation experiments were performed in a Beckman Optima XL-A instrument, at 20°C in 12.5mM MES, 150mM NaCl, 2mM βME, 1mM *tris*(2-carboxyethyl)phosphine (TCEP). Absorbance at 280 nm was measured to detect protein distribution. For sedimentation velocity experiments, 17µM of TRAF6, IRAK1Ct or a 1:1 molar ratio mixture of both proteins were centrifuged at 42500 rpm, at 20°C in 12.5mM MES, 150mM NaCl, 2mM βME, 1mM TCEP. Continuous distributions were calculated by *c*(*s*) analysis in SEDFIT (<http://www.analyticalultracentrifugation.com>) using solution and protein property estimates from SEDNTERP (<http://www.jphilo.mailway.com>). For sedimentation equilibrium experiments, TRAF6-C (45µM) and IRAK1Ct (15µM) with or without increasing concentrations of TRAF6-C (15, 30, 45µM) were centrifuged at 10,000, 15,000, and 20,000 rpm. Data were analyzed with SEDFIT and SEDPHAT (<http://www.analyticalultracentrifugation.com>).

Sedimentation equilibrium data were plotted as $\ln A_{280}$ against $(r^2 - r_0^2)/2$, where *r* is the radial position in the sample and *r*₀ is the radial position of the meniscus. This representation gives a straight line with a slope proportional to the average molecular mass of the sample.

HeteroAnalysis [85] was used to simulate sedimentation equilibrium data for 20, 40, 60, and 80kDa globular proteins.

BIBLIOGRAPHY

- 1 Kumar, H., Kawai, T. and Akira, S. (2011) Pathogen recognition by the innate immune system. *Int. Rev. Immunol.* **30**, 16–34.
- 2 Kawai, T. and Akira, S. (2010) The role of pattern-recognition receptors in innate immunity: update on Toll-like receptors. *Nat. Immunol.* **11**, 373–384.
- 3 Wertz, I. E. and Dixit, V. M. (2010) Signaling to NF-kappaB: regulation by ubiquitination. *Cold Spring Harbor Perspect. in Biol.* **2**, a003350.
- 4 Hershko, A. and Ciechanover, A. (1998) The ubiquitin system. *Annu. Rev. Biochem.* **67**, 425–479.
- 5 Rieser, E., Cordier, S. M. and Walczak, H. (2013) Linear ubiquitination: a newly discovered regulator of cell signalling. *Trends Biochem. Sci.* **38**, 94–102.
- 6 Chen, Z. J. and Sun, L. J. (2009) Nonproteolytic functions of ubiquitin in cell signaling. *Mol. Cell* **33**, 275–286.
- 7 Schauvliege, R., Janssens, S. and Beyaert, R. (2007) Pellino Proteins: Novel Players in TLR and IL-1R Signalling. *J. Cell. Mol. Med.* **11**, 453–461.
- 8 Moynagh, P. N. (2009) The Pellino family: IRAK E3 ligases with emerging roles in innate immune signalling. *Trends Immunol.* **30**, 33–42.
- 9 Jin, W., Chang, M. and Sun, S.-C. (2012) Peli: a family of signal-responsive E3 ubiquitin ligases mediating TLR signaling and T-cell tolerance. *Cell. Mol. Immunol.* **9**, 113–122.
- 10 Yang, S., Wang, B., Humphries, F., Jackson, R., Healy, M. E., Bergin, R., Aviello, G., Hall, B., McNamara, D., Darby, T., et al. (2013) Pellino3 ubiquitinates RIP2 and mediates Nod2-induced signaling and protective effects in colitis. *Nat. Immunol.* **14**, 927–936.
- 11 Schauvliege, R., Janssens, S. and Beyaert, R. (2006) Pellino proteins are more than scaffold proteins in TLR/IL-1R signalling: A role as novel RING E3-ubiquitin-ligases. *FEBS Lett.* **580**, 4697–4702.
- 12 Butler, M. P., Hanly, J. A. and Moynagh, P. N. (2007) Kinase-active Interleukin-1 Receptor-associated Kinases Promote Polyubiquitination and Degradation of the Pellino Family DIRECT EVIDENCE FOR PELLINO PROTEINS BEING UBIQUITIN-PROTEIN ISOPEPTIDE LIGASES. *J. Biol. Chem., ASBMB* **282**, 29729–29737.
- 13 Ordureau, A., Smith, H., Windheim, M., Peggie, M., Carrick, E., Morrice, N. and Cohen, P. (2008) The IRAK-catalysed activation of the E3 ligase function of Pellino isoforms induces the Lys63-linked polyubiquitination of IRAK1. *Biochem. J.* **409**, 43–52.
- 14 Krishnan, J., Selvarajoo, K., Tsuchiya, M., Lee, G. and Choi, S. (2007) Toll-like receptor signal transduction. *Exp. Mol. Med.* **39**, 421–438.
- 15 Ofengeim, D. and Yuan, J. (2013) Regulation of RIP1 kinase signalling at the crossroads of inflammation and cell death. *Nat. Rev. Mol. Cell Biol.* **14**, 727–736.
- 16 Xiao, H., Qian, W., Staschke, K., Qian, Y., Cui, G., Deng, L., Ehsani, M., Wang, X., Qian, Y. W., Chen, Z. J., et al. (2008) Pellino 3b Negatively Regulates Interleukin-1-induced TAK1-dependent NF B Activation. *J. Biol. Chem.* **283**, 14654–14664.
- 17 Chang, M., Jin, W. and Sun, S.-C. (2009) Peli1 facilitates TRIF-dependent Toll-like receptor signaling and proinflammatory cytokine production. *Nat. Immunol., Nature Publishing Group* **10**, 1089–1095.
- 18 Kim, T. W., Yu, M., Zhou, H., Cui, W., Wang, J., DiCorleto, P., Fox, P., Xiao, H. and Li, X. (2012) Pellino 2 Is critical for Toll-like Receptor/Interleukin-1 Receptor (TLR/IL-1R)-mediated Post-transcriptional Control. *J. Biol. Chem.* **287**, 25686–25695.
- 19 Wu, C.-J., Conze, D. B., Li, T., Srinivasula, S. M. and Ashwell, J. D. (2006) Sensing of Lys 63-linked polyubiquitination by NEMO is a key event in NF-kappaB activation. *Nat. Cell Biol.* **8**, 398–406.
- 20 Conze, D. B., Wu, C. J., Thomas, J. A., Landstrom, A. and Ashwell, J. D. (2008) Lys63-Linked Polyubiquitination of IRAK-1 Is Required for Interleukin-1 Receptor- and Toll-Like Receptor-Mediated NF-B Activation. *Mol. Cell. Biol.* **28**, 3538–3547.

- 21 Siednienko, J., Jackson, R., Mellett, M., Delagic, N., Yang, S., Wang, B., Tang, L. S., Callanan, J. J., Mahon, B. P. and Moynagh, P. N. (2012) Pellino3 targets the IRF7 pathway and facilitates autoregulation of TLR3- and viral-induced expression of type I interferons. *Nat. Immunol.* **13**, 1055–1062.
- 22 Enesa, K., Ordureau, A., Smith, H., Barford, D., Cheung, P. C. F., Patterson-Kane, J., Arthur, J. S. C. and Cohen, P. (2012) Pellino1 is required for interferon production by viral double-stranded RNA. *J. Biol. Chem.* **287**, 34825–34835.
- 23 Strober, W., Murray, P. J., Kitani, A. and Watanabe, T. (2006) Signalling pathways and molecular interactions of NOD1 and NOD2. *Nat. Rev. Immunol.* **6**, 9–20.
- 24 Kanayama, A., Seth, R. B., Sun, L., Ea, C.-K., Hong, M., Shaito, A., Chiu, Y.-H., Deng, L. and Chen, Z. J. (2004) TAB2 and TAB3 activate the NF-kappaB pathway through binding to polyubiquitin chains. *Mol. Cell* **15**, 535–548.
- 25 Chang, M., Jin, W., Chang, J.-H., Xiao, Y., Brittain, G. C., Yu, J., Zhou, X., Wang, Y.-H., Cheng, X., Li, P., et al. (2011) The ubiquitin ligase Peli1 negatively regulates T cell activation and prevents autoimmunity. *Nat. Immunol.* **12**, 1002–1009.
- 26 Smith-Garvin, J. E., Koretzky, G. A. and Jordan, M. S. (2009) T cell activation. *Annu. Rev. Immunol.* **27**, 591–619.
- 27 Cheng, J., Montecalvo, A. and Kane, L. P. (2011) Regulation of NF-κB induction by TCR/CD28. *Immunol. Res.* **50**, 113–117.
- 28 Yang, S., Wang, B., Tang, L. S., Siednienko, J., Callanan, J. J. and Moynagh, P. N. (2013) Pellino3 targets RIP1 and regulates the pro-apoptotic effects of TNF-α. *Nat. Commun.* **4**, 2583.
- 29 Xiao, Y., Jin, J., Chang, M., Chang, J.-H., Hu, H., Zhou, X., Brittain, G. C., Stansberg, C., Torkildsen, Ø., Wang, X., et al. (2013) Peli1 promotes microglia-mediated CNS inflammation by regulating Traf3 degradation. *Nat. Med.* **19**, 595–602.
- 30 Lin, C.-C., Huoh, Y.-S., Schmitz, K. R., Jensen, L. E. and Ferguson, K. M. (2008) Pellino proteins contain a cryptic FHA domain that mediates interaction with phosphorylated IRAK1. *Structure* **16**, 1806–1816.
- 31 Durocher, D., Henckel, J., Fersht, A. R. and Jackson, S. P. (1999) The FHA domain is a modular phosphopeptide recognition motif. *Mol. Cell* **4**, 387–394.
- 32 Durocher, D., Taylor, I. A., Sarbassova, D., Haire, L. F., Westcott, S. L., Jackson, S. P., Smerdon, S. J. and Yaffe, M. B. (2000) The molecular basis of FHA domain: phosphopeptide binding specificity and implications for phospho-dependent signaling mechanisms. *Mol. Cell, Elsevier* **6**, 1169–1182.
- 33 Durocher, D. and Jackson, S. P. (2002) The FHA domain. *FEBS Lett., Elsevier* **513**, 58–66.
- 34 Mahajan, A., Yuan, C., Lee, H., Chen, E. S. W., Wu, P.-Y. and Tsai, M.-D. (2008) Structure and function of the phosphothreonine-specific FHA domain. *Sci Signal* **1**, re12.
- 35 Pennell, S., Westcott, S., Ortiz-Lombardía, M., Patel, D., Li, J., Nott, T. J., Mohammed, D., Buxton, R. S., Yaffe, M. B., Verma, C., et al. (2010) Structural and Functional Analysis of Phosphothreonine-Dependent FHA Domain Interactions. *Structure, Elsevier Ltd* **18**, 1587–1595.
- 36 Jiang, Z. (2002) Pellino 1 Is Required for Interleukin-1 (IL-1)-mediated Signaling through Its Interaction with the IL-1 Receptor-associated Kinase 4 (IRAK4)-IRAK-Tumor Necrosis Factor Receptor-associated Factor 6 (TRAF6) Complex. *J. Biol. Chem.* **278**, 10952–10956.
- 37 Jensen, L. E. and Whitehead, A. S. (2003) Pellino2 activates the mitogen activated protein kinase pathway. *FEBS Lett.* **545**, 199–202.
- 38 Strelow, A., Kollwe, C. and Wesche, H. (2003) Characterization of Pellino2, a substrate of IRAK1 and IRAK4. *FEBS Lett.* **547**, 157–161.
- 39 Brooks, L., Heimsath, E. G., Loring, G. L. and Brenner, C. (2008) FHA-RING ubiquitin ligases in cell division cycle control. *Cell. Mol. Life Sci.* **65**, 3458–3466.
- 40 Karin, M. and Ben-Neriah, Y. (2000) Phosphorylation meets ubiquitination: the control of NF-κB activity. *Annu. Rev. Immunol.* **18**, 621–663.

- 41 Hunter, T. (2007) The age of crosstalk: phosphorylation, ubiquitination, and beyond. *Mol. Cell* **28**, 730–738.
- 42 Griffin, B. D., Mellett, M., Campos-Torres, A., Kinsella, G. K., Wang, B. and Moynagh, P. N. (2011) A poxviral homolog of the Pellino protein inhibits Toll and Toll-like receptor signalling. *Eur. J. Immunol.* **41**, 798–812.
- 43 Rich, T., Allen, R. L., Lucas, A.-M., Stewart, A. and Trowsdale, J. (2000) Pellino-related sequences from *Caenorhabditis elegans* and *Homo sapiens*. *Immunogenetics* **52**, 145–149.
- 44 Waterhouse, A. M., Procter, J. B., Martin, D. M. A., Clamp, M. and Barton, G. J. (2009) Jalview Version 2—a multiple sequence alignment editor and analysis workbench. *Bioinformatics* **25**, 1189–1191.
- 45 Smith, H., Peggie, M., Campbell, D. G., Vandermoere, F., Carrick, E. and Cohen, P. (2009) Identification of the phosphorylation sites on the E3 ubiquitin ligase Pellino that are critical for activation by IRAK1 and IRAK4. *Proc. Natl. Acad. Sci. U. S. A.* **106**, 4584–4590.
- 46 Huoh, Y.-S. and Ferguson, K. M. The Pellino E3 ubiquitin ligases recognize specific phosphothreonine motifs and have distinct substrate specificities. (Submitted to *Biochem. J.*)
- 47 Yaffe, M. B. and Smerdon, S. J. (2004) The use of in vitro peptide-library screens in the analysis of phosphoserine/threonine-binding domain structure and function. *Annu Rev Biophys Biomol Struct* **33**, 225–244.
- 48 Liao, H., Yuan, C., Su, M. I., Yongkiettrakul, S., Qin, D., Li, H., Byeon, I. J., Pei, D. and Tsai, M. D. (2000) Structure of the FHA1 domain of yeast Rad53 and identification of binding sites for both FHA1 and its target protein Rad9. *J. Mol. Biol.* **304**, 941–951.
- 49 Alderwick, L. J., Molle, V., Kremer, L., Cozzone, A. J., Dafforn, T. R., Besra, G. S. and Fütterer, K. (2006) Molecular structure of EmbR, a response element of Ser/Thr kinase signaling in *Mycobacterium tuberculosis*. *Proc. Natl. Acad. Sci. U. S. A.* **103**, 2558–2563.
- 50 Kollwe, C. (2003) Sequential Autophosphorylation Steps in the Interleukin-1 Receptor-associated Kinase-1 Regulate its Availability as an Adapter in Interleukin-1 Signaling. *J. Biol. Chem.* **279**, 5227–5236.
- 51 Mamidipudi, V., Lin, C., Seibenhener, M. L. and Wooten, M. W. (2004) Regulation of interleukin receptor-associated kinase (IRAK) phosphorylation and signaling by iota protein kinase C. *J. Biol. Chem.* **279**, 4161–4165.
- 52 Blom, N., Gammeltoft, S. and Brunak, S. (1999) Sequence and structure-based prediction of eukaryotic protein phosphorylation sites. *J. Mol. Biol.* **294**, 1351–1362.
- 53 Li, X., Commane, M., Burns, C., Vithalani, K., Cao, Z. and Stark, G. R. (1999) Mutant cells that do not respond to interleukin-1 (IL-1) reveal a novel role for IL-1 receptor-associated kinase. *Mol. Cell. Biol., Am Soc Microbiol* **19**, 4643–4652.
- 54 Lin, S.-C., Lo, Y.-C. and Wu, H. (2010) Helical assembly in the MyD88-IRAK4-IRAK2 complex in TLR/IL-1R signalling. *Nature* **465**, 885–890.
- 55 Bernstein, N. K., Williams, R. S., Rakovszky, M. L., Cui, D., Green, R., Karimi-Busheri, F., Mani, R. S., Galicia, S., Koch, C. A. and Cass, C. E. (2005) The Molecular Architecture of the Mammalian DNA Repair Enzyme, Polynucleotide Kinase. *Mol. Cell* **17**, 657–670.
- 56 Huen, M. S. Y., Grant, R., Manke, I., Minn, K., Yu, X., Yaffe, M. B. and Chen, J. (2007) RNF8 Transduces the DNA-Damage Signal via Histone Ubiquitylation and Checkpoint Protein Assembly. *Cell* **131**, 901–914.
- 57 McCoy, A. J., Grosse-Kunstleve, R. W., Adams, P. D., Winn, M. D., Storoni, L. C. and Read, R. J. (2007) Phaser crystallographic software. *Journal of Applied Crystallography* **40**, 658–674.
- 58 Arnold, K., Bordoli, L., Kopp, J. and Schwede, T. (2006) The SWISS-MODEL workspace: a web-based environment for protein structure homology modelling. *Bioinformatics* **22**, 195–201.
- 59 Gee, C. L., Papavinasasundaram, K. G., Blair, S. R., Baer, C. E., Falick, A. M., King, D. S., Griffin, J. E., Venghatakrishnan, H., Zukauskas, A., Wei, J.-R., et al. (2012) A

- phosphorylated pseudokinase complex controls cell wall synthesis in mycobacteria. *Sci Signal* **5**, ra7.
- 60 Machida, S. and Yuan, Y. A. (2013) Crystal Structure of Arabidopsis thaliana Dawdle Forkhead-Associated Domain Reveals a Conserved Phospho-Threonine Recognition Cleft for Dicer-Like 1 Binding. *Mol. Plant* **6**, 1290–1300.
- 61 Wu, H.-H., Wu, P.-Y., Huang, K.-F., Kao, Y.-Y. and Tsai, M.-D. (2012) Structural Delineation of MDC1-FHA Domain Binding with CHK2-pThr68. *Biochemistry* **51**, 575–577.
- 62 Adams, J. A. (2003) Activation loop phosphorylation and catalysis in protein kinases: is there functional evidence for the autoinhibitor model? *Biochemistry* **42**, 601–607.
- 63 Li, S., Strelow, A., Fontana, E. J. and Wesche, H. (2002) IRAK-4: a novel member of the IRAK family with the properties of an IRAK-kinase. *Proc. Natl. Acad. Sci. U. S. A.* **99**, 5567–5572.
- 64 Tun-Kyi, A., Finn, G., Greenwood, A., Nowak, M., Lee, T. H., Asara, J. M., Tsokos, G. C., Fitzgerald, K., Israel, E., Li, X., et al. (2011) Essential role for the prolyl isomerase Pin1 in Toll-like receptor signaling and type I interferon-mediated immunity. *Nat. Immunol.* **12**, 733–741.
- 65 Cui, W., Xiao, N., Xiao, H., Zhou, H., Yu, M., Gu, J. and Li, X. (2012) β -TrCP-mediated IRAK1 degradation releases TAK1-TRAF6 from the membrane to the cytosol for TAK1-dependent NF- κ B activation. *Mol. Cell. Biol.* **32**, 3990–4000.
- 66 Edinger, R. S., Lebowitz, J., Li, H., Alzamora, R., Wang, H., Johnson, J. P. and Hallows, K. R. (2009) Functional regulation of the epithelial Na⁺ channel by IkappaB kinase-beta occurs via phosphorylation of the ubiquitin ligase Nedd4-2. *J. Biol. Chem.* **284**, 150–157.
- 67 Songyang, Z., Shoelson, S. E., Chaudhuri, M., Gish, G., Pawson, T., Haser, W. G., King, F., Roberts, T., Ratnofsky, S. and Lechleider, R. J. (1993) SH2 domains recognize specific phosphopeptide sequences. *Cell* **72**, 767–778.
- 68 Liu, B. A., Engelmann, B. W. and Nash, P. D. (2012) The language of SH2 domain interactions defines phosphotyrosine-mediated signal transduction. *FEBS Lett., Federation of European Biochemical Societies* **586**, 2597–2605.
- 69 Bae, J. H., Lew, E. D., Yuzawa, S., TomE, F., Lax, I. and Schlessinger, J. (2009) The selectivity of receptor tyrosine kinase signaling is controlled by a secondary SH2 domain binding site. *Cell* **138**, 514–524.
- 70 Rotin, D., Margolis, B., Mohammadi, M., Daly, R. J., Daum, G., Li, N., Fischer, E. H., Burgess, W. H., Ullrich, A. and Schlessinger, J. (1992) SH2 domains prevent tyrosine dephosphorylation of the EGF receptor: identification of Tyr992 as the high-affinity binding site for SH2 domains of phospholipase C gamma. *EMBO J.* **11**, 559–567.
- 71 Machida, K., Thompson, C. M., Dierck, K., Jablonowski, K., Kärkkäinen, S., Liu, B., Zhang, H., Nash, P. D., Newman, D. K., Nollau, P., et al. (2007) High-throughput phosphotyrosine profiling using SH2 domains. *Mol. Cell* **26**, 899–915.
- 72 Gaurnier-Hausser, A., Patel, R., Baldwin, A. S., May, M. J. and Mason, N. J. (2011) NEMO-Binding Domain Peptide Inhibits Constitutive NF- κ B Activity and Reduces Tumor Burden in a Canine Model of Relapsed, Refractory Diffuse Large B-Cell Lymphoma. *Clin. Cancer Res.* **17**, 4661–4671.
- 73 Yao, J., Kim, T. W., Qin, J., Jiang, Z., Qian, Y., Xiao, H., Lu, Y., Qian, W., Gulen, M. F., Sizemore, N., et al. (2007) Interleukin-1 (IL-1)-induced TAK1-dependent Versus MEKK3-dependent NF κ B activation pathways bifurcate at IL-1 receptor-associated kinase modification. *J. Biol. Chem., ASBMB* **282**, 6075–6089.
- 74 Windheim, M., Stafford, M., Peggie, M. and Cohen, P. (2008) Interleukin-1 (IL-1) Induces the Lys63-Linked Polyubiquitination of IL-1 Receptor-Associated Kinase 1 To Facilitate NEMO Binding and the Activation of I κ B Kinase. *Mol. Cell. Biol.* **28**, 1783–1791.
- 75 Deshaies, R. J. and Joazeiro, C. A. P. (2009) RING domain E3 ubiquitin ligases. *Annu. Rev. Biochem.* **78**, 399–434.
- 76 Zheng, N., Wang, P., Jeffrey, P. D. and Pavletich, N. P. (2000) Structure of a c-Cbl-UbcH7

- complex: RING domain function in ubiquitin-protein ligases. *Cell* **102**, 533–539.
- 77 Yin, Q., Lin, S.-C., Lamothe, B., Lu, M., Lo, Y.-C., Hura, G., Zheng, L., Rich, R. L., Campos, A. D., Myszka, D. G., et al. (2009) E2 interaction and dimerization in the crystal structure of TRAF6. *Nat. Struct. Mol. Biol.* **16**, 658–666.
- 78 Ye, H., Arron, J. R., Lamothe, B., Cirilli, M., Kobayashi, T., Shevde, N. K., Segal, D., Dzivenu, O. K., Vologodskaia, M., Yim, M., et al. (2002) Distinct molecular mechanism for initiating TRAF6 signalling. *Nature* **418**, 443–447.
- 79 Poblenz, A. T., Jacoby, J. J., Singh, S. and Darnay, B. G. (2007) Inhibition of RANKL-mediated osteoclast differentiation by selective TRAF6 decoy peptides. *Biochem. Biophys. Res. Commun.* **359**, 510–515.
- 80 Zhang, P., Reichardt, A., Liang, H., Aliyari, R., Cheng, D., Wang, Y., Xu, F., Cheng, G. and Liu, Y. (2012) Single amino acid substitutions confer the antiviral activity of the TRAF3 adaptor protein onto TRAF5. *Sci Signal* **5**, ra81.
- 81 Park, Y. C., Burkitt, V., Villa, A. R., Tong, L. and Wu, H. (1999) Structural basis for self-association and receptor recognition of human TRAF2. *Nature* **398**, 533–538.
- 82 Niu, F., Ru, H., Ding, W., Ouyang, S. and Liu, Z.-J. (2013) Structural biology study of human TNF receptor associated factor 4 TRAF domain. *Protein Cell*.
- 83 Tropea, J. E., Cherry, S. and Waugh, D. S. (2009) Expression and purification of soluble His6-tagged TEV protease. In *Methods in Molecular Biology; High Throughput Protein Expression and Purification* (Doyle, S. A., ed.), pp 297–307, Humana Press, Totowa, NJ.
- 84 Otwinowski, Z. and Minor, W. (1997) Processing of X-ray diffraction data collected in oscillation mode. *Methods in Enzymology* **276**, 307–326.
- 85 Cole, J. L. (2004) Analysis of heterogeneous interactions. *Methods in Enzymology*, Elsevier **384**, 212–232.